UNIVERSITÀ
DEGLI STUDI
DI PADOVA

FACSIMILE FRONT PAGE

Head Office: Università degli Studi di Padova

Department of Biology

Ph.D. COURSE: Biosciences

CURRICULUM: Cell Biology and Physiology

SERIES: XXXV

Antagonising microRNAs that target the mitochondria shaping protein Opa1 ameliorates denervation-induced muscle atrophy

Thesis written with the financial contribution of Muscular Dystrophy Association (MDA) and Association Francaise contre les Myopathies (AFM)

Coordinator: Prof. Ildikò Szabò

Supervisor: Prof. Luca Scorrano

Ph.D. student: Andre Djalalvandi

Acknowledgements

First and foremost, I would like to thank my Family. Without their unrelenting support throughout the years none of my academic success would have been possible.

Next, I would like to thank my Professor, Luca, who has been a great mentor to me over the past three years, imparting sound scientific knowledge/advice, inspiration and making me feel a welcome member of the Lab.

I would like to thank all the people in the Scorrano Lab for their help, humour and moral support during my PhD. From VIMM, Keisuke developed the luciferase plasmids used in this project and we had many brainstorming sessions together. Lorenza and Martina taught me many wet-lab techniques and how to work with mice. Akiko has the special gift of making a person feel better when they are down; she helped me a lot during the PhD with her kind words and immense ability to make me laugh. Carlotta joined for a short period during the final phase of my PhD and helped contribute towards the in vivo worked produced in this project. From Vallisneri, I would like to thank Tiago, Erwan and Mauricio for being my brothers and helping me through stressful times. The experiences we have shared are mainly through playing football, exercising, getting f*cked and enjoying conferences.

I would like to thank Saman Sharifi from Alimonti lab who is my brother. We have had some nice scientific discussions at work and Sam has always been happy to share reagents with our lab when needed. Most importantly, we have embarked on some crazy adventures in Italy, both good and bad, and there will be more funny memories in the future for sure.

Lastly, I would like to acknowledge myself for doing a PhD.

Contents

Summary of thesis

Distorted mitochondrial cristae shape is a pathological hallmark of mitochondrial and disuse myopathies. Genetic overexpression of the master cristae shape regulator Optic atrophy 1 (OPA1) in models of mitochondrial and disuse myopathies ameliorates mitochondrial and muscle function and prolongs lifespan but translating this proof of principle approach into a pharmacological therapy to modulate OPA1 levels remains a challenge. Here we report that antagonising microRNAs (miRNAs) that regulate OPA1 mRNA levels ameliorates a model of disuse myopathy. By bioinformatic approaches we identified that mouse and human *OPA1* is regulated by miRNAs of the 148/152-3p family and by miR-128-3p. By using luciferase sensors, we show that these miRNAs specifically target and regulate mammalian OPA1 levels. Moreover, these OPA1-specific miRNAs are increased upon mitochondrial dysfunction, in complex IV deficient cell lines and in mice undergoing muscle atrophy induced by sciatic nerve denervation. Mechanistically, levels of these miRNAs appear under the control of endoplasmic reticulum stress pathways that are engaged upon mitochondrial dysfunction. Delivery of specific microRNA antagonizers (antagomiRs) increased OPA1 levels and curtailed muscular atrophy induced by denervation in vivo. Our results nominate OPA1-regulating miRNAs as therapeutic targets in mitochondrial myopathies.

Summary of thesis (Italian)

La forma distorta delle creste mitocondriali è un segno patologico delle miopatie mitocondriali e da disuso. La sovraespressione genetica del regolatore della forma delle creste master L'atrofia ottica 1 (OPA1) nei modelli di miopatie mitocondriali e da disuso migliora la funzione mitocondriale e muscolare e prolunga la durata della vita, ma tradurre questo approccio di prova di principio in una terapia farmacologica per modulare i livelli di OPA1 rimane una sfida. Qui riportiamo che l'antagonizzazione dei microRNA (miRNA) che regolano i livelli di mRNA di OPA1 migliora un modello di miopatia da disuso. Mediante approcci bioinformatici abbiamo identificato che l' OPA1 murino e umano è regolato dai miRNA della famiglia 148/152-3p e dal miR-128-3p. Utilizzando i sensori della luciferasi, dimostriamo che questi miRNA prendono di mira e regolano specificamente i livelli di OPA1 nei mammiferi. Inoltre, questi miRNA specifici per OPA1 sono aumentati in caso di disfunzione mitocondriale, in linee cellulari carenti di complesso IV e in topi sottoposti a atrofia muscolare indotta da denervazione del nervo sciatico. Meccanicisticamente, i livelli di questi miRNA appaiono sotto il controllo delle vie di stress del reticolo endoplasmatico che sono impegnate sulla disfunzione mitocondriale. La somministrazione di specifici antagonisti del microRNA (antagomiR) ha aumentato i livelli di OPA1 e ridotto l'atrofia muscolare indotta dalla denervazione in vivo. I nostri risultati nominano i miRNA che regolano OPA1 come bersagli terapeutici nelle miopatie mitocondriali.

Abbreviations

ADP	Adenosine diphosphate
ADOA	Autosomal dominant atrophy
AGO2)	Argonaute 2
ATF2	Activating transcription factor 2
ATP	Adenosine triphosphate
ATP5F1A	ATP synthase F1 subunit alpha
CCCP	Carbonyl cyanide m-chlorophenyl hydrazone
CCR4-NOT	Carbon Catabolite Repression—Negative On TATA-less
Cdk1	Cyclin-dependent protein kinase 1
CMT2A	Charcot-Marie-Tooth disease type 2A
CJ	Cristae junction
COX4-I	Cytochrome c oxidase subunit 4 isoform 1
COX15	Cytochrome C Oxidase Assembly Homolog COX15
DDX6	DEAD-Box Helicase 6
DCP2	Decapping protein 2
DNA	Deoxyribonucleic acid
DNM2	Dynamin-2
DRP1	Dynamin-related protein 1
ER	Endoplasmic reticulum
ETC	Electron transport chain
FADH	Flavin adenine dinucleotide
FGF21	Fibroblast growth factor 21
FIS1	Mitochondrial fission 1 protein

GTP	Guanosine triphosphate
HOTAIR	HOX transcript antisense RNA
Hsc70	Heat shock cognate 71 kDa protein
HSP90	Heat shock protein 90
IBM	Inner boundary membrane
IMM	Inner mitochondrial membrane
INF2	Inverted formin 2
LNA	Locked nucleic acid
MEF	Mouse embryonic fibroblast
MFF	Mitochondrial fission factor
MFN1	Mitofusin-1
MFN2	Mitofusin-2
MICOS	Mitochondrial contact site and cristae organizing system
MiD49	Mitochondrial dynamics protein 49
MiD51	Mitochondrial dynamics protein 51
miRNA	MicroRNA
mRNA	Messenger RNA
mtDNA	Mitochondrial DNA
MT-TL1	Mitochondrially encoded tRNA leucine 1
NADH	Nicotinamide adenine dinucleotide
NF-κB	Nuclear factor kappa-light-chain-enhancer of activated B cells
OMA1	Overlapping proteolytic activity with m-AAA protease 1
OMM	Outer mitochondrial membrane
OPA1	Optic atrophy 1

OXPHOS	Oxidative phosphorylation
PGC1α/β	Peroxisome proliferator-activated receptor gamma coactivator 1-alpha/beta
POLG1	DNA polymerase subunit gamma 1
RCC	Respiratory chain complex
RCS	Respiratory chain supercomplex
RISC	RNA-induced silencing complex
ROS	Reactive oxygen species
RNA	Ribonucleic acid
rRNA	Ribosomal RNA
tRNA	Transfer RNA
SURF1	Surfeit locus protein 1
TUDCA	Tauroursodeoxycholic acid
TCA	Tricarboxylic acid cycle
TNRC6	Trinucleotide repeat-containing gene 6A
VDAC	Voltage-dependent anion channel
XBP1s	X-box binding protein 1
XIST	X-inactive specific transcript
XRN1	5′-3′ exoribonuclease 1
YME1L	Yeast mitochondrial DNA escape 1-like
2’-MOE	2′- O -methoxethyl

Introduction

Mitochondria

Mitochondria are double-membrane organelles that supply the energy currency for the cell in the form of adenosine triphosphate (ATP). Other well-established roles of mitochondria include free radical scavenging, intrinsic apoptosis, Ca^{2+} buffering, stem cell fate and autophagy (Giacomello et al., 2020; Osellame et al., 2012). This organelle was first defined in 1857 by the anatomist Rudolf Albrecht von Koelliker who named them “sarcosomes”. Subsequently, microbiologist Carl Benda conjured up the word “mitochondria”, where “mitos" means thread and “chondros" means granule. According to the endosymbiotic theory by Margulis, mitochondria originated from a primordial rickettsia bacteria α-protobacteria that occupied a prototypical eukaryotic cell, in which the relationship between the two entities enhanced energy conversion to set in motion the rise of multicellular organisms (Margulis, 1971). Interestingly, mitochondria contain their own DNA (mtDNA) that is a double-stranded circular DNA molecule of ~16.5 kb encoding for 13 proteins, two ribosomal RNAs (rRNA) and 14 transfer RNAs (tRNA) (Greaves et al., 2012).

Mitochondrial compartments

Outer mitochondrial membrane

Akin to the eukaryotic cell membrane, the outer mitochondrial membrane (OMM) of mitochondria is composed of a phospholipid bilayer that is the external part of the organelle. This membrane is the entry point for nuclear-encoded mitochondrial proteins and contains pore-forming proteins such as voltage-dependent anion channels (VDAC) that are selectively permeable for the entry of metabolites and ions (Camara et al., 2017). Proteins residing on the OMM can form contacts with neighbouring organelles to carry out a wide variety of cellular functions (Giacomello et al., 2020). For example, mitochondria and endoplasmic reticulum (ER) form physical contacts for lipid exchange, mitochondrial calcium uptake and to support mitochondrial division. Lastly, mitophagic receptors localise on the OMM to initiate mitophagy for promoting a healthy turnover of mitochondria (Giacomello et al., 2020).

Intermembrane space

The intermembrane space is the area between the OMM and inner mitochondrial membrane (IMM). This space is where hydrogen ions accumulate as part of the electrochemical gradient for ATP generation and other mitochondrial processes.

Inner mitochondrial membrane

The IMM can be separated further into the inner boundary membrane (IBM), that runs parallel against the OMM, and the cristae which are deep invaginations in the membrane that increase the surface area of the IMM. The cristae membrane accommodates respiratory chain complexes (RCC) that form the electron transport

chain, and together with F_1F_0–ATP synthase, participate in ATP generation (see Fig. 1) (Osellame et al., 2012). Moreover, cristae junctions (CJs) that link cristae to the IBM act as diffusion barriers to sequester cytochrome C and other small molecules.

Mitochondrial matrix

The mitochondrial matrix is the central space of the mitochondria enclosed by the IMM. It is the site of mtDNA replication, transcription, and protein synthesis (Greaves et al., 2012). Moreover, enzymatic reactions such as the tricarboxylic acid cycle (TCA) take place here, which yields reducing intermediates NADH and $FADH_2$ that then feed electrons to complexes I and II of the ETC, respectively (Osellame et al., 2012).

Mitochondrial respiratory chain

Energy conversion takes place at the cristae. The ETC is composed of four RCCs, complexes I-IV, and two mobile electron carriers, ubiquinone and cytochrome C. It is the site of oxidative phosphorylation (OXPHOS) wherein electrons are stripped from reducing equivalents NADH and $FADH_2$ and transferred from the least electronegative complex (complex I) to the most electronegative complex (complex IV). Coupled to electron transfer is proton pumping by complexes I, III and IV across the IMM to generate an electrochemical gradient. This force drives H+ ions into the IMS that then enter F_1F_0–ATP synthase to stimulate its rotary function for ATP synthesis (see Fig. 1) (Osellame et al., 2012).

Interestingly, RCCs assemble into macromolecular structures known as respiratory chain supercomplexes (RCS), with the most abundant in mammalian mitochondria being RCS $I+III_2+IV_1$ (Signes & Fernandez-Vizarra, 2018). RCSs enhance mitochondrial respiration through improving electron flow channelling, stabilising individual complexes and reducing ROS accumulation (Baker et al., 2019; Signes & Fernandez-Vizarra, 2018). The assembly of RCSs is dependent on cristae morphology: a narrow CJ width favours RCS assembly (Cogliati et al., 2013), whereas widening of the CJ leads to RCS disassembly, and in certain cases, cytochrome C release out of the intracristal space and the induction of apoptosis (Cipolat et al., 2006; Frezza et al., 2006).

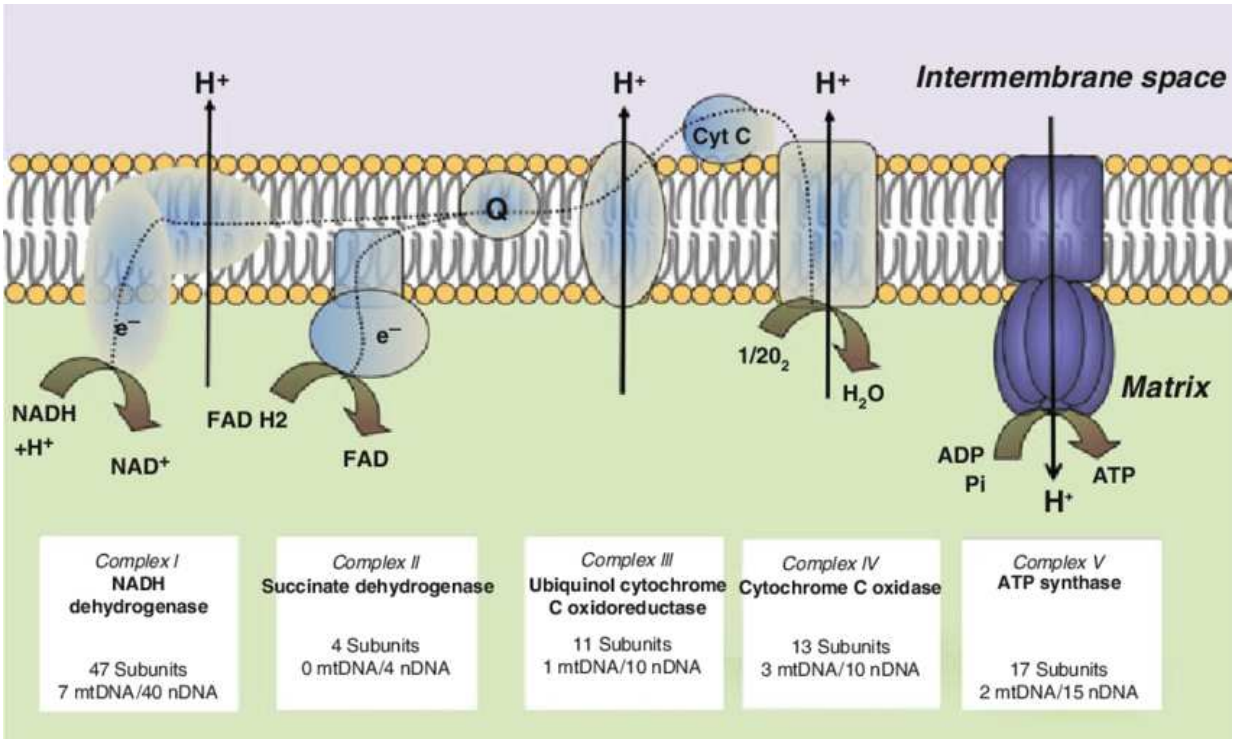

Figure 1. Schematic representation of the electron transport chain in mammalian mitochondria. Electrons from NADH and $FADH_2$ are donated to complex I and complex II, respectively. As electrons are passed down the chain from complex I to complex IV, the free energy from electron transfer is harnessed to pump protons from the matrix to the IMS by complex I, complex III and complex IV. Protons enter F_1F_0–ATP synthase to switch on its rotary function for catalysing the conversion of ADP to ATP. Image from Benard et al. (2011)

Mitochondrial dynamics and ultrastructure

Mitochondrial dynamics can be defined as the morphological changes mitochondria undergo to meet cellular demands. It accomplishes this by ongoing fusion, fission and cristae remodelling events (Giacomello et al., 2020; Pernas & Scorrano, 2016). Mitochondrial fusion and fission are evolutionary conserved processes that are chiefly controlled by dynamin-related GTPases Optic atrophy 1 (OPA1), Mitofusin 1 (MFN1), Mitofusin 2 (MFN2) and Dynamin-related protein 1 (DRP1). Mitofusins 1 and 2 mediate OMM fusion, OPA1 regulates IMM fusion and cristae remodelling, and DRP1 and its adaptor proteins execute mitochondrial fission (Pernas & Scorrano, 2016). Basically, rates of fusion and fission dictate mitochondrial shape. Unopposed fusion causes mitochondrial hyperfusion, whereas unopposed fission triggers mitochondrial fragmentation. Fusion and fission take place in a cyclic fashion to facilitate a healthy turnover of mitochondria. Additionally, mitochondrial dynamics influence the number, size and intracellular distribution of mitochondria (Pernas & Scorrano, 2016).

Optic atrophy 1

Optic atrophy 1 is located at the IMM and conserved from yeast (Mgm1 homolog) to human. The OPA1 gene is located on chromosome 3q28-q29 and spans over 100kb of genomic DNA for a total of 31 exons (Belenguer & Pellegrini, 2013). Eight isoforms exist that are alternatively spliced at exons 4, 4b, and 5b, and these are expressed differentially within each tissue (see Fig. 2) (Del Dotto et al., 2018). All OPA1 mRNA variants encode a protein of 924-1014 amino acids. There are three conserved regions on the OPA1 protein: GTPase domain, middle domain, and GTPase effector domain that contains a coiled-coil domain. The GTPase domain is the site at which guanosine triphosphate (GTP) is hydrolysed to stimulate IMM fusion. The middle domain and

coiled-coil domain allow for homotypic protein-protein interactions to form OPA1 oligomers that assist with cristae shaping (Del Dotto et al., 2018; MacVicar & Langer, 2016). Mitochondrial metalloproteases overlapping proteolytic activity with m-AAA protease 1 (OMA1) and yeast mitochondrial DNA escape 1-like (YME1L), proteolytically process OPA1 to generate short isoforms (S-OPA1) that lack the transmembrane domain (see Fig. 2). OPA1 long forms (L-OPA1) can be cleaved at S1 (OMA1-mediated) and S2 sites (YME1L-mediated). Isoforms 3, 5, 6 and 8, that include exon 4b, are completely cleaved into shorter forms (Del Dotto et al., 2018). At steady state, YME1L cleaves OPA1 in a manner coupled to OXPHOS. Separately, stress-induced OPA1 cleavage is performed by OMA1; it occurs during apoptosis, mitochondrial depolarisation and permeability transition. In basal conditions, a balanced ratio of long and short forms are required for optimal functioning of OPA1 (del Dotto et al., 2018).

A comprehensive list of *OPA1* mutations can be found on this database (http://opa1.mitodyn.org). Out of the 414 variants identified, around 60% are pathogenic, mostly from deletion mutations in the GTPase domain. In 50% of the pathogenic mutations, a premature stop codon is added, leading to a truncated mRNA that gets degraded, ultimately causing *OPA1* haploinsufficiency (Chao de la Barca et al., 2016). Pathogenic mutations of OPA1 mostly cause autosomal dominant atrophy syndrome (ADOA), but cases of encephalopathy, cardiomyopathy and non-syndromic Parkinsons disease have also been reported (Lynch et al., 2017; Spiegel et al., 2016).

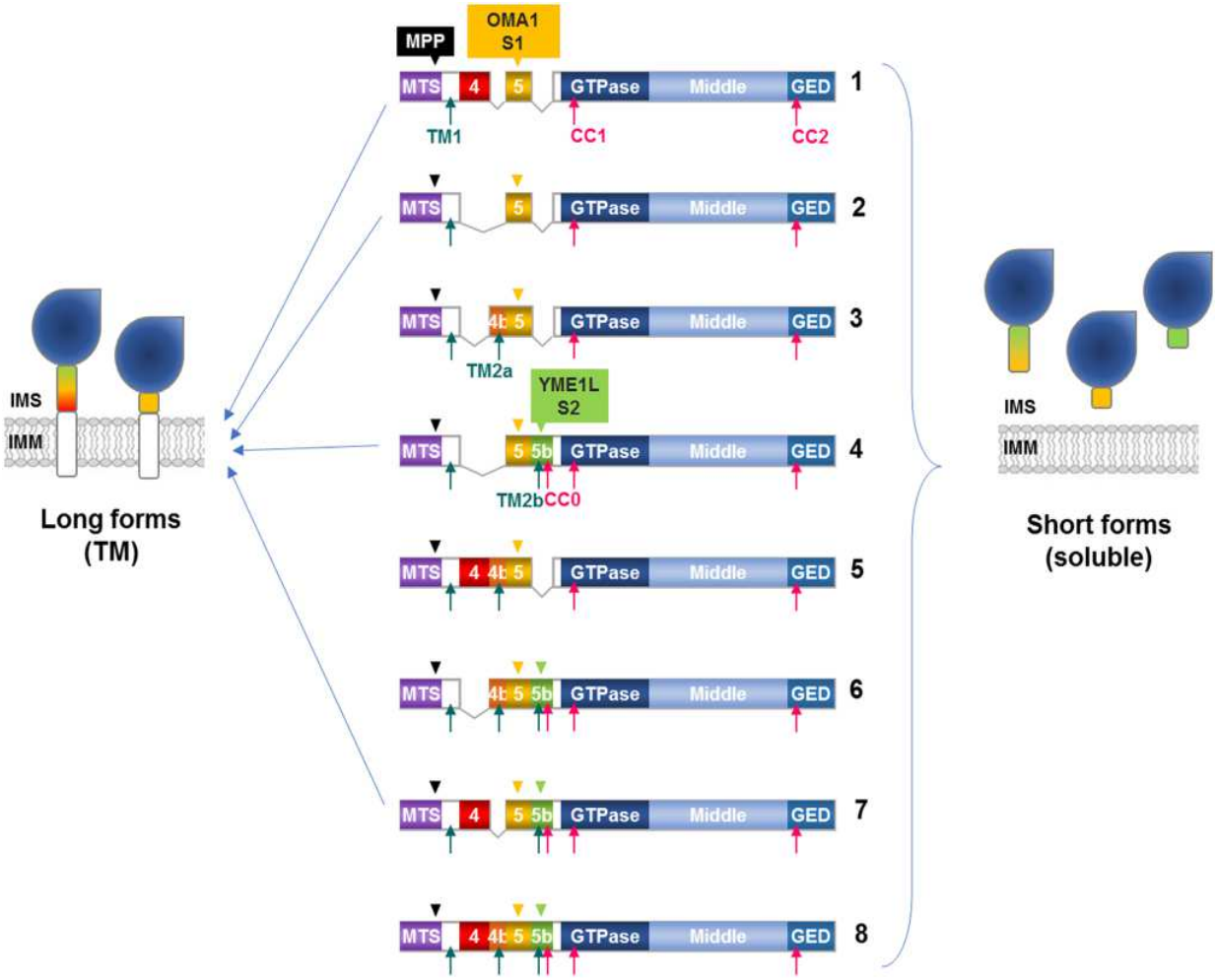

Figure 2. Protein structural domains of OPA1 and proteolytic processing sites. Eight isoforms of mammalian OPA1 protein exist that are cleaved at different locations to generate short OPA1 (S-OPA1) forms. OMA1 cleaves OPA1 at the S1 site located in the transmembrane domain and YME1L cleaves OPA1 at the S2 site that is also located in the transmembrane domain. Isoforms 3, 5, 6 and 8 that contain exon 4b are always cleaved into S-OPA1 forms. Image from Del Dotto et al. (2018)

Outer mitochondrial membrane fusion

The precise mechanism by which MFN1 and MFN2 facilitate OMM fusion remains equivocal. The overarching consensus was that heptad repeat 2 domains (HR2) of MFN1 and MFN2 mediate tethering of adjacent mitochondria, with heterotypic MFN1-MFN2 interactions displaying greater fusion activity than MFN1 and MFN2 homotypic interactions (Pernas & Scorrano, 2016). Then, crystallography studies engineering minimal recombinant MFN1 (predicted GTPase domain and a portion of C-terminal) showed that GTPase domains associate *in trans* for tethering (Chandhok et al., 2018). Taken together, it is plausible that HR2 domains bind for initial tethering to the adjoining mitochondria, followed by GTPase domain binding to set in motion a GTPase-dependent power stroke for pulling the OMMs together.

Despite sharing ~80% homology, MFN1 and MFN2 exhibit functional differences: MFN1 possesses greater tethering efficiency and GTPase activity (~8-fold higher) compared to MFN2 (Ishihara et al., 2004). Moreover, only MFN1 is indispensable for OPA1-mediated IMM fusion and is therefore a fundamental component of the fusion machinery (Cipolat et al., 2004). MFN2 has fusion-independent functions as it facilitates calcium ion homeostasis by tethering mitochondria to the ER (de Brito & Scorrano, 2008; Ivanova et al., 2017). The ER tethering function of MFN2 may be due to its ability to form sustained GTPase domain dimers, or its protein-protein interaction domain that is not present on MFN2 (Chandhok et al., 2018; Filadi et al., 2018). In mouse embryonic fibroblasts (MEFs), fragmented mitochondria were observed in MFN1-depleted cells, whereas MFN2-depleted cells displayed swollen spherical mitochondria (H. Chen et al., 2003a). When both Mitofusins were absent, mitochondria lacked the ability to fuse, causing impaired respiration and cellular growth impairments. Extending this, combined MFN1 and MFN2 ablation in mice is

embryonically lethal, highlighting the necessity for mitochondrial fusion in mammalian development (H. Chen et al., 2003b). Overexpressing MFN1 in MFN2 KO cells, or MFN2 in MFN1 KO cells, rescues mitochondrial fusion, yet surprisingly, in certain *MFN2* mutations only MFN1 overexpression could recover fusion activity (Pernas & Scorrano, 2016). These results imply that MFN1 and MFN2 have a redundancy relationship.

Inner mitochondrial membrane fusion

Inner mitochondrial membrane fusion finalises the unification of two mitochondria and is controlled by OPA1. In cellular and animal models, OPA1 ablation triggered mitochondrial fragmentation, and overexpressing OPA1 induced mitochondrial elongation (Cipolat et al., 2004) (Olichon et al., 2003). What is the physiological role of S-OPA1? When operating alone, S-OPA1 cannot perform IMM fusion (Ban et al., 2017). In contrast, when L-OPA1 processing was inhibited via YME1L deletion, mitochondria became fragmented (Mishra et al., 2014). Recent kinetics work employing evanescent field microscopy to monitor IMM fusion may help reconcile these inconsistencies (Ge et al., 2020). Mitochondrial tethering, membrane docking, lipid mixing and content release were analysed. It was revealed that superfluous S-OPA1 levels blocked pore opening, thereby disrupting the fusogenic ability of L-OPA1 (Ge et al., 2020). This phenomenon explains the pro-fission effects from S-OPA1 overexpression (Ishihara et al., 2006). Nevertheless, there is evidence of a synergistic relationship between L-OPA1 and S-OPA1 in performing IMM fusion (Ban et al., 2017). One study conducting an *in vitro* membrane fusion reaction found higher fusion rates in the L-OPA1 and S-OPA1 group (3:1 long-to-short ratio) compared to L-OPA1 alone (Ban et al., 2017). The proposed model for IMM fusion is as follows: L-OPA1

associates with cardiolipin on the opposite membrane to form a tether, with S-OPA1 providing structural support, then, GTP-hydrolysis stimulates membrane fusion.

Mitochondrial fission

The dominant member driving mitochondrial fission is the cytosolic mechanoenzyme DRP1 (Tilokani et al., 2018). DRP1 is recruited to the OMM where it arranges into spiral complexes around the preconstricted GTP-dependent fission site to sever the mitochondrion in two. DRP1 lacks membrane-binding domains, and so, to accomplish fission it interacts with OMM adaptor proteins: mitochondrial fission factor (MFF), mitochondrial fission protein 1 (FIS1) and mitochondrial dynamics proteins of 49 and 51 kDa (MiD49 and MiD51) (Tilokani et al., 2018). DRP1-dependent mitochondrial fission is initiated by phosphorylation-dephosphorylation reactions (Cereghetti et al., 2008; Taguchi et al., 2007). Responding to elevated cytosolic Ca^{2+} levels, calcineurin dephosphorylates DRP1 on Ser637 to prompt its translocation to mitochondria (Cereghetti et al., 2008). Cyclin-dependent protein kinase 1 (Cdk1)/cyclin B phosphorylates DRP1 on Ser616 (Ser585 in rat DRP1) to induce fission during mitosis (Taguchi et al., 2007). Mitochondrial division occurs at mitochondria-ER contacts; wherein ER tubules wrap around the mitochondria to mark the constriction site, and actin polymers formed by inverted formin 2 (INF2) and SPIRE1C, supplement DRP1 activity (Friedman et al., 2011; Korobova et al., 2013; Manor et al., 2015). Intriguingly, it has been shown that mitochondrial fission events are further influenced by lysosomes, to mark constriction sites (Wong et al., 2018), and Golgi-derived vesicles, to support late stages of division (Nagashima et al., 2020). Multiple organelles contributing towards mitochondrial fission exemplifies the complexity of mitochondrial dynamics and the social environment of the eukaryotic cell.

It was previously thought that Dynamin-2 (DNM2), acting downstream of DRP1, was necessary for executing mitochondrial scission. However, DNM2 ablation did not result in a hyperfused mitochondria network, confirming that DNM2 is not essential for fission completion (Fonseca et al., 2019). Cryo-electron microscopy (Cryo-EM) structures of DRP1-GTP and MiD49 and MiD51 complexes have shed light onto DRP1-dependent fission mechanisms (Kalia et al., 2018). GTP-binding to MiD49 and MiD51 formed linear copolymers, and subsequent GTP hydrolysis induced curling of DRP1 oligomers into ~16 nm diameter rings — a size feasible to constrict a double-membrane mitochondrion (Kalia et al., 2018). Abnormal DRP1 activity is associated with pathological states. In cellular models of Huntington's disease, elevated DRP1 levels caused mitochondrial fragmentation (Costa et al., 2010), suggesting that basal levels of DRP1 activity are vital for maintaining mitochondrial homeostasis.

Unlike yeast FIS1, mammalian FIS1 is dispensable for mitochondrial fission, although it is relied upon during stress-related fission (i.e., mitophagy and apoptosis stimulation) (Shen et al., 2014). Still, silencing and overexpressing FIS1 in mammalian cells has been demonstrated to induce mitochondrial elongation and fragmentation, respectively (Pernas & Scorrano, 2016). No existence of a yeast MFF homologue is suggestive of an evolutionary advancement in the fission machinery of mammals. In fact, MFF has emerged as the major receptor for DRP1-dependent mitochondrial fission. Overexpressing MFF fragmented the mitochondrial network while MFF silencing resulted in hyperfused mitochondria and interrupted DRP1 recruitment to mitochondria (Otera et al., 2010). Other DRP1 adaptors, MiD49 and MiD51, paradoxically elongated mitochondria when overexpressed [64-66]. A potential explanation is that the dissociation of MiD49 and MiD51 from DRP1 is required for

mitochondrial constriction (Kalia et al., 2018), thus, an overaccumulation of these proteins could consequently block fission activity.

Mitochondrial cristae dynamics

Mitochondrial cristae modify their shape in accordance with physiological stimuli. The seminal paper by Hackenbrock in the 60s proved that in conditions of low adenosine diphosphate (ADP) availability, mitochondria transition from a "condensed state" (compact matrix and enlarged cristae) to an "orthodox state" (less compact matrix and denser cristae) (Hackenbrock, 1966). Reports decades later substantiated these findings, in which cristae became denser during starvation in MEFs to increase mitochondrial respiration (Gomes et al., 2011). Separate from its bioenergetic role, cristae remodelling is the core event of the intrinsic apoptosis pathway (Cipolat et al., 2006; Frezza et al., 2006). Cristae junctions typically act as diffusion barriers but widen during apoptosis to release cytochrome c into the cytosol for activating killer caspases that precipitate cell death (Frezza et al., 2006). Recently, it has been reckoned that cristae act autonomously within a mitochondrion, as individual cristae were reported to carry varying levels of membrane potential (Wolf et al., 2019). Heterogeneous membrane potential is coherent with the "cristae fission and fusion model" wherein cristae were reported to fuse and divide with neighbouring cristae (Kondadi et al., 2020). This mechanism would enable protein and lipid intermixing, for diluting damaged respiratory complexes and increasing cardiolipin synthesis.

The key modulators of cristae architecture are OPA1, mitochondrial contact site and cristae organising system (MICOS) and F_1F_o-ATP synthase (Cogliati et al., 2016). OPA1 is anchored to the IMM where it oligomerises to form and maintain CJs to

prevent cytochrome C release (Frezza et al., 2006). Additionally, by keeping CJs tight, OPA1 promotes the assembly of respiratory chain supercomplexes (RCSs) that facilitate efficient electron transfer to enhance mitochondrial respiration (Cogliati et al., 2013). The MICOS complex spans the CJ and is composed of seven subcomplexes in mammals: MIC10, MIC12, MIC19, MIC25, MIC26, MIC27, MIC60. MIC60, a core component, connects the OMM to the IMM and stabilises cristae to the IBM, permitting a long CJ without affecting cristae width (Cogliati et al., 2016). Another central player is MIC10, that self-oligomerises to induce negative IMM curvature for CJ formation (Barbot et al., 2015). When MIC60 and MIC10 are ablated in cells, there is a loss of CJs, highlighting their essential role in the biogenesis and maintenance of these structures (Cogliati et al., 2016;van der Laan et al., 2016).

Shaping the opposing end of cristae is F_1F_o-ATP synthase: by assembling into "v-shaped" dimers, it bends the lipid bilayer at the cristae rim to induce positive membrane curvature (Blum et al., 2019; Strauss et al., 2008). Deleting dimer-specific subunits of F_1F_o-ATP led to cristae loss and mitochondria displaying onion-like morphologies (Davies et al., 2011). Proteomic experiments have revealed a dynamic interplay among these cristae-shaping proteins. MIC10 molecules promoted F_1F_o-ATP synthase dimerisation through physical interactions, indicating MIC10 acts to synchronise CJ and cristae rim remodelling (Rampelt et al., 2017). MIC60 associates with OPA1 in high molecular weight complexes to stabilise CJs, with OPA1 operating upstream of MIC60 in this pathway (Glytsou et al., 2016). OPA1-dependent cristae remodelling stimulated F_1F_o-ATP synthase dimerisation and its reversal activity to maintain the electrochemical gradient. Reciprocally, *ATP5a* (F_1F_o-ATP synthase subunit) silencing disassembled Opal oligomers (Quintana-Cabrera et al., 2018).

Mitochondrial diseases

Mitochondrial diseases encompass a wide range of progressive debilitating disorders that are characterised by OXPHOS malfunction due to defects in RCCs. These diseases affect ~1:5000 individuals, can manifest at childhood or adulthood, and are transmitted by any mode of inheritance (Gorman et al., 2016; Ylikallio & Suomalainen, 2012). To date, ~300 genes have been identified to have a causative role in mitochondrial disease manifestation, due to pathogenic mutations in nuclear DNA and mtDNA (Gorman et al., 2016). As mitochondria are ubiquitously found throughout the body, multiple organs can become pathological. Organs with high metabolic demand that heavily rely on mitochondria such as the brain and muscle are afflicted the most. It is not surprising then that a large portion of the clinical features reported in mitochondrial disease patients are neurological and muscle problems (see Fig. 3) (Gorman et al., 2016; Ylikallio & Suomalainen, 2012). Biochemically, complex I and complex IV deficiencies are the most common causes of OXPHOS defects in mitochondrial diseases (Ghezzi & Zeviani, 2018). Diseases with prominent muscle issues are sub categorised as mitochondrial myopathies (examples discussed below). A key feature in these diseases is skeletal muscle atrophy. This is pertinent as less muscle mass correlates with worse prognosis (Bonaldo & Sandri, 2013). Electron microscopy analysis of mitochondrial myopathy patients displayed a wide array of mitochondrial ultrastructure abnormalities, such as “onion-like” concentric cristae and “donut” mitochondria (see Fig. 4) (Vincent et al., 2016).

Autosomal dominant optic atrophy

Mutations in *OPA1* cause autosomal dominant optic atrophy (ADOA), which is defined by isolated retinal ganglion cell (RGC) degeneration, causing progressive visual loss (Chao de la Barca et al., 2016). The disease typically affects children but can manifest later in adulthood. Certain mutations in the GTPase domain cause autosomal dominant atrophy plus syndrome (ADOA+) that is of greater severity to normal ADOA as multiple organs are hit, causing myopathy and peripheral neuropathy (Chao de la Barca et al., 2016). Mitochondrial fragmentation, impaired respiration and mtDNA instability are biochemical features reported in ADOA patient fibroblasts (Amati-Bonneau et al., 2009).

Leigh syndrome

Leigh syndrome is a progressive neurodegenerative encephalopathy that affects infants and can be caused by mutations in nuclear and mtDNA genes. The majority of Leigh syndrome cases are due to mutations in genes involved in complex IV assembly or function (Schubert & Vilarinho, 2020). The most frequently mutated gene is surfeit locus protein 1 *(SURF1)* that is an assembly factor of complex IV. One Leigh syndrome patient had lactic acidosis, hypotonia and seizures and died before the first month of age. Another patient was 16 years old and had slower disease progression, exhibiting predominantly muscle and brain problems (Antonicka et al., 2003)

Charcot-Marie-Tooth type 2 disease

Charcot-Marie-Tooth (CMT2A) is a peripheral neuropathy caused mainly by pathogenic mutations in *MFN2* (Züchner et al., 2004). The disease hits peripheral nerves, causing chronic motor and sensory defects, particularly in the axonal region. Clinical reports have consistently recorded patients to have walking gait issues, associated with progressive muscle weakness, and atrophy in upper and lower extremities (Kijima et al., 2005).

Mitochondrial encephalomyopathy, lactic acidosis, and stroke-like syndrome (MELAS)

Mitochondrial encephalomyopathy, lactic acidosis and stroke-like episodes (MELAS) is a multisystem disorder often fatal in childhood. Most cases are caused by mutations in the mtDNA gene *MT-TL1* encoding tRNALeu (Galnares-Olalde et al., 2021). Rarer cases have been reported to occur from DNA polymerase subunit gamma 1 (POLG1) mutations. Symptoms manifest at around two years of age, namely motor function impairment, muscle and hearing loss, heart and kidney issues and lactic acid accumulation in bodily fluids. A unique feature of this disease is the occurrence of stroke-like episodes (Galnares-Olalde et al., 2021).

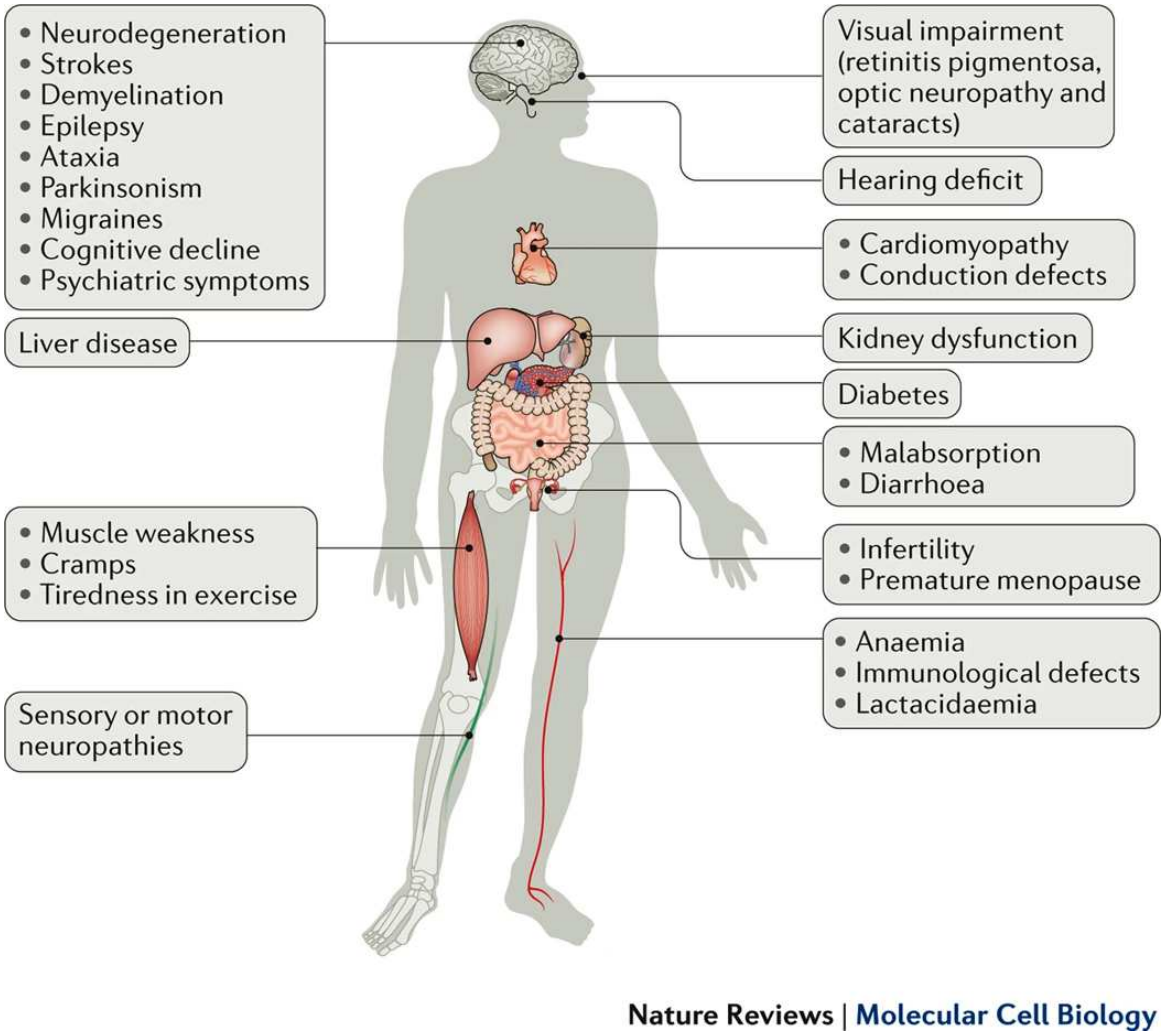

Figure 3. Pathological features of mitochondrial diseases. Mitochondrial disorders can manifest in childhood and adulthood and target multiple organs such as the brain, heart, pancreas, skeletal muscle and kidney. Tissue with high metabolic demands (brain and muscle) make up a large bulk of symptoms. Image from Suomalainen & Battersby (2018)

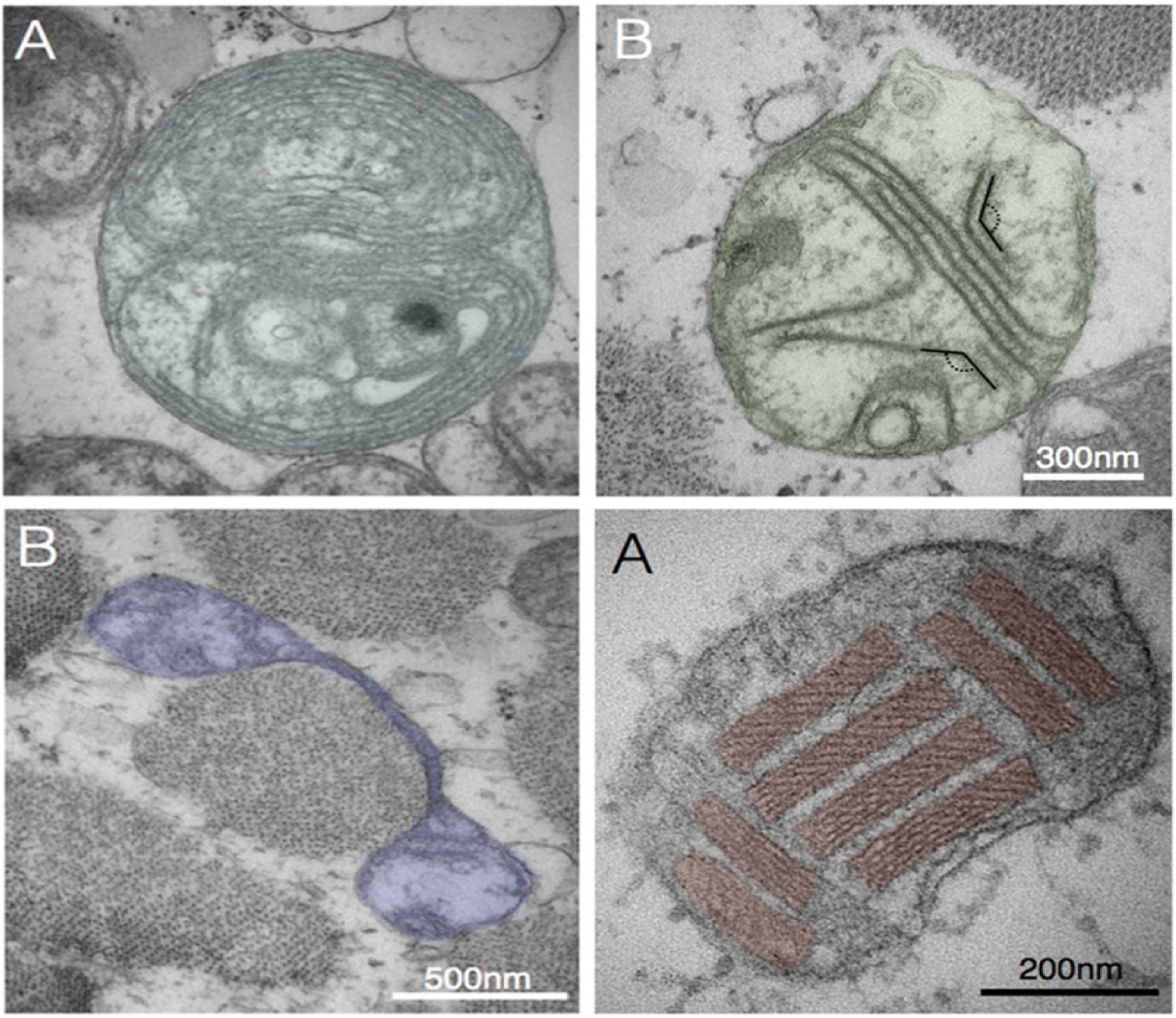

Figure 4. Ultrastructural analysis of skeletal muscle mitochondria from mitochondrial myopathy patients. Top left panel: mitochondrial cristae display the so-called "onion-like" morphology in a *m.*8344A>G patient. Top right panel: mitochondrial cristae are linearised also in a *m.*8344A>G patient. Bottom left panel: mitochondria form nanotunnels in a *m.*3243A>G patient. Paracrystalline inclusions are present in a patient with a single mtDNA deletion. Image from Vincent et al. (2016)

microRNA

microRNAs (miRNA) are a class of small non-coding RNAs (~22 nt long) that participate in translational repression (Bartel, 2018). They were discovered in *C.elegans* in 1993 when *lin-4*, a heterochronic gene that controls development timing, did not encode a protein but transcribed two pairs of small RNAs (Lee et al., 1993). The non-coding RNA was 22 nt long and contained complementarity sites to the 3'UTR region of *lin-4* mRNA, resulting in miRNA-mRNA binding and mRNA decay. Consequently, the translational repression triggered a pathway transition from the initial larval developmental stage to the next phase (R. C. Lee et al., 1993). Later in 2002, additional miRNAs were discovered in a range of species, including mice and humans (Lagos-Quintana et al., 2002). Currently on miRbase V22, a widely used searchable database of published miRNA sequences, there are 1234 annotated miRNA for mice and 1115 annotated miRNA for humans.

Pri-miRNA & pre-miRNA

Roughly 50% of miRNA are transcribed from introns of protein-coding mRNA, or exons of non-coding primary transcripts, while the other half are intergenic and regulated by their own promoters (Ha & Kim, 2014). In the nucleus, RNA polymerase II transcribes the miRNA gene which then folds back on itself to form a hairpin structure. The RNase Drosha and its molecular partner DGCR8 form a trimeric microprocessor complex that interacts with the miRNA hairpin. It operates as a molecular ruler to measure and then cut DNA strands to form a pre-miRNA with a 2' nt overhang (see Fig. 5) (Lee et al., 2003). Next, Exportin-5 and RAN-GTP bind together to form a transport complex that recognises the 2 nt 3' overhang and exports the pre-miRNA through a nuclear pore complex into the cytoplasm (Ha & Kim, 2014) . Dicer is another RNase that recognises

pre-miRNA (with preference for 2 nt overhang) and cuts both strands near the loop to create a 22nt miRNA duplex (see Fig. 5) (Lee et al., 2003).

Mature miRNA & miRISC

The miRNA duplex is loaded onto an argonaute 2 (AGO2) protein to form the RNA-induced silencing complex (RISC) (Bartel, 2018). RISC assembly involves two steps: loading and unwinding of the miRNA duplex. Heat shock cognate 71 kDa protein (Hsc70)/heat shock protein 90 (HSP90) use ATP to keep AGO2 in an open conformation for duplex binding to form pre-RISC (Bartel, 2018; Ha & Kim, 2014). During AGO2 loading, the most thermodynamically unstable miRNA strand, termed the guide strand, is loaded onto AGO2, while the other strand is degraded. AGO2 exposes the miRNA seed for pairing (2-5 nt) to the mRNA site. The seed region of the miRNA guides the RISC complex to the complementary site on the mRNA (typically at the 3'UTR) where it will enact translational repression (Bartel, 2009, 2018).

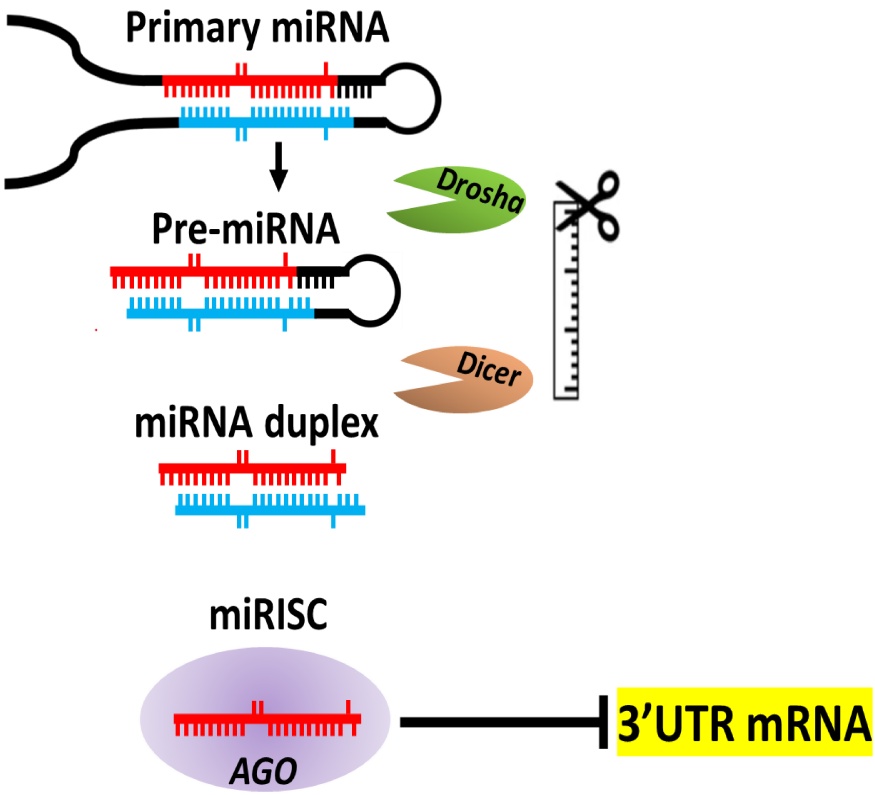

Figure 5. Schematic representation of the canonical microRNA biogenesis pathway. Primary miRNA transcripts are transcribed by RNA polymerase II and then further modified by miRNA processing enzymes Drosha and Dicer in the nucleus and cytoplasm, respectively. Next, the single miRNA strand is loaded onto an AGO2 complex to form the miRNA silencing complex (miRISC) that then travels towards an mRNA where it enacts mRNA decay or translational repression.

Mechanism of action

There are four canonical orientations in which miRNA bind to the target sequence on the mRNA. The most potent effector being the 8mer site that binds to the mRNA with optimal affinity (see Fig. 6) (Bartel, 2018). Other factors that influence miRNA repression efficiency are the presence of multiple target sites on an mRNA, especially sites that are between 8-40 nt of each other. Moreover, highly conserved sites are more susceptible to miRNA decay as they reside in optimal locations in the genome for silencing (Bartel, 2018; Selbach et al., 2008). Notably, in miR-223 KO cells, mRNA targets with 7mer or 8mer binding sites to this miRNA had a less than 2-fold increase, thus translational repression is modest—usually reductions of 50% and often less than 20% in protein content (Bartel, 2018). Once the miRNA is bound to the mRNA, there are two distinct mechanisms by which miRNA blocks protein translation: mRNA decay and translational repression.

By comparing data sets from mass spectrometry and real-time PCR, mRNA levels were observed to be downregulated more than protein levels, suggesting that mRNA decay is the dominant mechanism of action of miRNA. Indeed, mRNA decay accounts for around 70-90% target repression (Baek et al., 2008; Selbach et al., 2008). The mechanism in humans involves AGO2 recruitment of the adaptor protein Trinucleotide repeat-containing gene 6A (TNRC6) that interacts with CCR4-NOT to deadenylate the mRNA, followed by decapping by decapping protein 2 (DCP2) and finally 5'-to-3' degradation by exoribonuclease XRN1 (Jonas & Izaurralde, 2015). The proposed mechanism for pure translational repression involves CCR4-NOT recruitment of DEAD-Box Helicase 6 (DDX6), which binds the decapping complex and inhibits translation (Bartel, 2018).

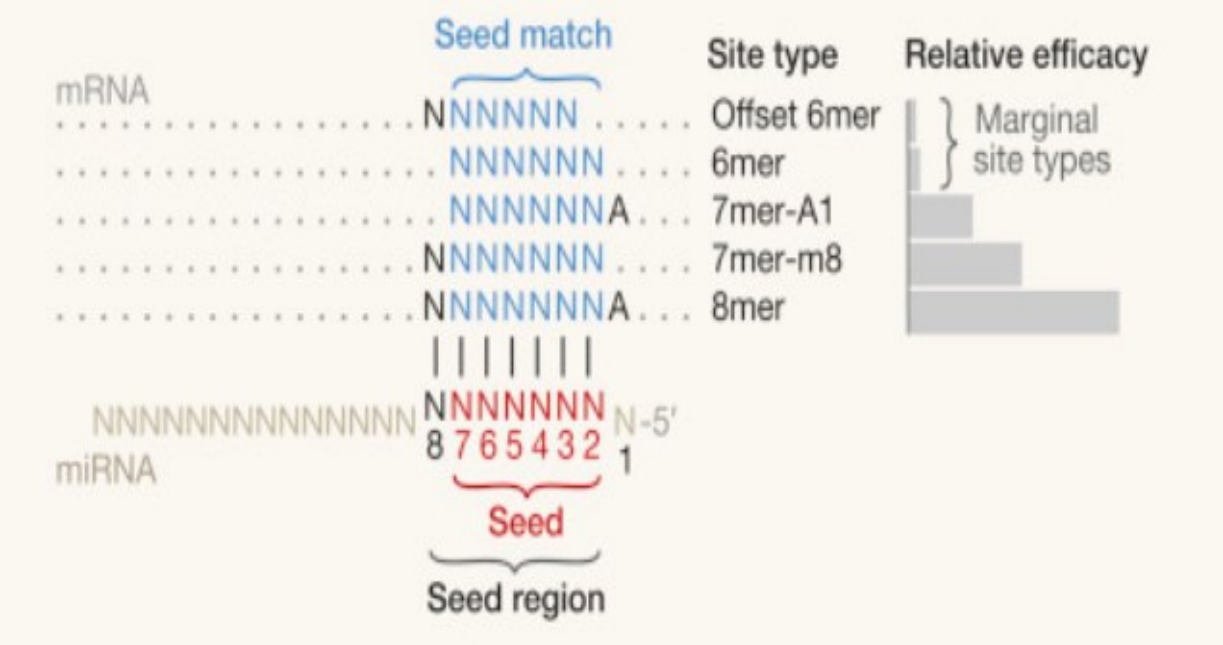

Figure 6. miRNA seed region base-pairs with mRNA in different orientations. Canonical sites for miRNA-mRNA interactions all contain a complementary seed region where complete binding occurs (positions 2-8 on an miRNA). The most potent orientation is 8mer and the least potent is 6mer. Image from Bartel (2018)

miRNA antagonisers

microRNA antagonisers (antagomiRs) are chemically modified oligonucleotides that base-pair with miRNA to silence its action (see Fig. 7) (Lennox & Behlke, 2011). This technology could therefore be harnessed to upregulate the expression of a gene of interest. Two types of antagomiRs have been developed with different mechanisms of action. One is via steric blocking of the RISC silencing complex, that has a locked nucleic acid (LNA) modification, whereas the other construct has a 2′- O -methoxethyl (2'-MOE) modification and physically degrades the miRNA. 2'-MOE constructs are more stable, less toxic, and can be recycled to silence additional miRNAs again after usage (Li & Rana, 2014). They have three chemical modifications to enhance stability and delivery 1) 2'-MOE sugar group 2) phosphorothioate backbone 3) cholesterol-moiety at 3′-end (tail). The 2'-MOE sugar modification enhances binding affinity, increases nuclease resistance and reduces immune activation. The phosphorothioate modification replaces an oxygen for sulfur in the phosphate backbone to further prevent nuclease attack (Lennox & Behlke, 2011). Phosphorothioate bonds help with absorption into blood and cellular uptake in most tissues. AntagomiRs are highly stable, with a half-life ranging from 1-4 weeks (Li & Rana, 2014). The cholesterol group at the 3' end assists delivery by reducing binding of serum proteins to lipoplexes (Lennox & Behlke, 2011).

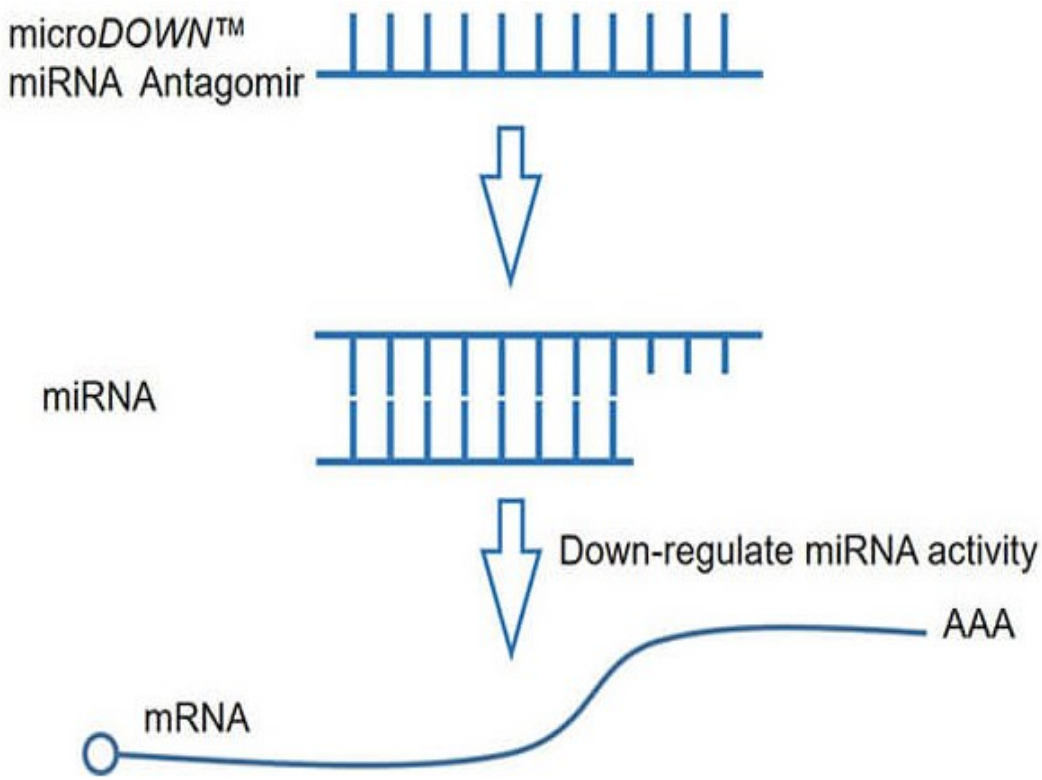

Figure 7. 2'-MOE AntagomiRs bind specifically to miRNA to inhibit its function. AntagomiRs possess perfect sequence complementarity to a miRNA and they base-pair together to block the silencing action of the miRNA, thereby allowing for more transcripts to be available for translation.

Aims and hypothesis of this study

- Verify if miRNAs of the 148/152-3p family and 128-3p regulate OPA1-dependent mitochondrial ultrastructure and function.
- Identify if miRNAs of the 148/152-3p family and 128-3p are increased in models of OXPHOS dysfunction and mitochondrial disease mouse models
- Verify if AntagomiRs specific for miRNAs of the 148/152-3p family and 128-3p can increase OPA1 to rescue muscle loss in mouse models of muscle atrophy

It was hypothesised that inhibiting the action of miRNAs of the 148/152-3p family and 128-3p, to increase OPA1 expression levels, provides protection against skeletal muscle atrophy.

Antagonising microRNAs that target the mitochondria shaping protein Opa1 ameliorates denervation-induced muscle atrophy

Andre Djalalvandi[1,2], Keisuke Takeda[1,2], Francesca Grespi[1,2], Martina Semenzato[1,2], Carlotta Barison[1,2], Davide Steffan[1,2], Camilla Bean[1,2], and Luca Scorrano[1,2§]

[1]Department of Biology, Via U. Bassi 58B, 35121 Padova, Italy

[2]Veneto Institute of Molecular Medicine, Via Orus 2, 35129 Padova,

[§]: address correspondence to luca.scorrano@unipd.it

Introduction

Mitochondria are central players in metabolism, signal transduction and cell fate. They are the chief energy converters in the cell and participate in anabolic and catabolic reactions, Ca^{2+} signalling, apoptosis, autophagy, and stem cell fate (Giacomello et al., 2020; Osellame et al., 2012). Defects in any of these processes lead to mitochondrial dysfunction that can ultimately drive pathology in several human diseases.

Primary mitochondrial diseases manifest predominantly by pathological mutations in mitochondrial DNA or nuclear DNA, causing neurodegeneration and/or muscle disease in children and adults. However, mitochondrial syndromes can involve other organs, individually or in combination with brain and muscle disease (Suomalainen & Battersby, 2018). The most frequent biochemical abnormalities in mitochondrial disorders include isolated or combined complex I/complex IV defects (Ghezzi & Zeviani, 2018). Collectively, these diseases are called mitochondrial disorders, a group of heterogeneous, and usually inherited (occasionally sporadic) conditions. Individually rare, when taken as a whole, mitochondrial disorders are among the most frequent genetic diseases in humans, affecting ~1 in 5,000 individuals (Gorman et al., 2016). Currently there is no effective treatment for mitochondrial disorders and there is therefore a clear need to develop new therapeutic strategies to tackle them.

Aberrant mitochondrial morphology is a pathological hallmark of mitochondrial diseases, irrespective of their mode of transmission and of the organ inspected (Vincent et al., 2016). Mitochondrial shape and membrane ultrastructure are controlled by GTPase dynamin-related proteins Mitofusins 1 and 2 (MFN1 & MFN2), Optic atrophy 1 (OPA1), Dynamin-related protein 1 (DRP1) and its adaptor proteins (Giacomello et al., 2020; Tilokani et al., 2018). Notably, cristae structure abnormalities

have been reported in skeletal muscle biopsies of mitochondrial disease patients (Vincent et al., 2016). Interestingly, correction of altered cristae ultrastructure by genetically increasing OPA1 levels not only interrupts denervation-induced muscle atrophy (Varanita et al., 2015) but can effectively ameliorate the phenotype in two mouse models of oxidative phosphorylation (OXPHOS) deficiency (Civiletto et al., 2015). These results therefore indicate that ultrastructural correction of mitochondria by increased OPA1 levels can be exploited to interrupt the pathogenic circle of mitochondrial diseases. However, a therapeutic strategy involving the increase in OPA1 levels represents a challenge. One possibility is to biologically modulate OPA1 transcription. Such a modulation can be achieved for example by using SINEUPs, a class of antisense long noncoding RNAs (lncRNAs) that can enhance the translation of their target mRNA (Carrieri et al., 2012). SINEUPs have been successfully employed for mitochondrial diseases, for example to correct frataxin levels in a Freidrich's Ataxia cellular model (Bon et al., 2019). Albeit developments are being made to reduce their size and their immunogenicity (Valentini et al., 2022), SINEUPs pharmacopoeia remains challenging. A different strategy might rely on targeting microRNAs (miRNAs) that endogenously modulate OPA1 levels. This approach surmises that (i) specific OPA1 targeting miRNAs exist; (ii) that these miRNAs are upregulated in mitochondrial and disuse myopathies; (iii) that delivery of miRNA antagonisers (antagomiRs) targeting them can restore OPA1 levels and mitochondrial ultrastructure and function.

With these questions in mind, we sought to identify miRNAs (miR) controlling OPA1 levels, to verify if they directly regulate OPA1 expression levels and if their inhibition using antagomiRs was sufficient to increase OPA1 levels and provide protection against muscle atrophy. We report the identification of four OPA1-targeting miRNAs.

Their levels are regulated by mitochondrial dysfunction induced ER stress and can be targeted by antagomiRs to restore OPA1 levels and reduce denervation induced muscle atrophy in vivo.

Results

miR-148/152-3p family and miR-128-3p are direct modulators of mammalian OPA1

To identify miRNAs that potentially target mammalian *Opa1*, three miRNA prediction websites were used: miRDB, TargetScan.org and miRwalk. miRNAs of the 148/152-3p family and miR-128-3p were predicted to target the 3'UTR of OPA1 with strong confidence and in an efficient orientation in mouse and human (Fig. 1) and were therefore selected for biological validation *in vitro*.

To understand if miR-148/152-3p and miR-128-3p control OPA1 expression levels, each miRNA was overexpressed and OPA1 mRNA and protein content were measured by real-time PCR and immunoblotting. Levels of OPA1 mRNA and protein were reduced in mouse and human cells that overexpressed miR-148/152-3p and miR-128-3p (Fig. 2A-C), suggesting that these miRNAs are effectively targeting OPA1 mRNA in mammals. To confirm the specificity of miR-148/152-3p and miR-128-3p on targeting OPA1, we devised a luciferase-based reporter assay of miRNA levels and activity. In this assay, the OPA1 3'UTR fragment to which the miRNAs were predicted to bind was coupled to firefly luciferase. A renilla luciferase was coexpressed from the same plasmid and used as an internal reference for ratiometric luciferase measurements. If a miRNA binds to the specific target sequence in the 3'UTR of the gene of interest, levels of the firefly luciferase and hence the firefly/renilla luciferase ratio decrease (Fig. 2D). Because transfection of cells expressing the luciferase sensor with miR-148/152-3p or with miR-128-3p resulted in a significant reduction in the measured ratio, we conclude that these miRNAs target and degrade the respective

mouse OPA1 3'UTR fragment to which they were predicted to bind (Fig. 2E,F). These experiments validate the prediction websites used and nominate these miRNAs as regulators of OPA1 levels.

miR-148b, 152-3p family and miR-128-3p regulate mitochondrial morphology

Because OPA1 participates in mitochondrial fusion as well as cristae biogenesis, we next turned to experiments of mitochondrial and cristae morphology to test whether levels of the identified miRNAs exerted a biological effect on mitochondria. By using transmission electron microscopy (TEM), we analysed mitochondrial size and cristae shape in cells that overexpressed the different miRNAs. In representative TEM micrographs, we observed that mitochondria in cells transfected with miR-148b-3p, miR-152-3p miR-128-3p appeared shorter and contained less cristae, whereas mitochondrial morphological changes were less evident in cells transfected with miR-148a-3p (Fig. 3A). This visual perception was confirmed by morphometric analyses of mitochondrial area, a proxy of mitochondrial elongation, and of cristae width, a proxy of the cristae bioenergetic activity of OPA1 (Glytsou et al., 2016). Indeed, we measured a significant reduction in the mitochondrial area and increase in cristae width (quantification not shown) only in cells transfected with miR-148b-3p, 152-3p and miR-128-3p mimics (Fig. 3B, C). These experiments indicate that miR-148b-3p, 152-3p and miR-128-3p modulate not only OPA1 levels, but also mitochondrial cristae shape and mitochondrial morphology.

Increased levels of miR-152-3p and miR-128-3p upon mitochondrial dysfunction.

The miRNAs identified here as capable of regulating OPA1 levels are found upregulated in primary human muscle diseases wherein mitochondrial dysfunction and ER stress are two key pathogenic features (Chen et al., 2009; Kim et al., 2014). We therefore decided to test whether miR-48/152-3p family and miR-128-3p accumulated in models of mitochondrial dysfunction and ER stress. We first treated mouse adult fibroblasts (MAFs) transfected with our miRNA-based sensors that track miRNA activity with mitochondrial toxins: actinonin (ACT), an inhibitor of mitochondrial translation that stalls ribosomes and causes OPA1 degradation (Richter et al., 2013, 2015), the ATP synthase inhibitor oligomycin (OLIGO) and the uncoupler carbonyl cyanide m-chlorophenylhydrazone (CCCP). We found that our sensors recorded an increase in miR-152-3p and miR-128-3p levels whereas miR-148a-3p and miR-148b-3p activity levels remained unchanged. In the case of miR-128-3p, we recorded an increase in its levels also in cells treated with the complex III inhibitor antimycin A (AA) (Fig. 4A, B). We next measured if the increase in miR-152-3p and miR-128-3p levels was functional and resulted in OPA1 downregulation. Using our sensors for miRNA binding to the OPA1 3'UTR fragment, we found that the luciferase containing the binding site for miR-148/152-3p was readily degraded when MAFs were treated with the mitochondrial toxins. Accordingly, we measured by RT-PCR a reduction in OPA1 mRNA levels when cells were treated with CCCP, rotenone and antimycin A, but surprisingly not when cells were treated with actinonin, suggesting that compensatory mechanisms exists when mitochondrial ribosomes are stalled (Richter et al., 2013) (Fig.4C, 4D). Thus, miR-152-3p contributes towards downregulating OPA1 mRNA

levels in conditions of mitochondrial respiratory chain and ATP synthesis inhibition as well as uncoupling, but not when mitochondrial ribosomes are stalled.

Next, we used a genetic model of mitochondrial dysfunction, human HEK293 cells where the gene encoding for COX4I1, a complex IV subunit mutated in cases of Fanconi anemia and Leigh-like syndrome (Abu-Libdeh et al., 2017; Quéméner-Redon et al., 2013) had been deleted by CRISPR/Cas9 (a kind gift of Dr. Peter Pecina, The Czech Academy of Sciences). Our sensors reported increased miR-152-3p and miR-128-3p activity compared to wild type HEK293 cells (Fig. 4E), supporting the data obtained in MAFs and indicating that these miRNAs represent a conserved response to genetic and pharmacological mitochondrial dysfunction.

We next wished to understand the mechanistic basis for the upregulation of these miRNAs. A common consequence of mitochondrial dysfunction is the induction of ER stress, and its reduction can mitigate the cellular and systemic consequences caused by mitochondrial defects (Debattisti et al., 2014; Kaspar et al., 2021; Tezze et al., 2017). Because an often overlooked component of ER stress is the induction of miRNAs (Maurel & Chevet, 2013), we decided to address whether alleviating ER stress with the chemical chaperone Tauroursodeoxycholic acid (TUDCA) (Debattisti et al., 2014) influenced levels of the measured miRNAs in cells exposed to mitochondrial toxins. Co-treatment with TUDCA lowered miR-152-3p activity in MAFs treated with actinonin and CCCP and miR-152-3p and miR-128-3p activity in COX4-I KO HEK293 cells (Fig 4F, 4G). Altogether, these results indicate that that pharmacologically and genetically induced mitochondrial dysfunction in mouse and human cells results in the upregulation of miR-152-3p and miR-128-3p that can be reverted by a pharmacological ER stress reducer.

miR-148a-3p and miR-152-3p levels are increased in denervation-induced muscle atrophy

As miR-148/152-3p family and miR-128-3p are apparently involved in muscle pathology, we sought to clarify whether they were induced upon muscle atrophy. A classic model of lower limb muscle atrophy induced by disuse is represented by sciatic nerve resection that causes mitochondrial dysfunction and morphological derangement (Varanita et al., 2015). We therefore performed sciatic nerve resection on mice and measured at different time points the cross-sectional area (CSA) of gastrocnemius fibers to identify the occurrence of muscular atrophy. Fourteen days post intervention CSA was clearly reduced, and fibers displayed central nuclei (Fig. 5A). We therefore elected to extract and quantify OPA1 mRNA and miRNA levels at 14d post-denervation. OPA1 transcript was almost obliterated compared to the levels observed in the contralateral sham operated gastrocnemius (Fig. 5B). Accordingly, levels of miR-148a-3p and miR-152-3p were significantly increased, whereas miR-148b-3p levels were significantly reduced (Fig. 5C). Thus, in a model of disuse myopathy two of the miRNAs controlling OPA1 levels are upregulated concomitantly with the reduction in OPA1 and in fiber size.

Silencing of miR-148b-3p, miR-152-3p and miR-128-3p rescue miRNA-dependent drops in OPA1 levels

Given that miRNAs controlling OPA1 levels were upregulated in vitro in models of mitochondrial dysfunction and in vivo in denervation-induced muscle atrophy, we sought to understand if we could block miRNA-dependent reductions in OPA1 levels. To this end, we tested the ability of antagomiRs miR-148/152-3p and miR-128-3p to curtail the effects of the corresponding miRNAs. First, we used our luciferase reporter

assay to verify if simultaneous transfection with antagomiRs reduced the effects of their respective miRNA. Indeed, antagomiRs 148/152-3p and 128-3p inhibited the action of the respective miRNA (Fig. 6A). Next, we measured OPA1 protein levels by immunoblotting in cells singly or doubly transfected with the miRNAs and their respective antagomir. While OPA1 levels were reduced by the expression of the miRNAs, co-transfection with their antagomiRs completely abolished the effects of the miRNAs and fully stabilised OPA1 levels (Fig. 6B).

Silencing of miR-148a-3p and miR-152-3p increases OPA1 levels to protect against denervation-induced muscle atrophy

Having established that antagomiRs could counteract the effects of miRNAs, we decided to test whether inhibiting miR-148a-3p and miR-152-3p activity levels in denervated mouse muscle could correct the pathology. We therefore devised an antagomiR intervention of triweekly intramuscular injections composed of a cocktail of antagomiRs 148/152-3p and miR-128-3p at a final does of 50 nM that we injected days 3, 5, 7, 9, 11, 13 after the denervation. The antagomiR mix could inhibit the miRNA induction observed in denervated muscles, most effectively for miR-148a-3p and miR-152-3p (Fig. 6A). We next measured OPA1 protein levels that as expected dropped upon denervation but were fully rescued in the muscles receiving the antagomir mix (Fig. 6b). Finally, we prepared histological sections of gastrocnemii from denervated and denervated, anatagomiRs treated muscles and measured fiber CSA values in antagomiR-treated denervated muscle compared to control-treated denervated muscle. While the anatagomiRs did not fully protect from denervation, they afforded a 60% increase in the CSA compared to the untreated, denervated muscles (Fig. 6C, 6D). Altogether, these data indicate that our antagomiR mix curtails the reduction in

OPA1 observed in vivo in denervated gastrocnemii and significantly protects them from atrophy caused by denervation.

Discussion

The cristae-remodelling protein OPA1 represents a promising therapeutic target for tackling mitochondrial myopathies. Yet, the identification of molecules to pharmacologically upregulate OPA1 expression levels remains a challenge. Here, we uncover four candidate miRNAs (miR-148/152-3p family and miR-128-3p) that specifically target mammalian OPA1 3'UTR to control its expression levels. Blocking the action of these OPA1-specific miRNAs by delivery of microRNA antagonisers (antagomiRs) *in vivo* was protective against muscle atrophy induced by denervation.

The miR-148/152-3p family and miR-128-3p investigated in this study are mainly known for their role in cancer, acting as tumour suppressors (Chen et al., 2013; Liu et al., 2016; Xu et al., 2015). In certain cancers (gastrointestinal, hepatocellular carcinoma, ovarian, colorectal, breast), miR-148/152-3p and miR-128-3p levels are decreased where OPA1 levels are increased. In breast cancer cells, miR-148/152-3p family are epistatic to OPA1, as their levels increased upon OPA1 ablation to inhibit tumour growth and invasion (Zamberlan et al., 2022). These data support our findings wherein miR-148/152-3p and miR-128-3p displayed a causal miRNA-mRNA relationship with OPA1. The role of miR-148/152-3p family and miR-128-3p in muscle pathology is less clear, although studies have reported an increased abundance of OPA1-regulating miRNAs in various human muscle diseases (Chen et al., 2009; Kim et al., 2014) and miR-148a-3p and miR-152-3p in denervation-induced muscle atrophy (Soares et al., 2014). Similarly, we found miR-148a-3p and miR-152-3p levels elevated upon 14 days of sciatic nerve denervation, and this was accompanied with reductions in OPA1 mRNA levels. These results suggest that miR-148a-3p and miR-

152-3p that participate in the atrophy program may contribute to muscle wasting by driving OPA1 downregulation. Whether miR-148a-3p and miR-152-3p are increased in other atrophic stimuli such as fasting, dexamethasone treatment and sarcopenia is unclear and would be an insightful area for future work.

AntagomiRs are a class of chemically engineered oligonucleotides that base-pair with miRNA to inhibit its silencing action. Owing to their miniscule size and chemical modifications, antagomiRs are well-tolerated, evoking minimal toxicity and immune responses, and are relatively stable in mammalian tissue (Jonas & Izaurralde, 2015; Krützfeldt et al., 2005; Lennox & Behlke, 2011). In this regard, RNA-based therapy can be placed above DNA-based and protein-based therapy. AntagomiRs have been tested in clinical trials for various human diseases, but with no pharmaceutical breakthrough yet. The most promising candidate is Miravirsen (or SPC3649) that reached phase II trials for hepatitis (clinical trial code: NCT01200420). Currently, no miRNA-based therapy has been identified to combat muscle atrophy in pathological conditions. Here, inhibiting the action of miR-148a-3p and miR-152-3p in denervated mouse muscle via triweekly intramuscular antagomiR treatment increased OPA1 protein levels and attenuated the reduction of CSA of gastrocnemius muscle. This agrees and extends with our previous work where we found that mild genetic overexpression of OPA1 (~1.5x increase) protected mice from denervation-induced muscle loss (Varanita et al., 2015).

OXPHOS malfunction and ER stress are pathological mechanisms in mitochondrial diseases (Debattisti et al., 2014; Kaspar et al., 2021). Levels of miR-152-3p and miR-128-3p were increased in MAFs upon treatment of well-known compounds that induce mitochondrial dysfunction (actinonin, CCCP, oligomycin). Additionally, OPA1 mRNA levels were reduced, suggesting that miR-152-3p and miR-128-3p can contribute

towards OPA1 downregulation when mitochondria are dysfunctional. HEK293 cells harbouring a COX4-I deletion to cause OXPHOS dysfunction also had increased levels of miR-152-3p and miR-128-3p, suggesting this stress-induced miRNA pathway is conserved in mice and humans. Interestingly, TUDCA reduced miR-152-3p levels in OXPHOS-defective conditions. Thus, we speculate that the levels of miR-152-3p are under the control of ER stress pathways that are engaged upon mitochondrial dysfunction.

In a set of preliminary experiments, we wished to extend our antagomiRs therapy to a mitochondrial myopathy mouse model, a *COX15* muscle-specific knockout characterised by defects in mitochondrial ultrastructure and function that lead to detriments in muscle size and function (Civiletto et al., 2015; Viscomi et al., 2011). Notably, genetic overexpression of OPA1 in these COX15 KO mice was well tolerated and corrected cristae shape and RCS assembly to rescue mitochondrial and muscle function (Civiletto et al., 2015). We therefore delivered our antagomiR mix treatment intramuscularly to these mice and found that a single injection could decrease their respective miRNA and ultimately increase OPA1 mRNA levels. Thus, OPA1-specific antagomiRs may serve as a promising therapy for mitochondrial myopathies. We are now performing time course intramuscular antagomiR treatments to examine the effects on mitochondrial ultrastructure and function and muscle pathology.

It is worthwhile to mention the limitations and future directions of this study. Pinpointing the effect of a single miRNA is complicated as they target 100s of different transcripts (Bartel, 2018). It is conceivable that miR-148/152-3p family and miR-128-3p target other genes influencing mitochondrial ultrastructure and function and further experiments are required to address whether they specifically act via OPA1 regulation. Skin fibroblasts extracted from mice were used as a model to check the specificity of

miRNAs on targeting OPA1 in this study, yet the tissue of interest was skeletal muscle. Therefore, whether miRNAs specifically regulate OPA1-dependent functions in skeletal muscle mitochondria still needs to be clarified. This could be approached by muscle-specific genetic deletion of OPA1 in skeletal muscle, followed by miRNA/antagomiR delivery of miR-148/152-3p and miR-128-3p to observe any alterations in mitochondrial ultrastructure and function. Elucidating the regulators of these OPA1-specific miRNAs is needed. Based on TUDCA treatment experiments, we speculate that ER stress transcription factors play a role in regulating miR-152-3p. Indeed, ER stress markers such as Activating Transcription Factor 2 (ATF2) and X-box binding protein 1 (XBP1s) are predicted to target miR-148a-3p, and NF-κB predicted to regulate miR-128-3p (miRcode and Starbase prediction databases). Moreover, X-inactive specific transcript (XIST) and HOX transcript antisense RNA (HOTAIR) are two long non-coding RNAs (lncRNA) predicted to regulate miR-148/152-3p activity by acting as miRNA sponges. Exploiting luciferase-based sensors to observe interactions between transcription factors/lncRNA and miRNA warrants investigation.

To conclude, the results in this study nominate OPA1-regulating miRNAs as potential therapeutic targets for mitochondrial myopathies. Here, an antagomiR-based treatment was effective at increasing OPA1 expression and rescuing muscle atrophy. From a clinical perspective, obtaining miRNA expression profiles from muscle biopsies of myopathy patients would be valuable, as this allows personalised therapies targeting OPA1-regulating miRNAs.

Materials and methods

Cell lines and reagents

All cell lines were cultured in Dulbecco's Modified Eagle Medium (DMEM) with supplements [10% inactivated FBS (Sigma-Aldrich), 5% non-essential amino acids (Lonza), 1 mM sodium pyruvate (Sigma-Aldrich), 5% penicillin/streptomycin (Lonza), 5% uridine (Sigma-Aldrich)] and maintained at 37 °C and 5% CO_2. Compounds to induce mitochondrial dysfunction were: 5 µM CCCP (Sigma-Aldrich), 50 µM actinonin (Sigma-Aldrich), 1 µM rotenone (Sigma-Aldrich), 2 µM antimycin A (Sigma-Aldrich), 2.5 µM oligomycin (Sigma-Aldrich). 30 µM microRNA (miRNA) mimics (Thermo Fisher Scientific) and 30-50 µM antagomiR constructs (Creative Biogene) were transfected with Lipofectamine RNAimax reagent (Thermo Fisher Scientific).

Generation of mouse adult fibroblasts

This procedure was performed on diaphragm tissue of C57BL/6J male mouse. Tissue was sliced up and transferred to a 15 ml falcon containing 10 ml of pre-warmed filtered digestion buffer (1 mg/ml collagenase type II in DMEM with supplements (20% FBS, 1% non-essential AA's, 1% P/S). The solution was resuspended 10x and incubated for 8 minutes at 37 °C in a water bath. This procedure was repeated twice, and the supernatant was collected and incubated on ice. Fresh digestion buffer was added to the remaining tissue and the resuspension step was repeated as previously mentioned. Supernatants were pooled together, filtered through a cell strainer, and centrifuged at 600 g for 5 minutes. After this, the supernatant was added to a 6-well plate overnight. Each well was replaced with fresh media 24 hours later.

Genotyping

Nucleic acid from mouse fingers and tails was extracted following the manufacturers protocol for DNA extraction. The mice with the correct genotype were selected on the basis of PCR genotyping on tail DNA with the use of the following primers: primer for *Opa1* flx detection (F: 5'- CAG TGT TGA TGA CAG CTC AG - 3', R: 5' - CAT CAC ACA CTA GCT TAC ATT TGC - 3').

Dual-Luciferase reporter assay

The dual-luciferase reporter system (Promega Corp) in this study utilised the psiCHECK-2 reporter vector that expressed luciferase genes *Renilla* (driven by the SV40 promoter) and *Firefly* (driven by the HSV-TK promoter) which were exploited to determine two distinct bioluminescent signals. miRNA mimic inserts and OPA1 3'UTR fragments were inserted downstream of the Renilla gene. The psiCHECK-2 reporter vector contained inserts of a two-repeat complementary sequence to the seed region of miR-148a-3p, miR-148b-3p, miR-152-3p and miR-128-3p, and a ~500bp fragment of mouse and human OPA1 3'UTR where miR-148/152-3p family and miR-128-3p are predicted to bind to (see Fig. 1). Cells were seeded at 0.5 x 10^4 cells per well in a 96-well plate, and 24h after plating, transfection of the psiCHECK-2 Vector (0.1 µg) into cells was performed using Lipofectamine 3000 (Thermo Fisher Scientific) according to the manufacturer's protocol. The ratio of plasmid (in µg) to lipofectamine reagent (in µl) was 2:1. Cells were washed with PBS then lysed for 10 minutes at room temperature on a shaker using 30 µl passive lysis buffer 5x (Promega Corp.). Protein lysate was homogenised by manual pipetting. 10 µl protein lysate was added to each well in a white 96-well plate and incubated on ice. Reagents that stimulate the bioluminescent signal, LARII (Firefly substrate) and Stop & Glo (Renilla substrate)

(Promega Corp) were thawed on ice. LARII reagent was added to lysate and Firefly luminescence was measured, followed by immediate addition of Stop & Glo reagent for measuring Renilla luminescence. The ratio between LARII and Stop & Glo luminescence scores from samples were used for analysis.

RT-PCR for mRNA

Total RNA from cells was extracted using the TRIzol (Thermo Fisher Scientific) method according to the manufacturer's protocol. 1 µg RNA was reverse transcribed using M-MLV Reverse Transcriptase (Bio-Rad) according to the manufacturer's protocol. Diluted complementary DNA template (50 ng/µl) was used for quantitative RT-PCR reactions using SYBR Green PCR Master Mix reagents (Thermo Fisher Scientific) and performed using thermocycler in a 384-well plate. Results were analysed using the $2^{-\Delta Ct}$ method.

RT-PCR for microRNA

Total RNA from cells was extracted using TRIzol (Thermo Fisher Scientific) method according to the manufacturer's protocol. In a two-step process, RNA was reverse transcribed into complementary miRNA using miRNA-specific stem-loop primers (Thermo Fisher Scientific) for the miR-148/152-3p and miR-128-3p family and U6 was used as a housekeeping gene. Diluted miRNA template (10 ng/µl) was used for quantitative RT-PCR reactions using TaqMan chemistry (Thermo Fisher Scientific) and performed using a thermocycler in a 384-well plate. All data were normalised to U6 gene. Results were analysed using the $2^{-\Delta Ct}$ method.

Transmission electron microscopy

Cells were washed twice with PBS and fixed for 60 minutes at room temperature using glutaraldehyde at a final concentration of 2.5% (v/v) in PBS. Thin sections were imaged on a Tecnai-20 electron microscope (Philips-FEI). Mitochondrial area and cristae width were measured using image J software.

Immunoblotting

Cells were lysed in RIPA Buffer (10mM Tris pH8.8, 1mM EDTA, 0,5mM EGTA, 1%Triton 100X. 0,1% DOC, 140mM NaCl, 0,1% SDS) supplemented with 1:100 Complete Mini Protease Inhibitor Cocktail and incubated on ice for 20 minutes in 1.5 ml tubes. Samples were centrifuged at 18 000 g for five minutes at 4 °C. The supernatant was transferred to a new 1.5 ml tube and a Bicinchoninic acid (BCA) assay to calculate the protein concentration of each sample. Samples were mixed with LDS Sample Buffer 4X (NuPage, Invitrogen) and heated at 95 °C for five minutes for protein denaturation. SDS-PAGE was performed using 20 µg protein that was loaded into a 3-8% Tris-acetate gel (NuPage, Invitrogen) and run at 120 V for 90 minutes in Tris-Acetate-SDS Running Buffer (NuPage, Invitrogen). Proteins were transferred onto a PVDF membrane (Bio-Rad) using the wet-transfer method. Membrane blocking was performed using 5% (w/v) Dried Skimmed Milk in tris-buffered saline with tween 0.5% Tween20 (TBST) for 60 minutes at room temperature on a tube roller. Membranes were incubated with primary antibodies in 2.5% (w/v) Dried Skimmed Milk in TBST solution overnight in 4 °C. After primary antibody incubation, the membrane was washed (3 x 10 min) in 5 ml TBST and the isotype-matched horseradish peroxidase-conjugated secondary antibody (Abcam) was applied onto the membrane for 60 minutes at room temperature. The membrane was washed (3 x 5 min) in 5 ml

TBST, followed by enhanced chemiluminescence (ECL) substrate (Thermo Fisher Scientific) administration to detect protein bands by chemiluminescence using a western blot developing machine. Densitometric analysis was performed using ImageJ to quantify relative levels of protein bands. Individual bands of interest were isolated and detected by the software. Membrane background was corrected by using the 'rolling disk' function and the density of each band was calculated. Using raw volume values, each band for the protein of interest was normalised to the corresponding protein band of the loading control using spreadsheet software (Microsoft Excel).

Animal work

All procedures were conducted under the Italy animals and local ethical review. The mice were kept on a C57BL6/J background, and wild-type littermates were used as controls. The animals were maintained in a temperature and humidity-controlled animal care facility, with a 12-hour light/dark cycle and free access to water and food, and were sacrificed by cervical dislocation

Sciatic nerve denervation

Male 3–5-month-old C57BL/6 mice were randomly assigned to two conditions: scramble control and antagomiR experimental. Sham (non-denervated) leg of animals was used as the control. All mice were maintained under the same conditions. Mice were anaesthetised by isoflurane and the sciatic nerve was excised and removed, followed by stitching up of the wounded area. Gastrocnemius muscles of mice having

undergone denervation were snap frozen and collected at 7d, 10d, 12d, and 14d to be used for biochemical and morphological analysis.

AntagomiR injection

Mice were anaesthetised by isoflurane. AntagomiRs specific for miR-148a, miR-148b, miR-152 and miR-128 were resuspended in PBS at a concentration of 50 nM and mixed. Mice were injected triweekly with an antagomiR mix or scramble control of at three distinct local injections (3 x 20 µl) in the gastrocnemius muscle.

Morphological analysis

Gastrocnemius muscle tissue was cut at 10 µM thin slices using a cryostat (Leica) and stained with hematoxylin and eosin reagents (Sigma-Aldrich) following the manufacturers protocol for histochemical examination.

Statistical analysis

Data are represented as box blots and bar charts of at least three independent experiments with mean ± SEM displayed. Shapiro-Wilk test was performed to test for normal distribution in the data. Paired t-test and one-way analysis of variance (ANOVA) were performed to determine whether data was statistically significant between groups with the alpha value set at $p = 0.05$. Statistical significance represented in figures by "*", where $*p \leq 0.05$; $**p \leq 0.01$; $***p \leq 0.005$.

Table 1. Media components for cell culture

Component	**Manufacturer**	**Vol (ml)**	**Concentration**
DMEM	Lonza	500	-
Foetal Bovine Serum	Sigma-Aldrich	50	10%
Penicillin/Streptomycin	Lonza	5	Penicillin: 100 IU/ml Streptomycin: 100 µg/ml
MEM Non-Essential Amino Acids	Lonza	5	0.1 mM
Sodium Pyruvate	Sigma-Aldrich	5	1 mM
Uridine	Sigma-Aldrich	0.6	5%

Table 2. Reagents and kits

Reagent	**Manufacturer**	**Code**
Anti-OPA1 mouse	BD Biosciences (1:2000)	612607
Anti-TOM40 rabbit	Santa Cruz Biotechnology (1:1000)	ab185543
Anti-Vinculin mouse	Abcam (1:10 000)	ab219649
Goat Anti-Mouse IgG	Abcam (1:2000)	ab205719
Goat Anti-Rabbit IgG	Abcam (1:2000)	ab205718
CCCP	Sigma-Aldrich	C2759
Actinonin	Sigma-Aldrich	A6671
Rotenone	Sigma-Aldrich	R8875
Antimycin	Sigma-Aldrich	A8674
Oligomycin	Sigma-Aldrich	75351
TUDCA	Millipore	580549
mirVana miRNA mimic	Thermo Fisher Scientific	4464066
microDOWN AntagomiR	Creative Biogene	CBGAB0584-4
Dual-Luciferase® Reporter Assay	Promega	E1910
iScript cDNA Kit	Bio-Rad	1708890
SYBR™ Green PCR Master Mix	Thermo Fisher Scientific	A25741
TaqMan™ Universal PCR Master Mix	Thermo Fisher Scientific	4304437
Pierce protein BCA assay	Thermo Fisher Scientific	23227

Table 3. Real-time PCR primers

Gene	**Sequence**
Opa1	FWD: AGCCTCGCAGGAATTTTTGG REV: AGCCGATCCTAGTATGAGATAGC
Ribosomal 18s	FWD: AACTTAAAGRAATTGACGGA REV: TCCGTCAATTYCTTTAAGTT
Ribosomal Protein L7	FWD: GCAGATGTACCGCACTGAGATTC REV: ACCTTTGGGCTTACTCCATTGATA
GAPDH	FWD: CGACTTCAACAGCGACACTCAC REV: CCCTGTTGCTGTAGCCAAATTC

References

Abu-Libdeh, B., Douiev, L., Amro, S., Shahrour, M., Ta-Shma, A., Miller, C., Elpeleg, O., & Saada, A. (2017). Mutation in the COX4I1 gene is associated with short stature, poor weight gain and increased chromosomal breaks, simulating Fanconi anemia. *European Journal of Human Genetics : EJHG*, *25*(10), 1142–11146. https://doi.org/10.1038/EJHG.2017.112

Amati-Bonneau, P., Milea, D., Bonneau, D., Chevrollier, A., Ferré, M., Guillet, V., Gueguen, N., Loiseau, D., Crescenzo, M. A. P. de, Verny, C., Procaccio, V., Lenaers, G., & Reynier, P. (2009). OPA1-associated disorders: phenotypes and pathophysiology. *The International Journal of Biochemistry & Cell Biology*, *41*(10), 1855–1865. https://doi.org/10.1016/J.BIOCEL.2009.04.012

Antonicka, H., Mattman, A., Carlson, C. G., Glerum, D. M., Hoffbuhr, K. C., Leary, S. C., Kennaway, N. G., & Shoubridge, E. A. (2003). Mutations in COX15 produce a defect in the mitochondrial heme biosynthetic pathway, causing early-onset fatal hypertrophic cardiomyopathy. *American Journal of Human Genetics*, *72*(1), 101–114. https://doi.org/10.1086/345489

Baek, D., Villén, J., Shin, C., Camargo, F. D., Gygi, S. P., & Bartel, D. P. (2008). The impact of microRNAs on protein output. *Nature*. https://doi.org/10.1038/nature07242

Ban, T., Ishihara, T., Kohno, H., Saita, S., Ichimura, A., Maenaka, K., Oka, T., Mihara, K., & Ishihara, N. (2017). Molecular basis of selective mitochondrial fusion by heterotypic action between OPA1 and cardiolipin. *Nature Cell Biology*, *19*(7). https://doi.org/10.1038/ncb3560

Barbot, M., Jans, D. C., Schulz, C., Denkert, N., Kroppen, B., Hoppert, M., Jakobs, S., & Meinecke, M. (2015). Mic10 oligomerizes to bend mitochondrial inner membranes at cristae junctions. *Cell Metabolism*, *21*(5), 756–763. https://doi.org/10.1016/J.CMET.2015.04.006

Bartel, D. P. (2009). MicroRNAs: Target Recognition and Regulatory Functions. In *Cell* (Vol. 136, Issue 2, pp. 215–233). https://doi.org/10.1016/j.cell.2009.01.002

Bartel, D. P. (2018). Metazoan MicroRNAs. In *Cell* (Vol. 173, Issue 1, pp. 20–51). Cell Press. https://doi.org/10.1016/j.cell.2018.03.006

Belenguer, P., & Pellegrini, L. (2013). The dynamin GTPase OPA1: More than mitochondria? In *Biochimica et Biophysica Acta - Molecular Cell Research* (Vol. 1833, Issue 1, pp. 176–183). https://doi.org/10.1016/j.bbamcr.2012.08.004

Benard, G., Bellance, N., Jose, C., & Rossignol, R. (2011). Relationships Between Mitochondrial Dynamics and Bioenergetics. *Mitochondrial Dynamics and Neurodegeneration*, 47–68. https://doi.org/10.1007/978-94-007-1291-1_2

Blum, T. B., Hahn, A., Meier, T., Davies, K. M., & Kühlbrandt, W. (2019). Dimers of mitochondrial ATP synthase induce membrane curvature and self-assemble into rows. *Proceedings of the National Academy of Sciences of the United States of America*. https://doi.org/10.1073/pnas.1816556116

Bon, C., Luffarelli, R., Russo, R., Fortuni, S., Pierattini, B., Santulli, C., Fimiani, C., Persichetti, F., Cotella, D., Mallamaci, A., Santoro, C., Carninci, P., Espinoza, S., Testi, R., Zucchelli, S., Condò, I., & Gustincich, S. (2019). SINEUP non-coding RNAs rescue defective frataxin expression and activity in a cellular model of Friedreich's Ataxia. *Nucleic Acids Research*, *47*(20), 10728–10743. https://doi.org/10.1093/NAR/GKZ798

Bonaldo, P., & Sandri, M. (2013). Cellular and molecular mechanisms of muscle atrophy. *Disease Models & Mechanisms*, *6*(1), 25–39. https://doi.org/10.1242/dmm.010389

Camara, A. K. S., Zhou, Y. F., Wen, P. C., Tajkhorshid, E., & Kwok, W. M. (2017). Mitochondrial VDAC1: A key gatekeeper as potential therapeutic target. *Frontiers in Physiology*, *8*(JUN), 460. https://doi.org/10.3389/FPHYS.2017.00460/BIBTEX

Carrieri, C., Cimatti, L., Biagioli, M., Beugnet, A., Zucchelli, S., Fedele, S., Pesce, E., Ferrer, I., Collavin, L., Santoro, C., Forrest, A. R. R., Carninci, P., Biffo, S., Stupka, E., & Gustincich, S. (2012). Long non-coding antisense RNA controls Uchl1 translation through an embedded SINEB2 repeat. *Nature 2012 491:7424*, *491*(7424), 454–457. https://doi.org/10.1038/nature11508

Cereghetti, G. M., Stangherlin, A., Martins De Brito, O., Chang, C. R., Blackstone, C., Bernardi, P., & Scorrano, L. (2008). Dephosphorylation by calcineurin regulates translocation of Drp1 to mitochondria. *Proceedings of the National Academy of Sciences of the United States of America*, *105*(41), 15803–15808. https://doi.org/10.1073/PNAS.0808249105

Chandhok, G., Lazarou, M., & Neumann, B. (2018). Structure, function, and regulation of mitofusin-2 in health and disease. *Biological Reviews*, *93*(2), 933–949. https://doi.org/10.1111/brv.12378

Chao de la Barca, J. M., Prunier-Mirebeau, D., Amati-Bonneau, P., Ferré, M., Sarzi, E., Bris, C., Leruez, S., Chevrollier, A., Desquiret-Dumas, V., Gueguen, N., Verny, C., Hamel, C., Miléa, D., Procaccio, V., Bonneau, D., Lenaers, G., & Reynier, P. (2016). OPA1-related disorders: Diversity of clinical expression, modes of inheritance and pathophysiology. *Neurobiology of Disease*, *90*, 20–26. https://doi.org/10.1016/j.nbd.2015.08.015

Chen, H., Detmer, S. A., Ewald, A. J., Griffin, E. E., Fraser, S. E., & Chan, D. C. (2003a). Mitofusins Mfn1 and Mfn2 coordinately regulate mitochondrial fusion and are essential for embryonic development. *The Journal of Cell Biology*, *160*(2), 189. https://doi.org/10.1083/JCB.200211046

Chen, H., Detmer, S. A., Ewald, A. J., Griffin, E. E., Fraser, S. E., & Chan, D. C. (2003b). Mitofusins Mfn1 and Mfn2 coordinately regulate mitochondrial fusion and are essential for embryonic development. *Journal of Cell Biology*, *160*(2), 189–200. https://doi.org/10.1083/JCB.200211046/VIDEO-3

Chen, J. F., Callis, T. E., & Wang, D. Z. (2009). microRNAs and muscle disorders. *Journal of Cell Science*. https://doi.org/10.1242/jcs.041723

Chen, Y., Song, Y.-X., & Wang, Z.-N. (2013). The MicroRNA-148/152 Family: Multi-faceted Players. *Molecular Cancer*, *12*(1), 43. https://doi.org/10.1186/1476-4598-12-43

Cipolat, S., Martins De Brito, O., Zilio, B. D., & Scorrano, L. (2004). *OPA1 requires mitofusin 1 to promote mitochondrial fusion*. www.pnas.orgcgidoi10.1073pnas.0407043101

Cipolat, S., Rudka, T., Hartmann, D., Costa, V., Serneels, L., Craessaerts, K., Metzger, K., Frezza, C., Annaert, W., D'Adamio, L., Derks, C., Dejaegere, T., Pellegrini, L., D'Hooge, R., Scorrano, L., & de Strooper, B. (2006). Mitochondrial rhomboid PARL regulates cytochrome c release during apoptosis via OPA1-dependent cristae remodeling. *Cell*, *126*(1), 163–175. https://doi.org/10.1016/j.cell.2006.06.021

Civiletto, G., Varanita, T., Cerutti, R., Gorletta, T., Barbaro, S., Marchet, S., Lamperti, C., Viscomi, C., Scorrano, L., & Zeviani, M. (2015). Opa1 overexpression ameliorates the phenotype of two mitochondrial disease mouse models. *Cell Metabolism*, *21*(6), 845–854. https://doi.org/10.1016/j.cmet.2015.04.016

Cogliati, S., Enriquez, J. A., & Scorrano, L. (2016). Mitochondrial Cristae: Where Beauty Meets Functionality. In *Trends in Biochemical Sciences* (Vol. 41, Issue 3, pp. 261–273). Elsevier Ltd. https://doi.org/10.1016/j.tibs.2016.01.001

Cogliati, S., Frezza, C., Soriano, M. E., Varanita, T., Quintana-Cabrera, R., Corrado, M., Cipolat, S., Costa, V., Casarin, A., Gomes, L. C., Perales-Clemente, E., Salviati, L., Fernandez-Silva, P., Enriquez, J. A., & Scorrano, L. (2013). Mitochondrial cristae shape determines respiratory chain supercomplexes assembly and respiratory efficiency. *Cell*, *155*(1), 160–171. https://doi.org/10.1016/j.cell.2013.08.032

Costa, V., Giacomello, M., Hudec, R., Lopreiato, R., Ermak, G., Lim, D., Malorni, W., Davies, K. J. A., Carafoli, E., & Scorrano, L. (2010). Mitochondrial fission and cristae disruption increase the response of cell models of Huntington's disease to

apoptotic stimuli. *EMBO Molecular Medicine*, *2*(12), 490–503. https://doi.org/10.1002/EMMM.201000102

Davies, K. M., Strauss, M., Daum, B., Kief, J. H., Osiewacz, H. D., Rycovska, A., Zickermann, V., & Kühlbrandt, W. (2011). Macromolecular organization of ATP synthase and complex I in whole mitochondria. *Proceedings of the National Academy of Sciences of the United States of America*. https://doi.org/10.1073/pnas.1103621108

de Brito, O. M., & Scorrano, L. (2008). Mitofusin 2 tethers endoplasmic reticulum to mitochondria. *Nature 2008 456:7222*, *456*(7222), 605–610. https://doi.org/10.1038/nature07534

Debattisti, V., Pendin, D., Ziviani, E., Daga, A., & Scorrano, L. (2014). Reduction of endoplasmic reticulum stress attenuates the defects caused by Drosophila mitofusin depletion. *Journal of Cell Biology*, *204*(3), 303–312. https://doi.org/10.1083/JCB.201306121

del Dotto, V., Fogazza, M., Carelli, V., Rugolo, M., & Zanna, C. (2018). Eight human OPA1 isoforms, long and short: What are they for? In *Biochimica et Biophysica Acta - Bioenergetics* (Vol. 1859, Issue 4, pp. 263–269). Elsevier B.V. https://doi.org/10.1016/j.bbabio.2018.01.005

East African Scholars Journal of Medical Sciences Abbreviated Key Title: East African Scholars J Med Sci. (n.d.). https://doi.org/10.36349/EASJMS.2019.v02i09.016

Filadi, R., Pendin, Di., & Pizzo, P. (2018). Mitofusin 2: From functions to disease. In *Cell Death and Disease* (Vol. 9, Issue 3, pp. 1–13). Nature Publishing Group. https://doi.org/10.1038/s41419-017-0023-6

Fonseca, T. B., Sánchez-Guerrero, Á., Milosevic, I., & Raimundo, N. (2019). Mitochondrial fission requires DRP1 but not dynamins. *Nature 2019 570:7761*, *570*(7761), E34–E42. https://doi.org/10.1038/s41586-019-1296-y

Frezza, C., Cipolat, S., Martins de Brito, O., Micaroni, M., Beznoussenko, G. v., Rudka, T., Bartoli, D., Polishuck, R. S., Danial, N. N., de Strooper, B., & Scorrano, L. (2006). OPA1 Controls Apoptotic Cristae Remodeling Independently from Mitochondrial Fusion. *Cell*, *126*(1), 177–189. https://doi.org/10.1016/j.cell.2006.06.025

Friedman, J. R., Lackner, L. L., West, M., DiBenedetto, J. R., Nunnari, J., & Voeltz, G. K. (2011). ER tubules mark sites of mitochondrial division. *Science (New York, N.Y.)*, *334*(6054), 358–362. https://doi.org/10.1126/SCIENCE.1207385

Galnares-Olalde, J. A., López-Hernández, J. C., Benitez-Alonso, E. O., de Montellano, D. J. D. O., May-Mas, R. N., Briseño-Godínez, M. E., Pérez-Valdez, E. Y., Pérez-Jovel, E., Fernández-Valverde, F., León-Manríquez, E., & Vargas-Cañas, E. S. (2021). Mitochondrial Encephalomyopathy, Lactic Acidosis, and Stroke-like Episodes (MELAS) Syndrome: Frequency, Clinical Features, Imaging,

Histopathologic, and Molecular Genetic Findings in a Third-level Health Care Center in Mexico. *The Neurologist*, *26*(4), 143–148. https://doi.org/10.1097/NRL.0000000000000331

Ge, Y., Shi, X., Boopathy, S., McDonald, J., Smith, A. W., & Chao, L. H. (2020). Two forms of opa1 cooperate to complete fusion of the mitochondrial inner-membrane. *ELife*, *9*. https://doi.org/10.7554/ELIFE.50973

Ghezzi, D., & Zeviani, M. (2018). Human diseases associated with defects in assembly of OXPHOS complexes. In *Essays in Biochemistry* (Vol. 62, Issue 3, pp. 271–286). Portland Press Ltd. https://doi.org/10.1042/EBC20170099

Giacomello, M., Pyakurel, A., Glytsou, C., & Scorrano, L. (2020). The cell biology of mitochondrial membrane dynamics. *Nature Reviews Molecular Cell Biology 2020 21:4*, *21*(4), 204–224. https://doi.org/10.1038/s41580-020-0210-7

Glytsou, C., Calvo, E., Cogliati, S., Mehrotra, A., Anastasia, I., Rigoni, G., Raimondi, A., Shintani, N., Loureiro, M., Vazquez, J., Pellegrini, L., Enriquez, J. A., Scorrano, L., & Soriano, M. E. (2016). Optic Atrophy 1 Is Epistatic to the Core MICOS Component MIC60 in Mitochondrial Cristae Shape Control. *Cell Reports*, *17*(11), 3024–3034. https://doi.org/10.1016/j.celrep.2016.11.049

Gomes, L. C., Benedetto, G. di, & Scorrano, L. (2011). During autophagy mitochondria elongate, are spared from degradation and sustain cell viability. *Nature Cell Biology*, *13*(5), 589–598. https://doi.org/10.1038/ncb2220

Gorman, G. S., Chinnery, P. F., DiMauro, S., Hirano, M., Koga, Y., McFarland, R., Suomalainen, A., Thorburn, D. R., Zeviani, M., & Turnbull, D. M. (2016). Mitochondrial diseases. *Nature Reviews Disease Primers*, *2*(1), 16080. https://doi.org/10.1038/nrdp.2016.80

Greaves, L. C., Reeve, A. K., Taylor, R. W., & Turnbull, D. M. (2012). Mitochondrial DNA and disease. *The Journal of Pathology*, *226*(2), 274–286. https://doi.org/10.1002/PATH.3028

Ha, M., & Kim, V. N. (2014). Regulation of microRNA biogenesis. In *Nature Reviews Molecular Cell Biology* (Vol. 15, Issue 8, pp. 509–524). Nature Publishing Group. https://doi.org/10.1038/nrm3838

Hackenbrock, C. R. (1966). Ultrastructural bases for metabolically linked mechanical activity in mitochondria. I. Reversible ultrastructural changes with change in metabolic steady state in isolated liver mitochondria. *The Journal of Cell Biology*, *30*(2), 269–297. https://doi.org/10.1083/jcb.30.2.269

Ishihara, N., Eura, Y., & Mihara, K. (2004). Mitofusin 1 and 2 play distinct roles in mitochondrial fusion reactions via GTPase activity. *Journal of Cell Science*, *117*(26), 6535–6546. https://doi.org/10.1242/JCS.01565

Ishihara, N., Fujita, Y., Oka, T., & Mihara, K. (2006). Regulation of mitochondrial morphology through proteolytic cleavage of OPA1. *The EMBO Journal*, *25*(13), 2966. https://doi.org/10.1038/SJ.EMBOJ.7601184

Ivanova, H., Kerkhofs, M., Rovere, R. M. L., & Bultynck, G. (2017). Endoplasmic Reticulum–Mitochondrial Ca2+ Fluxes Underlying Cancer Cell Survival. *Frontiers in Oncology*, *7*(MAY), 1. https://doi.org/10.3389/FONC.2017.00070

Jonas, S., & Izaurralde, E. (2015). Towards a molecular understanding of microRNA-mediated gene silencing. In *Nature Reviews Genetics* (Vol. 16, Issue 7, pp. 421–433). Nature Publishing Group. https://doi.org/10.1038/nrg3965

Kalia, R., Wang, R. Y. R., Yusuf, A., Thomas, P. v., Agard, D. A., Shaw, J. M., & Frost, A. (2018). Structural basis of mitochondrial receptor binding and constriction by DRP1. *Nature 2018 558:7710*, *558*(7710), 401–405. https://doi.org/10.1038/s41586-018-0211-2

Kaspar, S., Oertlin, C., Szczepanowska, K., Kukat, A., Senft, K., Lucas, C., Brodesser, S., Hatzoglou, M., Larsson, O., Topisirovic, I., & Trifunovic, A. (2021). Adaptation to mitochondrial stress requires CHOP-directed tuning of ISR. *Sci. Adv*, *7*, 971–997. https://www.science.org

Kijima, K., Numakura, C., Izumino, H., Umetsu, K., Nezu, A., Shiiki, T., Ogawa, M., Ishizaki, Y., Kitamura, T., Shozawa, Y., & Hayasaka, K. (2005). Mitochondrial GTPase mitofusin 2 mutation in Charcot-Marie-Tooth neuropathy type 2A. *Human Genetics*, *116*(1–2), 23–27. https://doi.org/10.1007/S00439-004-1199-2

Kim, J. Y., Park, Y. K., Lee, K. P., Lee, S. M., Kang, T. W., Kim, H. J., Dho, S. H., Kim, S. Y., & Kwon, K. S. (2014). Genome-wide profiling of the microRNA-mRNA regulatory network in skeletal muscle with aging. *Aging*. https://doi.org/10.18632/aging.100677

Kondadi, A. K., Anand, R., Hänsch, S., Urbach, J., Zobel, T., Wolf, D. M., Segawa, M., Liesa, M., Shirihai, O. S., Weidtkamp-Peters, S., & Reichert, A. S. (2020). Cristae undergo continuous cycles of membrane remodelling in a MICOS-dependent manner. *EMBO Reports*, *21*(3), e49776. https://doi.org/10.15252/EMBR.201949776

Korobova, F., Ramabhadran, V., & Higgs, H. N. (2013). An Actin-Dependent Step in Mitochondrial Fission Mediated by the ER-Associated Formin INF2. *Science (New York, N.Y.)*, *339*(6118), 464–467. https://doi.org/10.1126/SCIENCE.1228360

Krützfeldt, J., Rajewsky, N., Braich, R., Rajeev, K. G., Tuschl, T., Manoharan, M., & Stoffel, M. (2005). Silencing of microRNAs in vivo with “antagomirs.” *Nature*, *438*(7068), 685–689. https://doi.org/10.1038/NATURE04303

L Margulis. (1971). Symbiotic theory of the origin of eukaryotic organelles; criteria for proof. *Sci Am*, *225*((2)), 48–57.

Lagos-Quintana, M., Rauhut, R., Yalcin, A., Meyer, J., Lendeckel, W., & Tuschl, T. (2002). Identification of tissue-specific MicroRNAs from mouse. *Current Biology*, *12*(9), 735–739. https://doi.org/10.1016/S0960-9822(02)00809-6

Lee, R. C., Feinbaum, R. L., & Ambros, V. (1993). The C. elegans heterochronic gene lin-4 encodes small RNAs with antisense complementarity to lin-14. *Cell*, *75*(5), 843–854. https://doi.org/10.1016/0092-8674(93)90529-Y

Lee, Y., Ahn, C., Han, J., Choi, H., Kim, J., Yim, J., Lee, J., Provost, P., Rådmark, O., Kim, S., & Kim, V. N. (2003). The nuclear RNase III Drosha initiates microRNA processing. *Nature*, *425*(6956), 415–419. https://doi.org/10.1038/nature01957

Lennox, K. A., & Behlke, M. A. (2011). Chemical modification and design of anti-miRNA oligonucleotides. In *Gene Therapy*. https://doi.org/10.1038/gt.2011.100

Li, Z., & Rana, T. M. (2014). Therapeutic targeting of microRNAs: current status and future challenges. *Nature Reviews Drug Discovery 2014 13:8*, *13*(8), 622–638. https://doi.org/10.1038/nrd4359

Liu, X., Li, J., Qin, F., & Dai, S. (2016). MiR-152 as a tumor suppressor microRNA: Target recognition and regulation in cancer. In *Oncology Letters* (Vol. 11, Issue 6, pp. 3911–3916). Spandidos Publications. https://doi.org/10.3892/ol.2016.4509

Lynch, D. S., Loh, S. H. Y., Harley, J., Noyce, A. J., Martins, L. M., Wood, N. W., Houlden, H., & Plun-Favreau, H. (2017). Nonsyndromic Parkinson disease in a family with autosomal dominant optic atrophy due to OPA1 mutations. *Neurology: Genetics*, *3*(5). https://doi.org/10.1212/NXG.0000000000000188

MacVicar, T., & Langer, T. (2016). OPA1 processing in cell death and disease - the long and short of it. In *Journal of Cell Science* (Vol. 129, Issue 12, pp. 2297–2306). Company of Biologists Ltd. https://doi.org/10.1242/jcs.159186

Manor, U., Bartholomew, S., Golani, G., Christenson, E., Kozlov, M., Higgs, H., Spudich, J., & Lippincott-Schwartz, J. (2015). A mitochondria-anchored isoform of the actin-nucleating spire protein regulates mitochondrial division. *ELife*, *4*(AUGUST2015). https://doi.org/10.7554/ELIFE.08828

Maurel, M., & Chevet, E. (2013). Endoplasmic reticulum stress signaling: the microRNA connection. *American Journal of Physiology. Cell Physiology*, *304*(12). https://doi.org/10.1152/AJPCELL.00061.2013

Mishra, P., Carelli, V., Manfredi, G., & Chan, D. C. (2014). Proteolytic cleavage of Opa1 stimulates mitochondrial inner membrane fusion and couples fusion to oxidative phosphorylation. *Cell Metabolism*. https://doi.org/10.1016/j.cmet.2014.03.011

Nagashima, S., Tábara, L. C., Tilokani, L., Paupe, V., Anand, H., Pogson, J. H., Zunino, R., McBride, H. M., & Prudent, J. (2020). Golgi-derived PI(4)P-containing vesicles drive late steps of mitochondrial division. *Science*, *367*(6484), 1366–

1371. https://doi.org/10.1126/SCIENCE.AAX6089/SUPPL_FILE/AAX6089_S9.MOV

Olichon, A., Baricault, L., Gas, N., Guillou, E., Valette, A., Belenguer, P., & Lenaers, G. (2003). Loss of OPA1 perturbates the mitochondrial inner membrane structure and integrity, leading to cytochrome c release and apoptosis. *The Journal of Biological Chemistry*, *278*(10), 7743–7746. https://doi.org/10.1074/JBC.C200677200

Osellame, L. D., Blacker, T. S., & Duchen, M. R. (2012). Cellular and molecular mechanisms of mitochondrial function. *Best Practice & Research. Clinical Endocrinology & Metabolism*, *26*(6), 711. https://doi.org/10.1016/J.BEEM.2012.05.003

Otera, H., Wang, C., Cleland, M. M., Setoguchi, K., Yokota, S., Youle, R. J., & Mihara, K. (2010). Mff is an essential factor for mitochondrial recruitment of Drp1 during mitochondrial fission in mammalian cells. *The Journal of Cell Biology*, *191*(6), 1141. https://doi.org/10.1083/JCB.201007152

Pernas, L., & Scorrano, L. (2016). Mito-Morphosis: Mitochondrial Fusion, Fission, and Cristae Remodeling as Key Mediators of Cellular Function. *Annual Review of Physiology*, *78*(1), 505–531. https://doi.org/10.1146/annurev-physiol-021115-105011

Quéméner-Redon, S., Bénech, C., Audebert-Bellanger, S., Friocourt, G., Planes, M., Parent, P., & Férec, C. (2013). A small de novo 16q24.1 duplication in a woman with severe clinical features. *European Journal of Medical Genetics*, *56*(4), 211–215. https://doi.org/10.1016/J.EJMG.2013.01.001

Quintana-Cabrera, R., Quirin, C., Glytsou, C., Corrado, M., Urbani, A., Pellattiero, A., Calvo, E., Vázquez, J., Enríquez, J. A., Gerle, C., Soriano, M. E., Bernardi, P., & Scorrano, L. (2018). The cristae modulator Optic atrophy 1 requires mitochondrial ATP synthase oligomers to safeguard mitochondrial function. *Nature Communications*, *9*(1). https://doi.org/10.1038/s41467-018-05655-x

Rampelt, H., Bohnert, M., Zerbes, R. M., Horvath, S. E., Warscheid, B., Pfanner, N., & van der Laan, M. (2017). Mic10, a Core Subunit of the Mitochondrial Contact Site and Cristae Organizing System, Interacts with the Dimeric F1Fo-ATP Synthase. *Journal of Molecular Biology*, *429*(8), 1162–1170. https://doi.org/10.1016/J.JMB.2017.03.006

Richter, U., Lahtinen, T., Marttinen, P., Myöhänen, M., Greco, D., Cannino, G., Jacobs, H. T., Lietzén, N., Nyman, T. A., & Battersby, B. J. (2013). A Mitochondrial Ribosomal and RNA Decay Pathway Blocks Cell Proliferation. *Current Biology*, *23*(6), 535–541. https://doi.org/10.1016/J.CUB.2013.02.019

Richter, U., Lahtinen, T., Marttinen, P., Suomi, F., & Battersby, B. J. (2015). Quality control of mitochondrial protein synthesis is required for membrane integrity and

cell fitness. *Journal of Cell Biology*, *211*(2), 373–389. https://doi.org/10.1083/jcb.201504062

Schubert, M. B., & Vilarinho, L. (2020). Molecular basis of Leigh syndrome: a current look. *Orphanet Journal of Rare Diseases 2020 15:1*, *15*(1), 1–14. https://doi.org/10.1186/S13023-020-1297-9

Selbach, M., Schwanhäusser, B., Thierfelder, N., Fang, Z., Khanin, R., & Rajewsky, N. (2008). Widespread changes in protein synthesis induced by microRNAs. *Nature*. https://doi.org/10.1038/nature07228

Shen, Q., Yamano, K., Head, B. P., Kawajiri, S., Cheung, J. T. M., Wang, C., Cho, J. H., Hattori, N., Youle, R. J., & van der Bliek, A. M. (2014). Mutations in Fis1 disrupt orderly disposal of defective mitochondria. *Molecular Biology of the Cell*, *25*(1), 145. https://doi.org/10.1091/MBC.E13-09-0525

Signes, A., & Fernandez-Vizarra, E. (2018). Assembly of mammalian oxidative phosphorylation complexes I–V and supercomplexes. In *Essays in Biochemistry* (Vol. 62, Issue 3, pp. 255–270). Portland Press Ltd. https://doi.org/10.1042/EBC20170098

Soares, R. J., Cagnin, S., Chemello, F., Silvestrin, M., Musaro, A., de Pitta, C., Lanfranchi, G., & Sandri, M. (2014). Involvement of MicroRNAs in the regulation of muscle wasting during catabolic conditions. *Journal of Biological Chemistry*, *289*(32), 21909–21925. https://doi.org/10.1074/jbc.M114.561845

Spiegel, R., Saada, A., Flannery, P. J., Burté, F., Soiferman, D., Khayat, M., Eisner, V., Vladovski, E., Taylor, R. W., Bindoff, L. A., Shaag, A., Mandel, H., Schuler-Furman, O., Shalev, S. A., Elpeleg, O., & Yu-Wai-Man, P. (2016). Short report: Fatal infantile mitochondrial encephalomyopathy, hypertrophic cardiomyopathy and optic atrophy associated with a homozygous OPA1 mutation. *Journal of Medical Genetics*, *53*(2), 127. https://doi.org/10.1136/JMEDGENET-2015-103361

Strauss, M., Hofhaus, G., Schröder, R. R., & Kühlbrandt, W. (2008). Dimer ribbons of ATP synthase shape the inner mitochondrial membrane. *EMBO Journal*. https://doi.org/10.1038/emboj.2008.35

Suomalainen, A., & Battersby, B. J. (2018). Mitochondrial diseases: The contribution of organelle stress responses to pathology. In *Nature Reviews Molecular Cell Biology* (Vol. 19, Issue 2, pp. 77–92). Nature Publishing Group. https://doi.org/10.1038/nrm.2017.66

Taguchi, N., Ishihara, N., Jofuku, A., Oka, T., & Mihara, K. (2007). Mitotic phosphorylation of dynamin-related GTPase Drp1 participates in mitochondrial fission. *The Journal of Biological Chemistry*, *282*(15), 11521–11529. https://doi.org/10.1074/JBC.M607279200

Tezze, C., Romanello, V., Desbats, M. A., Fadini, G. P., Albiero, M., Favaro, G., Ciciliot, S., Soriano, M. E., Morbidoni, V., Cerqua, C., Loefler, S., Kern, H., Franceschi, C., Salvioli, S., Conte, M., Blaauw, B., Zampieri, S., Salviati, L., Scorrano, L., & Sandri, M. (2017). Age-Associated Loss of OPA1 in Muscle Impacts Muscle Mass, Metabolic Homeostasis, Systemic Inflammation, and Epithelial Senescence. *Cell Metabolism*, *25*(6), 1374-1389.e6. https://doi.org/10.1016/j.cmet.2017.04.021

Tilokani, L., Nagashima, S., Paupe, V., & Prudent, J. (2018). Mitochondrial dynamics: Overview of molecular mechanisms. In *Essays in Biochemistry* (Vol. 62, Issue 3, pp. 341–360). Portland Press Ltd. https://doi.org/10.1042/EBC20170104

Valentini, P., Pierattini, B., Zacco, E., Mangoni, D., Espinoza, S., Webster, N. A., Andrews, B., Carninci, P., Tartaglia, G. G., Pandolfini, L., & Gustincich, S. (2022). Towards SINEUP-based therapeutics: Design of an in vitro synthesized SINEUP RNA. *Molecular Therapy. Nucleic Acids*, *27*, 1092. https://doi.org/10.1016/J.OMTN.2022.01.021

van der Laan, M., Horvath, S. E., & Pfanner, N. (2016). Mitochondrial contact site and cristae organizing system. In *Current Opinion in Cell Biology* (Vol. 41, pp. 33–42). Elsevier Ltd. https://doi.org/10.1016/j.ceb.2016.03.013

Varanita, T., Soriano, M. E., Romanello, V., Zaglia, T., Quintana-Cabrera, R., Semenzato, M., Menabò, R., Costa, V., Civiletto, G., Pesce, P., Viscomi, C., Zeviani, M., di Lisa, F., Mongillo, M., Sandri, M., & Scorrano, L. (2015). The Opa1-dependent mitochondrial cristae remodeling pathway controls atrophic, apoptotic, and ischemic tissue damage. *Cell Metabolism*, *21*(6), 834–844. https://doi.org/10.1016/j.cmet.2015.05.007

Vincent, A. E., Ng, Y. S., White, K., Davey, T., Mannella, C., Falkous, G., Feeney, C., Schaefer, A. M., McFarland, R., Gorman, G. S., Taylor, R. W., Turnbull, D. M., & Picard, M. (2016). The Spectrum of Mitochondrial Ultrastructural Defects in Mitochondrial Myopathy. *Scientific Reports*. https://doi.org/10.1038/srep30610

Viscomi, C., Bottani, E., Civiletto, G., Cerutti, R., Moggio, M., Fagiolari, G., Schon, E. A., Lamperti, C., & Zeviani, M. (2011). In vivo correction of COX deficiency by activation of the AMPK/PGC-1α axis. *Cell Metabolism*, *14*(1), 80–90. https://doi.org/10.1016/j.cmet.2011.04.011

Wolf, D. M., Segawa, M., Kondadi, A. K., Anand, R., Bailey, S. T., Reichert, A. S., Bliek, A. M. van der, Shackelford, D. B., Liesa, M., & Shirihai, O. S. (2019). Individual cristae within the same mitochondrion display different membrane potentials and are functionally independent. *The EMBO Journal*, *38*(22). https://doi.org/10.15252/EMBJ.2018101056

Wong, Y. C., Ysselstein, D., & Krainc, D. (2018). Mitochondria–lysosome contacts regulate mitochondrial fission via RAB7 GTP hydrolysis. *Nature 2018 554:7692*, *554*(7692), 382–386. https://doi.org/10.1038/nature25486

Xu, Y., Chen, B., George, S. K., & Liu, B. (2015). Downregulation of MicroRNA-152 contributes to high expression of DKK1 in multiple myeloma. *RNA Biology*, *12*(12), 1314–1322. https://doi.org/10.1080/15476286.2015.1094600

Ylikallio, E., & Suomalainen, A. (2012). Mechanisms of mitochondrial diseases. *Annals of Medicine*, *44*(1), 41–59. https://doi.org/10.3109/07853890.2011.598547

Zamberlan, M., Boeckx, A., Muller, F., Vinelli, F., Ek, O., Vianello, C., Coart, E., Shibata, K., Christian, A., Grespi, F., Giacomello, M., Struman, I., Scorrano, L., & Herkenne, S. (2022). Inhibition of the mitochondrial protein Opa1 curtails breast cancer growth. *Journal of Experimental & Clinical Cancer Research : CR*, *41*(1). https://doi.org/10.1186/S13046-022-02304-6

Züchner, S., Mersiyanova, I. v., Muglia, M., Bissar-Tadmouri, N., Rochelle, J., Dadali, E. L., Zappia, M., Nelis, E., Patitucci, A., Senderek, J., Parman, Y., Evgrafov, O., de Jonghe, P., Takahashi, Y., Tsuji, S., Pericak-Vance, M. A., Quattrone, A., Battologlu, E., Polyakov, A. v., … Vance, J. M. (2004). Mutations in the mitochondrial GTPase mitofusin 2 cause Charcot-Marie-Tooth neuropathy type 2A. *Nature Genetics*, *36*(5), 449–451. https://doi.org/10.1038/NG1341

Figure legends

Figure 1. In silico analysis predicts miRNAs 148/152-3p and 128-3p target the 3'UTR of Opa1 in mouse and human

(A, B) Three renowned miRNA prediction websites were used: miRDB, Target Scan and miRwalk. The inclusion criteria accepted miRNA with 7mer-m8 or 8mer binding orientations to mouse and human Opa1. The miRNAs that were consistently shown across two or more prediction engines were then selected for biological validation.

Figure 2. miRNAs 148/152-3p and 128-3p specifically degrade the 3'UTR of OPA1 to reduce its expression at the mRNA and protein level in mouse and human

(A, B) MAF and HEK293 cells were transfected with the indicated miRNA mimic (30 nM) for 24h, followed by immunoblotting to determine OPA1 protein content (levels normalised to vinculin). n=4 independent experiments

(C) MAF and HEK293 cells were transfected with the indicated miRNA mimic (30 nM) for 24h, followed by real-time PCR to determine OPA1 mRNA levels. n=3 independent experiments

(D, E) MAFs were transfected with miRNA-148/152-3p and 128-3p mimics (30 nM) and luciferase-based sensor plasmids encoding the OPA1 3'UTR binding site of miR-148/152-3p and miR-128-3p. After 24h, dual-luciferase assay was used to quantify luminescence. n=4 independent experiments

Figure 3. Overexpression of miR-148b-3p, miR-152-3p and miR-128-3p leads to mitochondrial fragmentation

(A) Representative TEM images of mitochondria in MAFs transfected with the indicated miRNA mimic (30 nM) for 24h

(B) Quantification of mitochondrial area by ImageJ analysis software. ~150 mitochondria were collectively analysed from three independent experiments per condition

Figure 4. Treatment with pharmacological compounds that trigger mitochondrial dysfunction increase miR-152-3p and miR-128-3p activity levels

(A, B) MAFs were transfected with luciferase-based sensor plasmids encoding a 2x repeat complementary seed sequence for OPA1-specific miRNAs to detect miRNA activity. After 24h, cells were treated with compounds known to induce mitochondrial dysfunction for 16h, followed by dual-luciferase assay to quantify luminescence. ACT: Actinonin (50μM), CCCP (5μM), AA: Antimycin (2μM), OLIGO: Oligomycin (2.5μM). n=5 independent experiments

(C) MAFs were transfected with luciferase-based sensor plasmids encoding the OPA1 3'UTR binding site for miR-148/152-3p. The same experiment was performed as in (A, B). n=4 independent experiments

(D) MAFs were treated with compounds known to induce mitochondrial dysfunction for 16h. Real-time PCR determined OPA1 mRNA expression. n=4 independent experiments

(E) COX4-I KO HEK293 cells were transfected with luciferase-based sensor plasmids encoding a 2x repeat complementary seed sequence for OPA1-specific miRNAs. After 24h, dual-luciferase assay quantified luminescence. n=6 independent experiments

(F) MAFs underwent the same procedure as stated in (A, B), with the exception of pre-treatment of TUDCA for 6h. n=5 independent experiments

(G) COX4-I KO HEK293 cells were transfected with luciferase-based sensor plasmids encoding a 2x repeat complementary seed sequence for OPA1-specific miRNAs. After 24h, cells were pre-treated with TUDCA for 6h, followed by drug treatment for 16h. Dual luciferase assay quantified luminescence. n=3 independent experiments

Figure 5. miR-148a-3p and miR-152-3p levels are elevated in denervated mouse muscle and OPA1 levels and gastrocnemius CSA are reduced

(A) Gastrocnemius muscles were extracted from C57BL/6 mice having undergone 14d of sciatic nerve denervation, and from this tissue, microRNA expression levels were quantified by real-time PCR. n=6 independent experiments

(B) Gastrocnemius muscle tissue from 14d denervated mice was extracted and OPA1 mRNA levels were quantified by real-time PCR. n=3 independent experiments

(C) Hematoxylin and eosin staining in gastrocnemius muscle of C57BL/6 mice that underwent 14d of sciatic nerve denervation. Non-denervated muscle (sham) used as control. Cross sectional area (CSA) was measured using Fiji software, 500 fibers/condition. n=3 independent experiments

Figure 6. AntagomiRs 148/152-3p and 128-3p inhibit the action of the respective miRNA to stabilise OPA1 protein levels

(A) MAFs were transfected with antagomiRs 148/152-3p and 128-3p (30 nM) and luciferase-based sensor plasmids encoding the OPA1 3'UTR binding sites. After 24h, MAFs were transfected with miR-148/152-3p and miR-128-3p mimics (30 nM). n=3 independent experiments

(B) MAFs were transfected with antagomiRs 148/152-3p and 128-3p (30 nM). After 24h, the respective miRNA mimic (30 nM) was transfected for another 24h, followed by immunoblotting to determine OPA1 protein levels.

Figure 7. Intramuscular antagomiR treatment (148/152-3p and 128-3p mix) inhibits the action of the respective miRNA to increase OPA1 levels and attenuate muscle loss incurred from sciatic nerve injury in mice

(A) Gastrocnemius muscle tissue was extracted from 14d denervated mice treated with antagomir cocktail (50 nM of 148/152-3p and 128-3p mix) for immunoblotting analysis to determine OPA1 protein levels. n=3 independent biological samples

(B) RNA was extracted from gastrocnemius muscle of 14d denervated mice treated with antagomir cocktail (50 nM of 148/152-3p and 128-3p mix) for real-time PCR quantification of miRNA expression levels. n=4 independent experiments

(C, D) Cross sectional area (CSA) of 14d denervated mice treated with antagomiR cocktail (50 nM of 148/152-3p and 128-3p mix) was measured and quantified as stated in (figure 5C), 500 fibers/condition. n=3 independent experiments

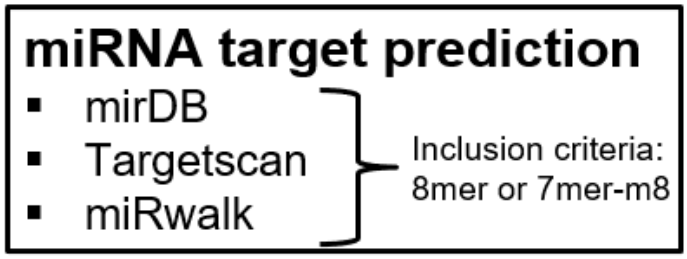

A

MOUSE

miRNA	Predicted binding site	Site type
OPA1 3'UTR mmu-miR-148a-3p	5'...CCAUGUCGUCACUGUGCACUGU... 3' UGUUUCAAGACAUCACGUGACU	7mer-m8
OPA1 3'UTR mmu-miR-148b-3p	5'...CCAUGUCGUCACUGUGCACUGU... 3' UGUUUCAAGACACUACGUGACU	7mer-m8
OPA1 3'UTR mmu-miR-152-3p	5'...CAUGUCGUCACUGUGCACUGU... 3' GGUUCAAGACAGUACGUGACU	7mer-m8
OPA1 3'UTR mmu-miR-128-3p	5'...GUCGUCACUGUGCACUGUGA... 3' UUUCUCUGGCCAAGUGACACU	8mer

B

HUMAN

miRNA	Predicted binding site	Site type
OPA1 3'UTR hsa-miR-148a-3p	5'...CUUGUUUUCACUUGUGCACUGU... 3' UGUUUCAAGACAUCACGUGACU	7mer-m8
OPA1 3'UTR hsa-miR-148b-3p	5'...CUUGUUUUCACUUGUGCACUGU... 3' UGUUUCAAGACACUACGUGACU	7mer-m8
OPA1 3'UTR hsa-miR-152-3p	5'...UUGUUUUCACUUGUGCACUGU... 3' GGUUCAAGACAGUACGUGACU	7mer-m8
OPA1 3'UTR hsa-miR-128-3p	5'...GUUUUCACUUGUGCACUGUGA... 3' UUUCUCUGGCCAAGUGACACU	8mer

Figure 1

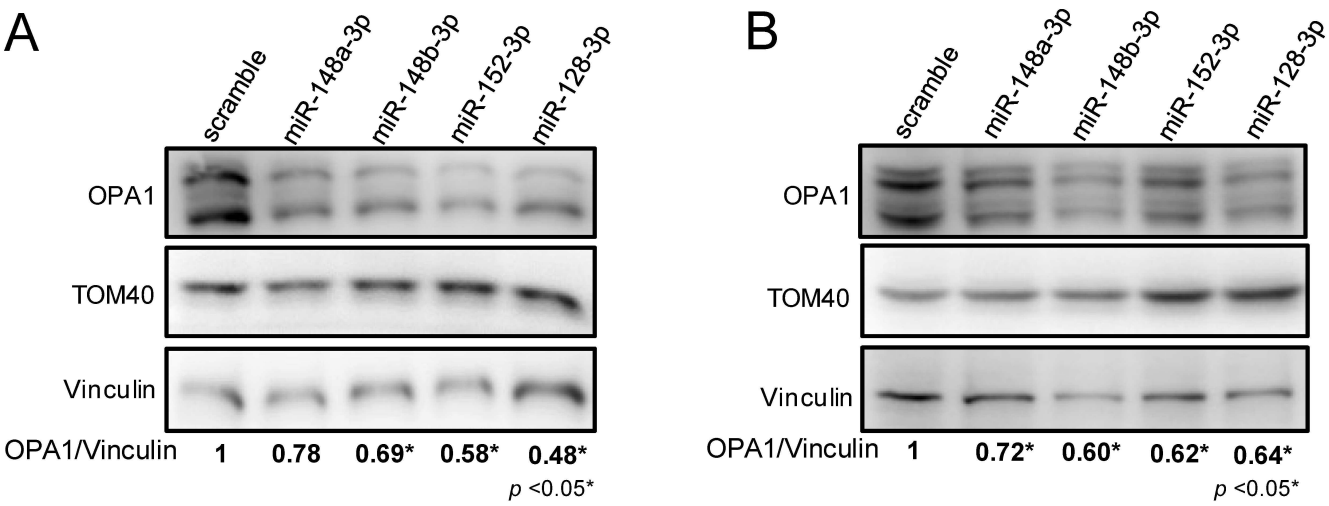
A
scramble
miR-148a-3p
miR-148b-3p
miR-152-3p
miR-128-3p
OPA1
TOM40
Vinculin
OPA1/Vinculin 1 0.78 0.69* 0.58* 0.48*
p <0.05*
B
scramble
miR-148a-3p
miR-148b-3p
miR-152-3p
miR-128-3p
OPA1
TOM40
Vinculin
OPA1/Vinculin 1 0.72* 0.60* 0.62* 0.64*
p <0.05*

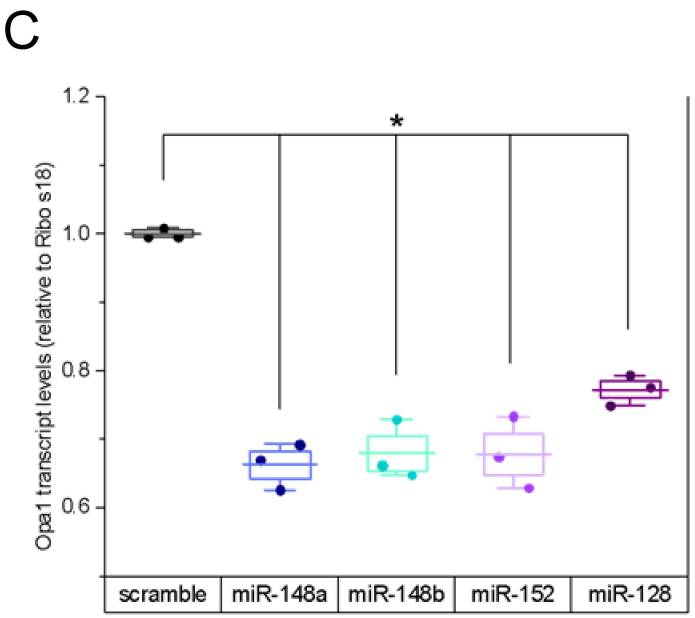
C
Opa1 transcript levels (relative to Ribo s18)
1.2
1.0
0.8
0.6
*
scramble
miR-148a
miR-148b
miR-152
miR-128

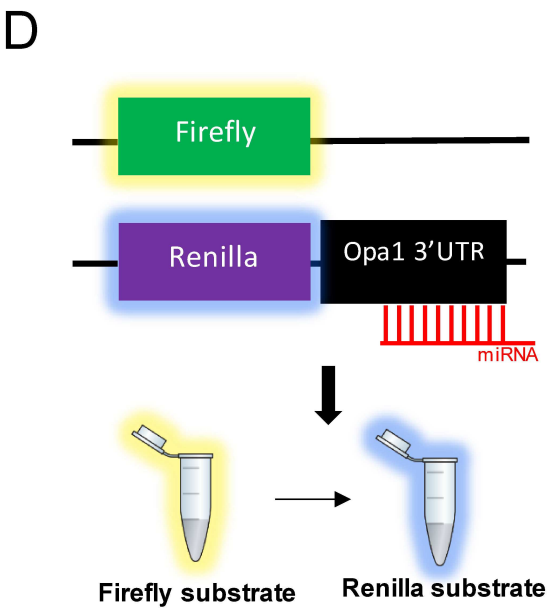
D
Firefly
Renilla
Opa1 3'UTR
miRNA
Firefly substrate
Renilla substrate

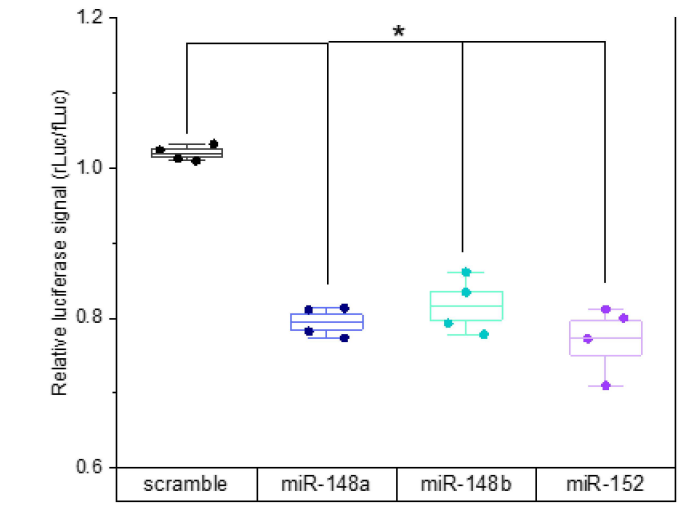
E
Relative luciferase signal (rLuc/fLuc)
1.2
1.0
0.8
0.6
*
scramble
miR-148a
miR-148b
miR-152

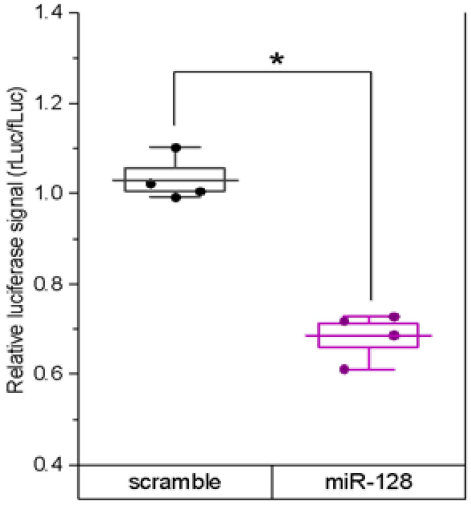
F
Relative luciferase signal (rLuc/fLuc)
1.4
1.2
1.0
0.8
0.6
0.4
*
scramble
miR-128

Figure 2

A

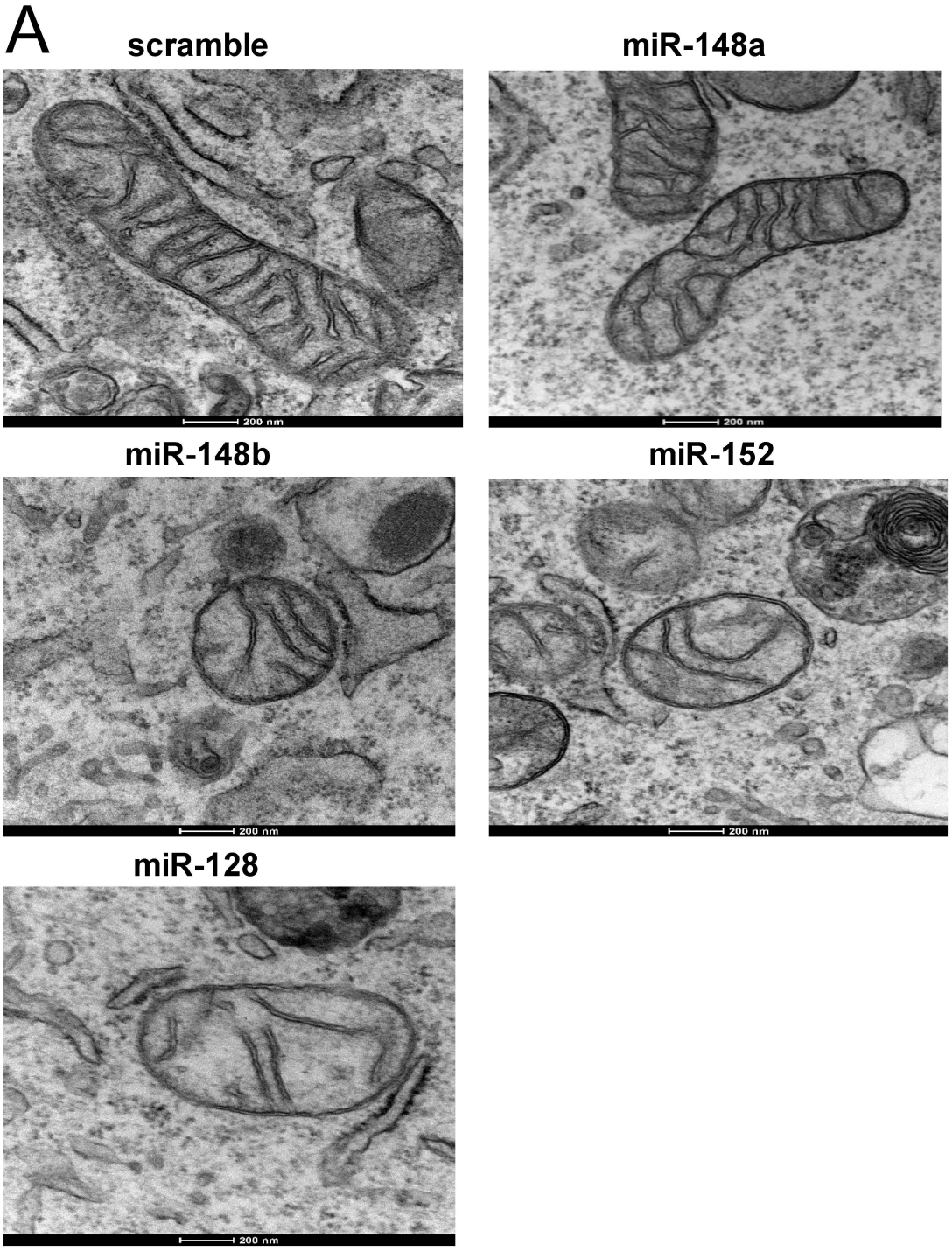
scramble
miR-148a
miR-148b
miR-152
miR-128
200 nm

B

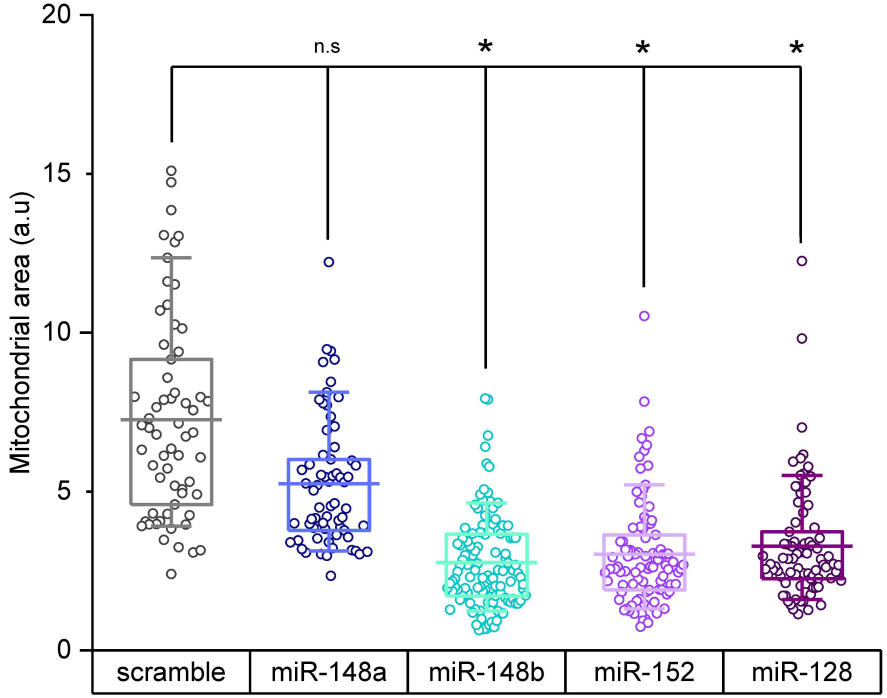
Mitochondrial area (a.u)
20
15
10
5
0
n.s
*
*
*
scramble
miR-148a
miR-148b
miR-152
miR-128

Figure 3

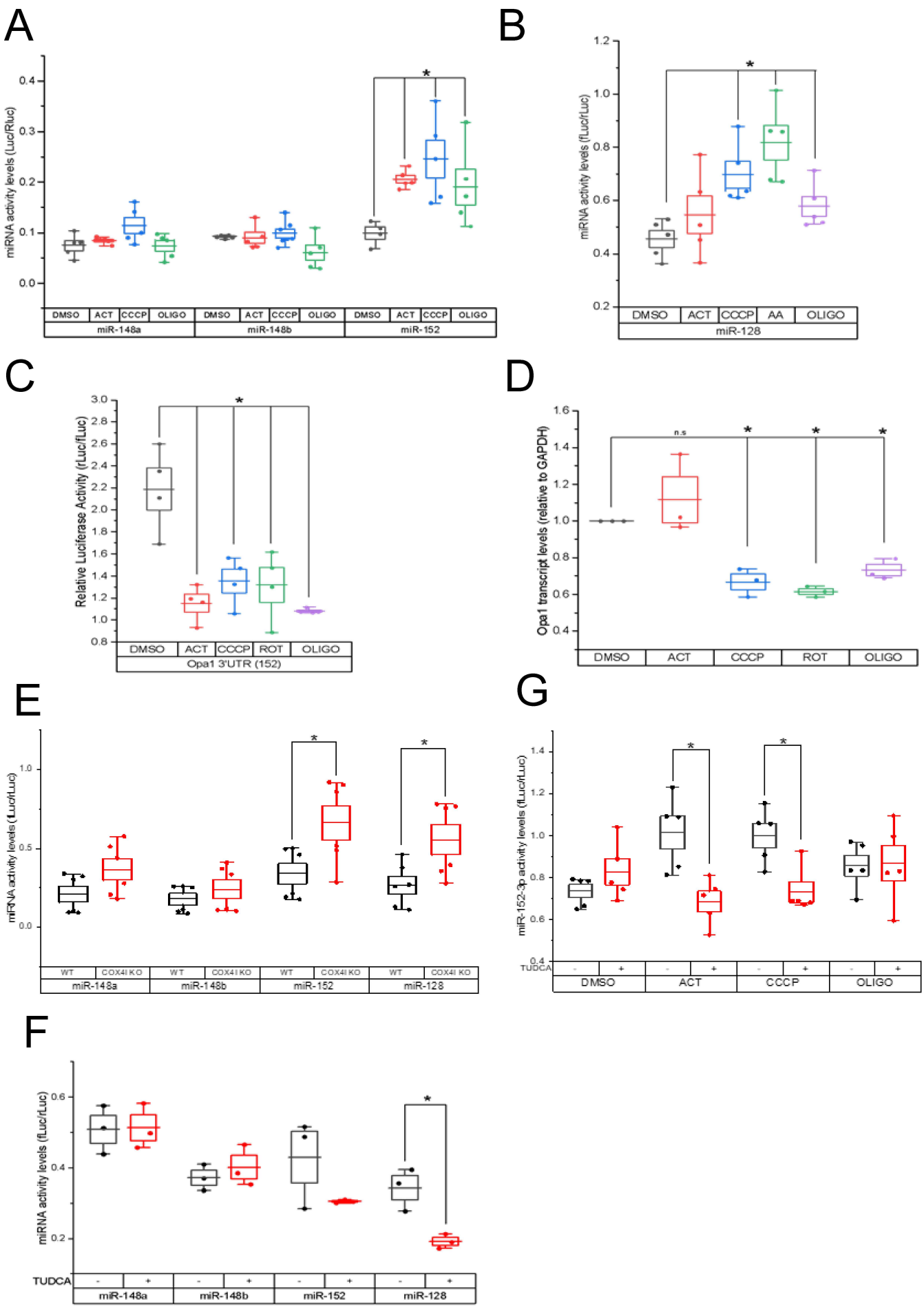
A
miRNA activity levels (Luc/Rluc)
DMSO ACT CCCP OLIGO
miR-148a
miR-148b
miR-152
B
miRNA activity levels (fLuc/rLuc)
DMSO ACT CCCP AA OLIGO
miR-128
C
Relative Luciferase Activity (rLuc/fLuc)
DMSO ACT CCCP ROT OLIGO
Opa1 3'UTR (152)
D
Opa1 transcript levels (relative to GAPDH)
n.s
DMSO ACT CCCP ROT OLIGO
E
miRNA activity levels (fLuc/rLuc)
WT COX4I KO
miR-148a
miR-148b
miR-152
miR-128
G
miR-152-3p activity levels (fLuc/rLuc)
TUDCA
DMSO ACT CCCP OLIGO
F
miRNA activity levels (fLuc/rLuc)
TUDCA
miR-148a
miR-148b
miR-152
miR-128

Figure 4

A

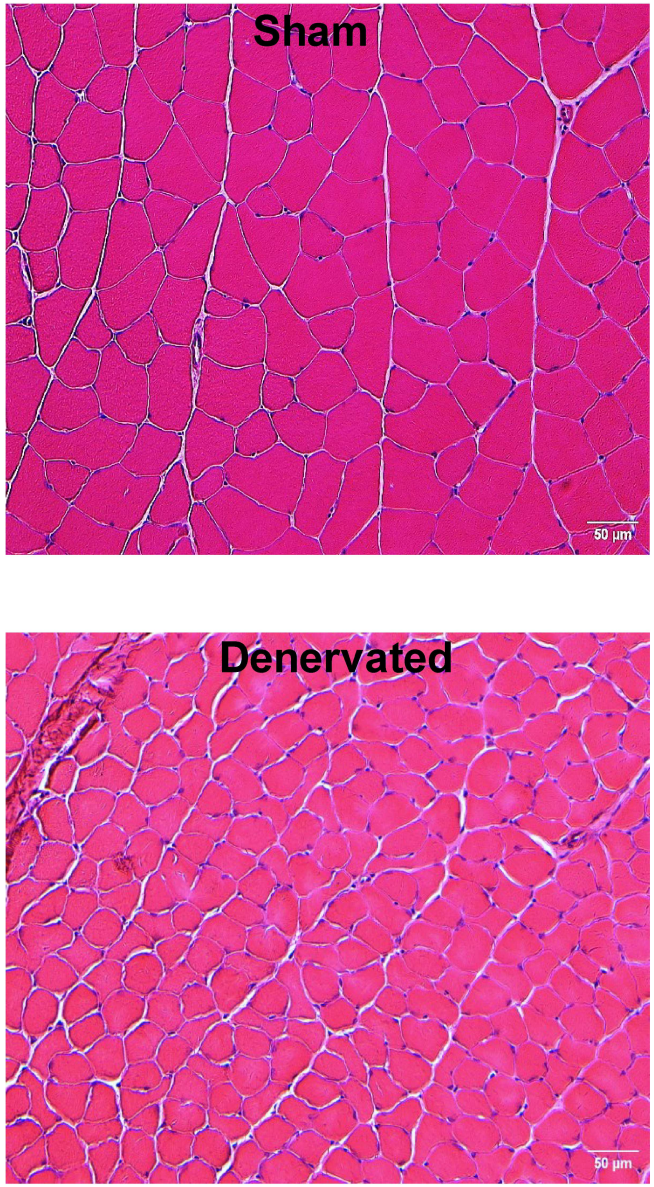
Sham
50 µm
Denervated
50 µm

B

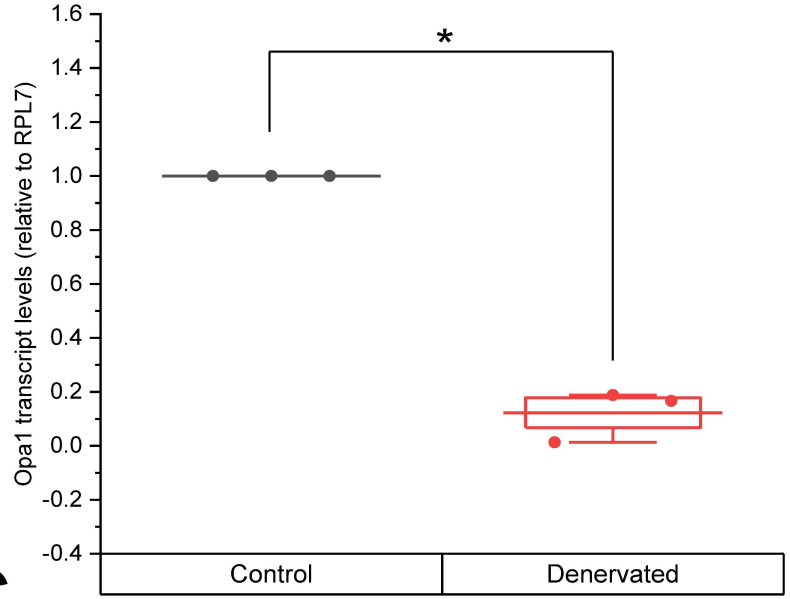
Opa1 transcript levels (relative to RPL7)
1.6
1.4
1.2
1.0
0.8
0.6
0.4
0.2
0.0
-0.2
-0.4
*
Control
Denervated

C

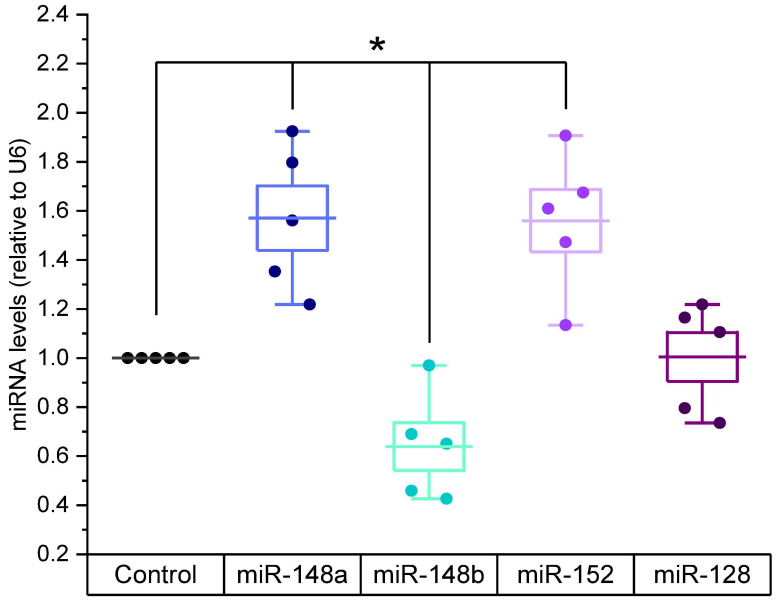
miRNA levels (relative to U6)
2.4
2.2
2.0
1.8
1.6
1.4
1.2
1.0
0.8
0.6
0.4
0.2
*
Control
miR-148a
miR-148b
miR-152
miR-128

Figure 5

A

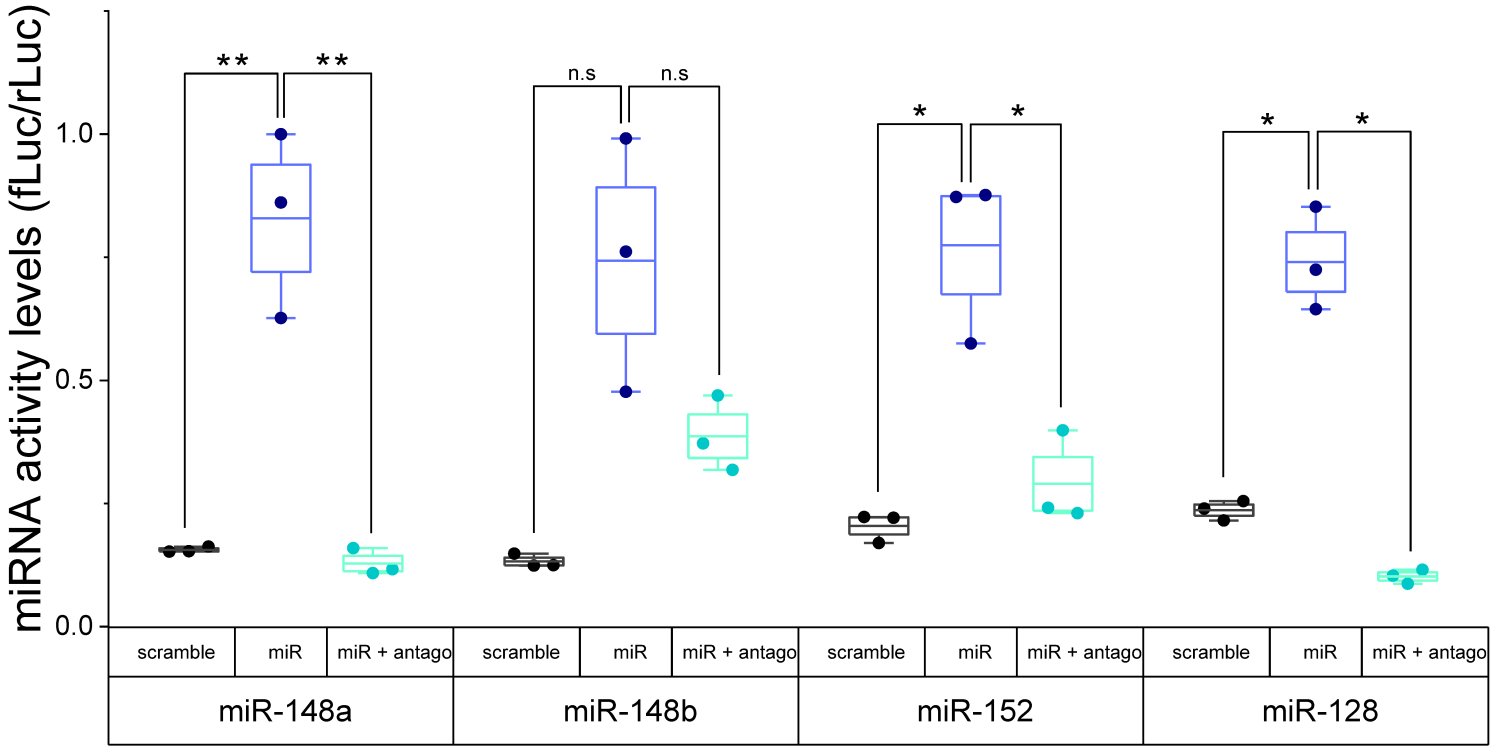

B

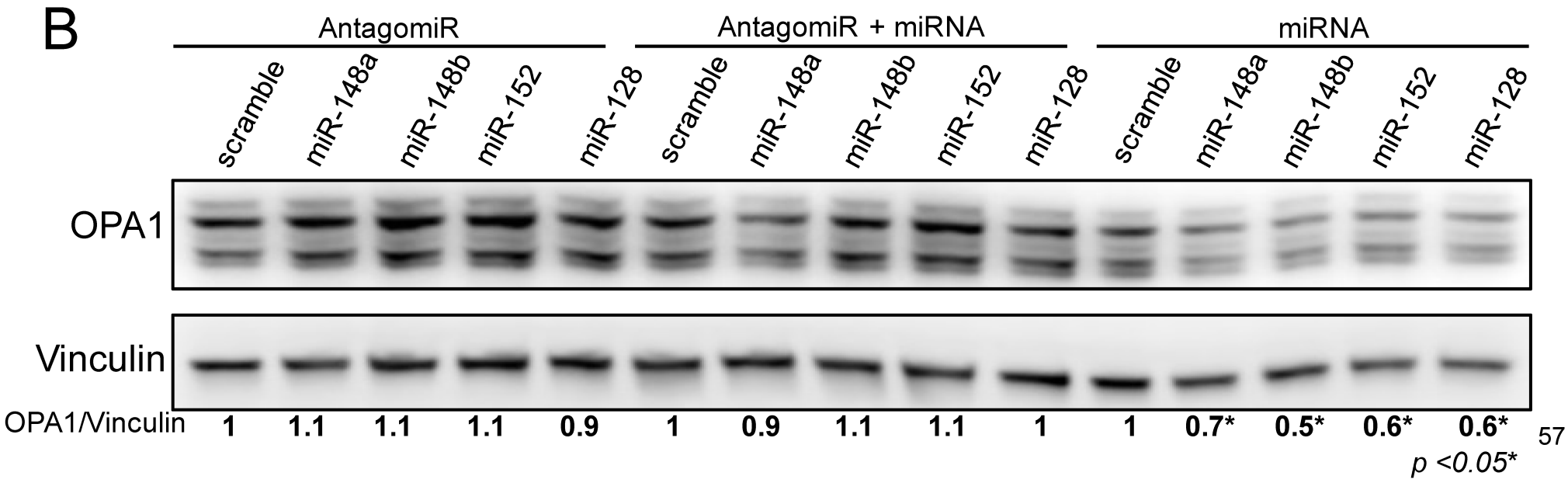

57

Figure 6

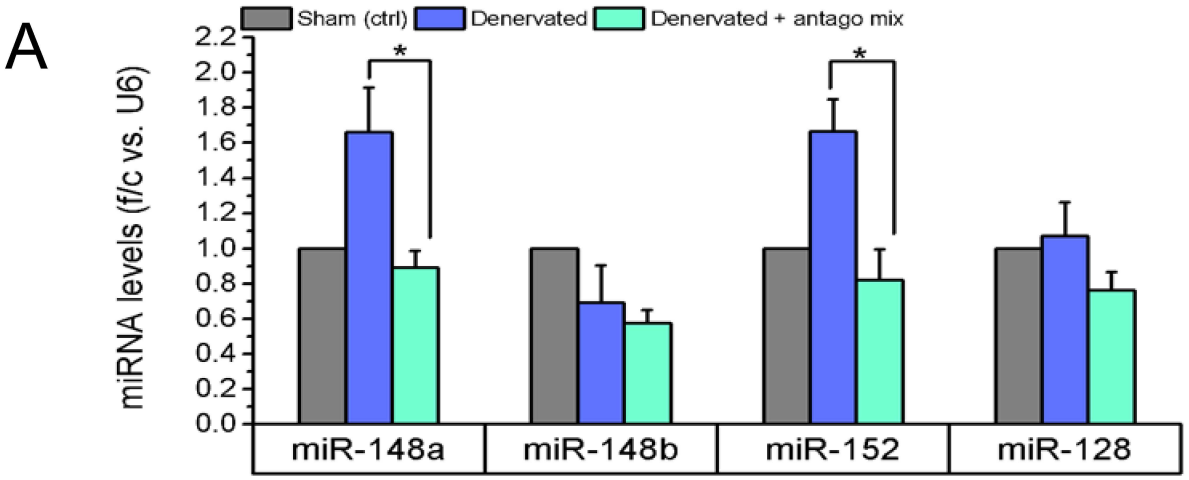
A
Sham (ctrl)
Denervated
Denervated + antago mix
miRNA levels (f/c vs. U6)
2.2
2.0
1.8
1.6
1.4
1.2
1.0
0.8
0.6
0.4
0.2
0.0
*
*
miR-148a
miR-148b
miR-152
miR-128

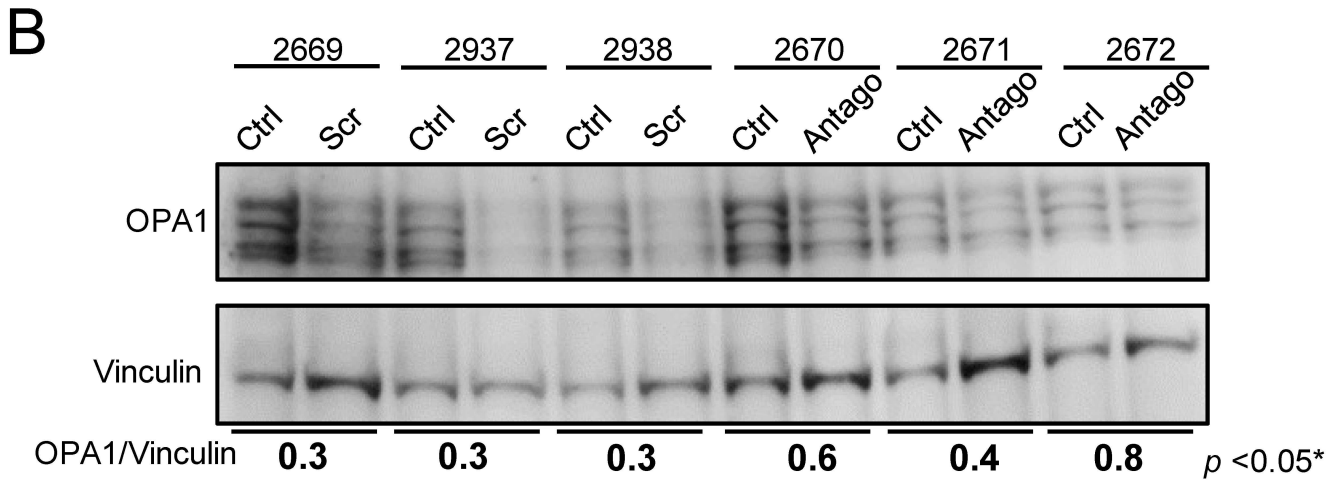
B
2669
2937
2938
2670
2671
2672
Ctrl
Scr
Ctrl
Scr
Ctrl
Scr
Ctrl
Antago
Ctrl
Antago
Ctrl
Antago
OPA1
Vinculin
OPA1/Vinculin
0.3
0.3
0.3
0.6
0.4
0.8
p <0.05*

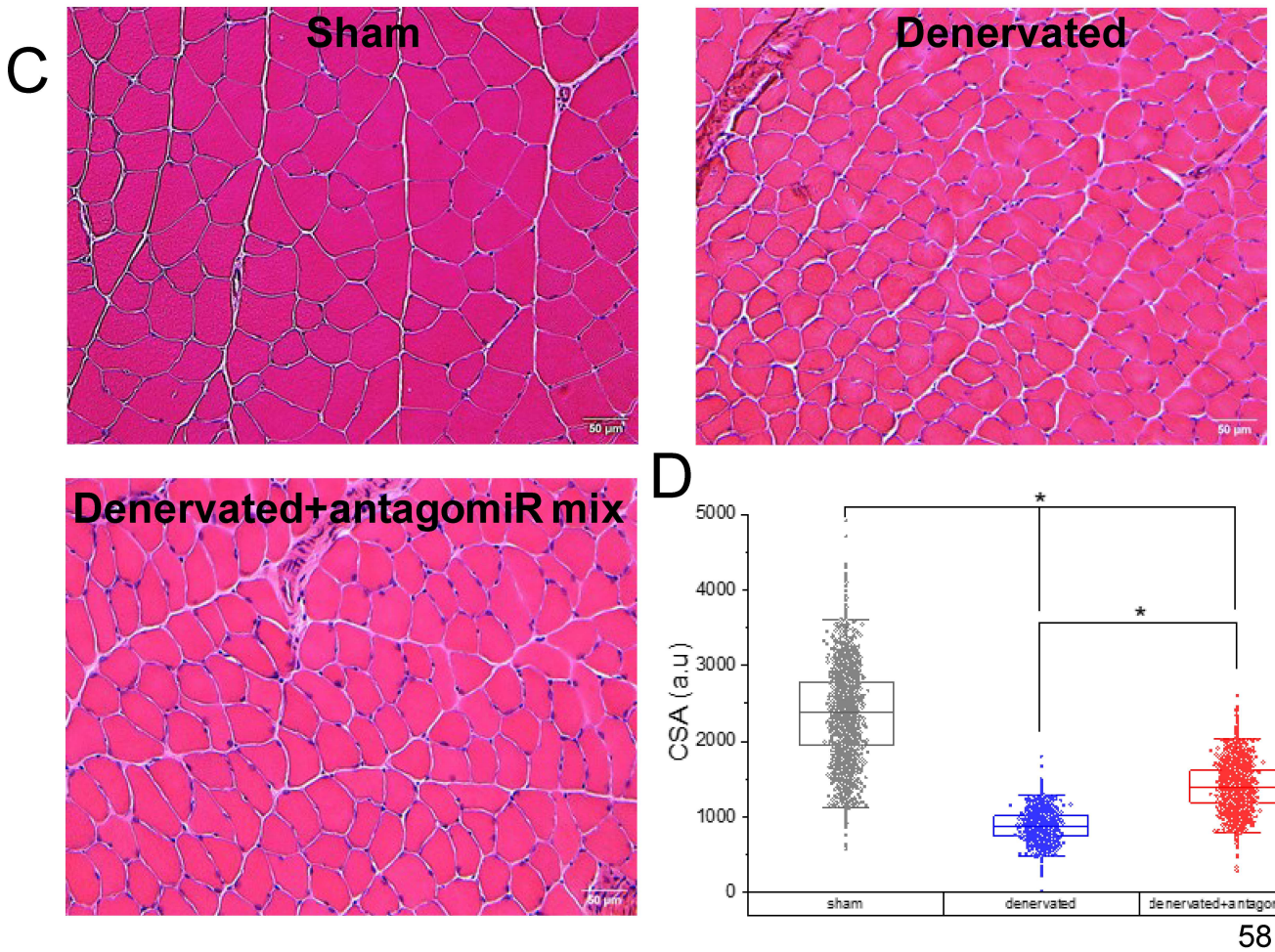
C
Sham
Denervated
Denervated+antagomiR mix
D
CSA (a.u)
5000
4000
3000
2000
1000
0
*
*
sham
denervated
denervated+antagomiR mix

Figure 7

Publication

Available online at www.sciencedirect.com

ScienceDirect

Current Opinion in Physiology

Mitochondrial dynamics: roles in exercise physiology and muscle mass regulation

Andre Djalalvandi[1,2] and Luca Scorrano[1,2,*]

How mitochondria alter their morphology to meet cellular demands epitomizes the 'form follows function' architectural principle. These remodeling events are collectively termed 'mitochondrial dynamics'. The influence of mitochondrial dynamics and of the mitochondria-shaping proteins that control it on skeletal muscle physiology has become clearer. Endurance exercise prompts mitochondrial morphological changes that augment the respiratory capacity of the worked muscles. Mechanistically, exercise training increases mitochondrial fusion protein levels in skeletal muscle to promote the development of a hyperfused mitochondrial network that possesses denser cristae. Conversely, disruptions to the mitochondrial network through imbalances in mitochondrial dynamics lead to muscle atrophy. Insight into the connection between mitochondrial morphology and muscle-mass maintenance will help to pinpoint therapeutic targets that can be exploited to counteract sarcopenia and muscle atrophy in pathological conditions.

Addresses
[1] Veneto Institute of Molecular Medicine, Via Orus 2, 35139 Padua, Italy
[2] Department of Biology, University of Padua, Via Ugo Bassi 58/B, 35121 Padua, Italy

Corresponding author: Luca Scorrano (luca.scorrano@unipd.it)
* Twitter account: @LabScorrano

Current Opinion in Physiology 2022, **27**:100550

This review comes from a themed issue on **Mitochondria Physiology**

Edited by **Iain Scott** and **Kelsey Fisher-Wellman**

For complete overview of the section, please refer to the article collection, "Mitochondria Physiology"

Online publication date: 25 May 2022

https://doi.org/10.1016/j.cophys.2022.100550

Introduction

Mitochondria are double-membrane organelles wherein the surface area of the inner mitochondrial membrane (IMM) is manyfold greater than the outer mitochondrial membrane (OMM). This is due to the presence of deep invaginations named cristae, which accommodate respiratory-chain complexes I–IV and F_1F_0–ATP synthase that participate in ATP generation. Mitochondria continually fuse, divide, and remodel their cristae in a manner tightly coupled to the physiological requirements of the cell [1,2]. These mechanisms have been christened 'mitochondrial dynamics' and are predominantly controlled by a family of GTP-dependent dynamin-related proteins. Mitofusins 1 and 2 (MFN1 & MFN2) are involved in OMM fusion and optic atrophy 1 (OPA1) mediates IMM fusion and cristae shaping. Dynamin-related protein-1 (DRP1) and its adaptor proteins execute mitochondrial fission [1]. Essentially, the ratio between fusion and fission rates determines mitochondrial morphology. When rates of fusion exceed fission, mitochondria become elongated and form a reticulum. Mitochondrial fusion is a two-step process, whereby OMMs of neighboring mitochondria merge together, followed by IMM merging, this permits the transfer of mitochondrial DNA (mtDNA), proteins, metabolites, and electrochemical energy between mitochondria [1]. By contrast, overriding fission rates dismantle the mitochondrial network, leading to the division of one mitochondrion into two daughter mitochondria (Figure 1).

Mitochondrial fission allows for the removal of damaged or depolarized mitochondria by mitophagy — the selective degradation of mitochondria by autophagy. Notably, expression levels of DRP1, MFN1, MFN2, and OPA1 in skeletal muscle correlate with lifelong exercise and muscle disuse, pointing to an interrelation between mitochondrial dynamics and muscle-health preservation [3–5]. This review discusses the mechanisms as to how mitochondrial dynamics impinge on skeletal muscle physiology during endurance exercise, in addition to examining the intimate relationship between mitochondrial shape and muscle-mass maintenance (Figure 2).

Mitochondrial dynamics and exercise

Exercise activates potent mitohormetic responses that have been documented to safeguard muscles from decay and disease [6–9]. Hence, mitochondrial fitness is tied to skeletal muscle health. Three-dimensional high-resolution analysis identified four mitochondrial populations that form a continuous network in skeletal muscle [10]. Paravascular mitochondria near capillaries are connected to fiber-parallel mitochondria, cross-fiber connection mitochondria, and I-band mitochondria. The mitochondrial reticulum acts as a conductive pathway to rapidly transmit electrochemical energy from the muscle periphery to contractile elements. This phenomenon is

Nomenclature

AMPK	AMP-activated protein kinase
CFCM	cross-fiber connection mitochondria
DRP1	Dynamin-related protein 1
FGF21	fibroblast growth factor 21
FPM	fiber parallel mitochondria
IBM	I-band mitochondria
IMJs	inter-mitochondrial junctions
IMM	inner mitochondrial membrane
MFN1	Mitofusin 1
MFN2	Mitofusin 2
mtDNA	Mitochondrial DNA
MuRF1	muscle RING-finger protein-1
OMM	outer mitochondrial membrane
OPA1	Optic atrophy 1
PGC1α	peroxisome proliferator-activated receptor γ coactivator-1alpha
PGC1β	peroxisome proliferator-activated receptor γ coactivator-1beta
PVM	Paravascular mitochondria
RCS	respiratory chain complexes
ROS	reactive oxygen species
SCAF1	supercomplex assembly factor 1
SR	sarcoplasmic reticulum

Figure 1

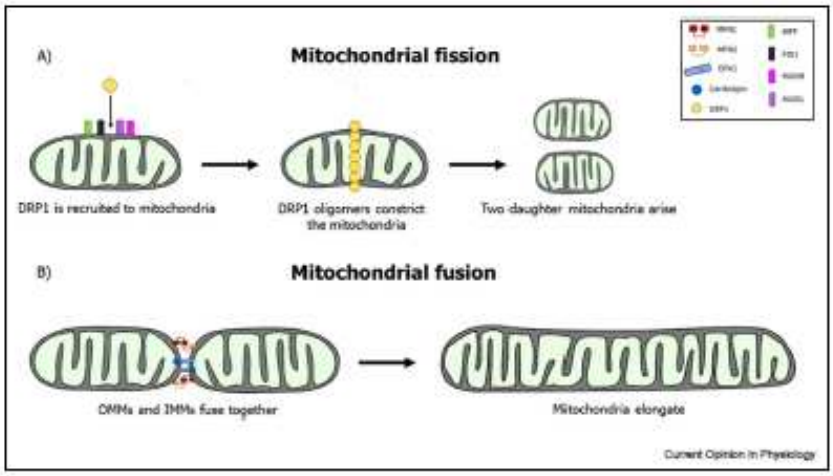

Mitochondrial fission and fusion in mammals. **(a)** Schematic representation of the mitochondrial fission process. The initial step of mitochondrial fission is DRP1 translocation from the cytosol to the mitochondria. Adaptor proteins, MFF, mitochondrial fission protein-1 (FIS1), and mitochondrial dynamics proteins of 49 and 51 kDa (MID49 and MID51) recruit DRP1 to the OMM where it arranges into spiral complexes around the preconstricted GTP-dependent fission site. Next, the GTPase domain on DRP1 hydrolyzes to constrict the OMM and sever the mitochondrion into two. **(b)** Schematic representation of the OMM and IMM fusion process. Fusion is initiated by OMM tethering between adjoining mitochondria and is coordinated through *in trans* interactions between MFN1 and MFN2, at HR2 domains, and/or GTPase domains. Following this, GTPase domains on MFN1 and MFN2 hydrolyze to enable OMMs to fuse together. For IMM fusion, OPA1 forms a bridge with cardiolipin on the opposing mitochondria. The adjacent IMMs are pulled together via GTP-dependent hydrolysis of Opa1, which finalizes the fusion of two mitochondria.

crucial, as muscles contracting maximally can account for 90% of whole-body oxygen uptake and ATP-turnover rates can near-instantaneously increase ~100-fold higher than resting rates [11,12]. Landmark studies in the 60s uncovered that skeletal muscle from endurance-trained rats expressed higher levels of mitochondrial proteins [13], and electron microscopy images displayed mitochondrial-shape alterations from exercise [14,15]. Accumulating evidence is helping to define in molecular detail the effects of endurance-based exercise on mitochondrial dynamics.

Acute exercise impacts on mitochondrial morphology

Throughout the acute-exercise period (one single-exercise bout), mitochondria-shaping proteins are differentially expressed in skeletal muscle. In rodent studies encompassing various endurance-exercise modalities, increased DRP1 phosphorylation on Ser616 was observed in the worked muscles, indicating exercise triggers mitochondrial fission [16–19]. Indeed, in skeletal muscles of mice that performed an exhaustive running protocol, DRP1 phosphorylation on Ser616 was accompanied with sarcoplasmic reticulum (SR)–mitochondrial

Figure 2

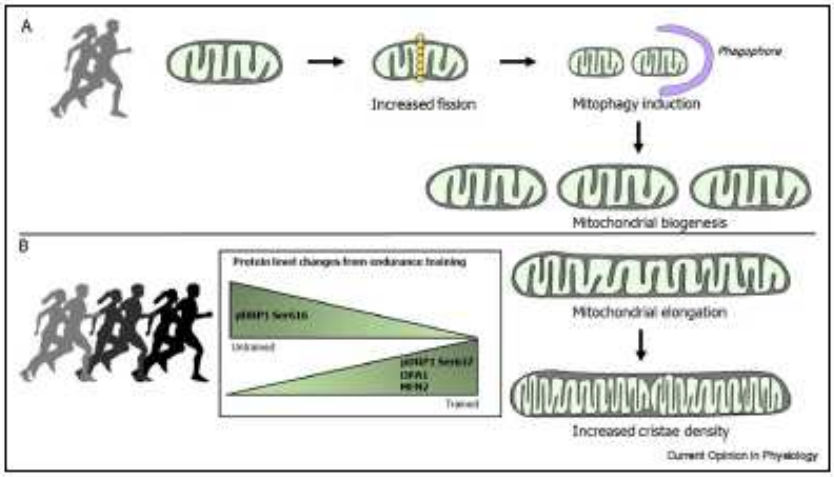

Alterations in mitochondrial dynamics from acute and chronic endurance exercise. **(a)** Schematic representation of the changes in mitochondrial dynamics and mitochondrial quality control during one single-exercise bout. The exercise stimulus increases fission rates to segregate damaged mitochondria and support mitochondrial-turnover mechanisms (i.e. mitophagy and biogenesis), thereby providing the worked muscles with a fitter, fresher pool of mitochondria. **(b)** Schematic representation of the changes in expression levels of fission and fusion proteins from long-term exercise training. As mitochondria become more resilient to exercise-incurred damage, fission activity is dampened, demonstrated by concomitant drops in DRP1 phosphorylation on Ser616 and increases in DRP1 phosphorylation on Ser637. Additionally, MFN2 and OPA1 levels increase. Overriding fusion rates lead to an expansion of the mitochondrial network to enhance the oxidative capacity of the trained muscles. When attaining athlete levels of fitness, mitochondrial volume reaches a spatial limit, and as a result, cristae become denser to further increase mitochondrial respiration in the muscle.

constrictions that likely represented the fission site [16]. The stimulus provoking fission during exercise is uncertain, perhaps, it arises from mechanical forces generated by contracting muscles [20], or an overaccumulation of exercise-induced reactive oxygen species (ROS) [21]. A noteworthy limitation to the exercise studies highlighted was the use of C5BL/6J mouse strains that naturally harbor nonfunctional supercomplex assembly factor 1 (SCAF1) [16,17,19]; these mice exhibit exercise-performance detriments due to aberrations in SCAF1-dependent respiratory-chain supercomplex (RCS) assembly [22]. Nevertheless, increased levels of phosphorylated DRP1 on Ser616 were also found in human skeletal muscle following a 1-h cycling session, supporting the data in rodents [23]. Does exercise activate mitophagy? Mitophagy was tracked *in vivo* using a pMitoTimer, a fluorescent mitochondrial reporter gene, in the skeletal muscle of mice that ran for 90 min [17]. It was revealed that AMP-activated protein kinase (AMPK) phosphorylated autophagy-activating kinase 1 (ULK) in muscles to stimulate mitophagy 6 h post exercise [17]. This finding suggests that mitophagy becomes activated during the recovery period to remove damaged-muscle mitochondria incurred from exercise.

Abundant in striated muscle, intermitochondrial junctions (IMJs) are electron-dense structures aligning cristae between adjacent mitochondria. The physiological function of IMJs is not clear-cut but it is probably to assist in distributing electrochemical potential throughout the muscle cell. Three hours of voluntary exercise led to a 1.9-fold increase in IMJs in mouse skeletal muscle [24]. Evidence that acute exercise enhanced inter-mitochondrial communication in skeletal muscle contradicts studies reporting increased fission activity [16–18]. While fission studies examined type-2 glycolytic muscle fibers, Picard and colleagues analyzed soleus muscles [24], a type-1 slow oxidative fiber abundant in mitochondria that possess high fusion activity, and consequently, would form a larger mitochondrial network [25]. Moreover, the exercise modality implemented by Picard's group was voluntary, so it is possible that the mice did not exert themselves sufficiently enough to stimulate exercise-induced fission. To that end, exercise intensity and muscle-fiber type are confounding factors that need to be acknowledged when evaluating the effects of mitochondrial dynamics during acute exercise.

Mitochondrial-morphology adaptations to long-term exercise

One of the hallmark adaptations to endurance exercise is mitochondrial biogenesis, controlled by coactivators peroxisome proliferator-activated receptor γ coactivator-1alpha (PGC1α) and 1beta [26]. Yet how mitochondria modify their shape during exercise training is less clear. How does lack of the fusion and fission machineries

impact exercise-training adaptations? Single ablation of MFN1 and MFN2 in mice had no effect on exercise performance, however, simultaneous deletion of MFN1 and MFN2 reduced complex-I and complex-IV subunit expression and impaired exercise performance [27]. Surprisingly, in haploinsufficient *OPA1* mice ($OPA1^{+/-}$) that underwent exercise training, treadmill-running performance was improved in comparison with wild-type mice. The compensatory adaptations seen in $OPA1^{+/-}$ mice included higher left ventricular hypertrophy and an improved capacity to utilize fatty acids [28]. Regarding fission machinery, hampered muscle-mass gains and impaired exercise performance were displayed in trained muscle-specific *DRP1* heterozygous mice [19]. Taken together, these studies illustrate that an imbalance in mitochondrial dynamics perturbs exercise-induced adaptations, and for the most part, is maladaptive toward performance.

Remarkably, 30 days of endurance-exercise training concomitantly reduced levels of DRP1 phosphorylation on Ser616 while increasing activity of DRP1 phosphorylation on Ser637 in mouse skeletal muscle [19]. This raises the possibility that training-induced adaptive responses steer toward remodeling mitochondria in favor of a profusion phenotype. In fact, human training studies give credence to this notion [3,29–35]. After a six-week endurance-training program, MFN2 protein content increased and mitochondria were enlarged in the muscles of healthy males [29]. Muscles from obese and aging individuals were similarly found to have higher MFN2 protein levels following a 12-week training program [30]. Increased MFN2-dependent fusion from endurance training may have been modulated transcriptionally by PGC1α [36]. Alternatively, exercise-induced increases in oxidized glutathione to generate disulfide-mediated MFN2 oligomers could have elevated fusion activity [37]. Other reports found that 12 weeks of endurance training increased the ratio of fusion-to-fission rates in human skeletal muscle [29], and OPA1 protein levels were higher in skeletal muscles of endurance-trained individuals compared with untrained muscle [3,30]. Interestingly, MFN2 and OPA1 protein levels were elevated in the muscles of human athletes throughout an intense exercise bout. This suggests a profusion environment arises in well-adapted muscle during exercise, presumably to meet the higher energy demands [32].

Cristae remodeling from exercise training

Higher cristae density was reported in skeletal muscle mitochondria of endurance-trained athletes [38]. Intriguingly, it was identified that cristae density was a stronger correlator of maximal oxygen uptake (i.e. VO_2 max) than mitochondrial content in endurance athletes. However, in sedentary individuals having completed 10 weeks of endurance training, there were no changes in cristae density [38]. These findings imply that cristae alterations do not occur through short-term training.

Cristae shape dictates RCS assembly [39]. The widely acknowledged 'plasticity model' posits that isolated respiratory complexes and RCSs coexist and reorganize their stoichiometry in conformity with the environment [40]. Evidence of this plasticity has been documented in endurance-trained muscles [41,42]. Four months of endurance training in sedentary adults promoted the assembly of complexes I, III, and IV into functional RCSs $I + III_2 + IV$, which were associated with increased muscle respiration [41]. A combination of blue native and mass spectrometry experiments enabled the identification of novel subunits of complex II and complex V that formed super-assembled structures in mouse muscle [42]. It is speculated that the function of RCS II + V is to enhance the stability of the complexes, although more work is needed to confirm this and to identify other potential functions. Furthermore, whether RCSs comprising complex II and complex V are present in human skeletal muscle needs clarifying. In contrast to human muscle, complex I and complex III failed to assemble into RCSs in endurance-trained mice, these discrepancies could be due to species-specific RCS assembly or training-modality differences.

Mitochondrial dynamics and muscle-mass maintenance

When mitochondrial homeostasis is disturbed in skeletal muscle, an array of atrophic signals become activated that induce myofiber degradation [26]. Imbalances in fusion and fission activity are one example of this dyshomeostasis, as seen in certain human myopathies. Regarding fusion, pathogenic *OPA1* and *MFN2* mutations cause autosomal-dominant optical atrophy and Charcot–Marie–Tooth neuropathy type 2A, respectively, these are human neuromuscular disorders characterized by muscle wasting [43,44]. For fission, a homozygous mutation in *MIEF1* gene, encoding for MiD49, caused progressive muscle weakness and exercise intolerance in a 15-year-old male [45], and mitochondrial fission factor (*MFF*) loss-of-function mutations have been reported to cause neuromuscular defects [46,47]. Put together, these clinical reports on myopathy patients lend support to the view that genes involved in mitochondrial dynamics are critical regulators of skeletal muscle homeostasis.

Mitofusins in skeletal muscle

Muscle-specific double deletion of *Mfn1* and *Mfn2* in mice gives rise to a phenotype resembling a mitochondrial myopathy. Pathological features included an increase in mtDNA mutations, mitochondrial proliferation, impaired respiration, and muscle atrophy [48]. Moreover, double *Mfn* KO mice had higher post-exercise lactate

levels, indicating an intolerance to exercise. *Mfn2* deletion in skeletal muscle accelerated age-related sarcopenia, which was attributed to mitochondrial dysfunction, ROS overproduction, and impaired autophagy [49]. Conversely, catabolic signaling activated the E3 ligase HUWE1 that specifically ubiquitinated MFN2 for its degradation [50]. This hints at a reciprocal relationship between MFN2 and muscle-mass regulation. Naturally then, can MFN2 overexpression counteract skeletal muscle atrophy? Muscle-specific overexpression of PGC1α stimulated MFN2 expression, preventing muscle loss in hindlimb-unloaded mice [5], and overexpressing MFN2 in C2C12 mouse myotubes attenuated tumor necrosis factor-α-induced atrophy [51]. These data highlight a role for MFN2 in curtailing muscle atrophy, although direct interrogation using muscle-specific *Mfn2*-overexpression models in atrophic conditions is needed. Dysregulated MFN2–SR contacts might contribute toward pathology in muscle disease [52–54]. Knocking down MFN2 in mouse muscle caused a 40% reduction in mitochondrial Ca^{2+} uptake that was associated with reduced MFN2–SR tethering interactions [52]. Consistently, EM images of human skeletal muscle revealed that MFN2 levels correlated with the number of mitochondria–SR contacts [54]. Owing to its multifunctional nature, more research is needed to untangle the MFN2-dependent mechanisms on muscle-mass preservation.

Optic atrophy 1 in skeletal muscle

Ablating *Opa1* in skeletal muscle led to a more severe phenotype than simultaneous deletion of *Mfn1* and *Mfn2*, underscoring additional functions that are controlled by OPA1 in this tissue. Inducible deletion of OPA1 in adult mouse skeletal muscle caused rapid reductions in myofiber Cross-sectional area (CSA) and muscle force, leading to premature death within three months [3]. *Opa1* deficiency in skeletal muscle distorted cristae shape and caused mitochondrial dysfunction. This triggered ER stress and systemic inflammation, resulting in the induction of major atrophy-related E3 ubiquitin ligases, muscle RING-finger protein-1 (MuRF1), and Atrogin-1, that coordinated myofiber breakdown [3,55]. Increased expression of fibroblast growth factor 21 (FGF21), a pleiotropic cytokine involved in catabolism, was observed in OPA1-deficient skeletal muscle [3,55,56]. The consequences of elevated FGF21 levels were investigated through muscle-specific simultaneous deletion of *Opa1* and full-body deletion of *Fgf21*, which rescued the systemic aging phenotype, but had minimal effects on reversing muscle mass [3]. These data imply that atrogenes were the main instigators of atrophy in muscles lacking OPA1. Contrastingly, mild OPA1 overexpression (~1.5-fold increase) blunted muscle atrophy by restoring mitochondrial function in denervated mouse muscle and in a mouse myopathy model caused by a muscle-specific gene deletion of *COX15* [57,58]. These results suggest that OPA1 in skeletal muscle can block the atrophy program in acute and chronic settings. Mechanistically, OPA1 overexpression remodeled cristae architecture in favor of enhanced RCS stabilization to increase mitochondrial respiration in *COX15* mutant mice. The health outcomes were prolonged lifespan and improved muscle endurance in respect to control mice [58].

Dynamin-related protein 1 in skeletal muscle

The connection between mitochondrial fragmentation and skeletal muscle mass preservation was recognized when the muscles of mice subjected to denervation and 48 h of fasting displayed a disorganized mitochondrial network [59]. In the same vein, DRP1 overexpression caused mitochondrial fragmentation and reduced ATP levels, thereby initiating AMPK retrograde signaling toward the nucleus to induce muscle atrophy in a FoxO3-dependent manner [59]. Chronic DRP1 overexpression in mouse skeletal muscle activated the eIF2α–ATF4–FGF21 pathway that inhibited growth-hormone stimulation, stalling protein-synthesis rates and muscle growth [60]. In contrast, blocking fission in starved muscles prevented atrophy, suggesting that an intact mitochondrial network is protective against acute muscle atrophy [59]. However, long-term muscle-specific depletion of *Drp1* in mice caused severe muscle loss and mitochondrial dysfunction [61,62], indicating that chronic inhibition of mitochondrial fission has deleterious consequences for muscle health. Mitochondria in DRP1-lacking muscles were enlarged and dysfunctional, which resulted in ER stress activation and increased mitochondrial Ca^{2+} uptake, leading to myofiber loss [61]. Collectively, these data reveal that overactivation and underactivation of DRP1-dependent fission disrupt mitochondrial homeostasis, and through perturbed Ca^{2+} signaling and stress responses, cause muscle wasting. Remarkably, fission inhibition, by muscle-specific ablation of *Drp1* in *Opa1*-deficient muscles, partially recovered muscle defects, alleviated oxidative stress and inflammation, and averted the lethal phenotype seen in *Opa1* KO mice [63]. Re-equilibrating mitochondrial dynamics to ameliorate the pathological phenotype agrees with other reports [64–67]. In essence, simultaneous abolishment of fusion and fission machineries seems to be less detrimental toward systemic health than an imbalance in mitochondrial dynamics.

Conclusions and perspectives

Dramatic progress has been made in recent years regarding our understanding of how mitochondrial morphology impacts on skeletal muscle homeostasis. Clearly, mitochondrial- shape adaptations are instrumental toward the resultant fitness gains in exercised muscles. Exercise is a pillar of health and is akin to medicine for alleviating muscle defects in several human

Table 1

Impact of acute endurance exercise on proteins regulating mitochondrial dynamics in rodent and human skeletal muscle. High-intensity high-volume training (HIHVT), sprint-interval training (SIT).

Acute responses to exercise

Citation	Organism	Experimental procedure	DRP1 alterations	Mitofusin alterations	OPA1 alterations
Picard et al. (2013) [24]	C57BL/6J mouse	3 h of voluntary running (~1.8 km covered) Soleus muscle extracted and analyzed	Unchanged	MFN2 protein levels unchanged	n/a
Jamart et al. (2013) [18]	C57BL/6 mouse	90 min (55% $\dot{V}O_2$ max) of treadmill running Gastrocnemius muscle extracted and analyzed	↑ DRP1 Ser616 phosphorylation levels	Unchanged	n/a
Laker et al. (2017) [17]	C57BL/6J mouse	90 min of treadmill running Flexor digitorum brevis muscle extracted and analyzed	↑ DRP1 Ser616 phosphorylation levels 0–3 h post exercise ↑ DRP1 Ser637 phosphorylation levels 3–6 h post exercise	MFN2 protein levels unchanged	n/a
Lavorato et al. (2016) [16]	C57BL/6J mouse	45–60 min of treadmill running to exhaustion Extensor digitorum brgus muscle extracted and analyzed	↑ DRP1 Ser616 phosphorylation levels post exercise	n/a	n/a
Kruse et al. (2016) [23]	Human	1 h (70% $\dot{V}O_2$ max) cycling Skeletal muscle biopsy extracted and analyzed	↑ DRP1 Ser616 phosphorylation levels post exercise	↑ MFN2 protein levels post exercise	Unchanged
Huertas et al. (2019)	Human (trained athletes)	HIHVT (10 × 200 m with 40-s intervals) SIT (10 × 50 m max effort every 4 min) Triceps brachii muscle extracted and analyzed	n/a	↑ MFN2 protein levels 3 h post HIHVT and SIT exercise	↑ OPA1 protein levels 3 h post HIHVT exercise

Table 2

Impact of long-term exercise training on proteins regulating mitochondrial dynamics in rodent and human skeletal muscle. Moderate-intensity continuous training (MICT), sprint-interval training (SIT), and high-intensity interval training (HIIT).

Long-term responses to exercise training

Citation	Organism	Experimental procedure	DRP1 alterations	Mitofusin alterations	OPA1 alterations
Caffin et al. (2013) [28]	Opa1$^{+/+}$/Opa1$^{+/-}$ C3H × C57/B6 mouse	60-day treadmill- running training Gastrocnemius muscle extracted and analyzed	n/a	n/a	↑ OPA1 protein levels post exercise training in Opa1$^{+/-}$ mice
Moore et al. (2019) [19]	C57BL/6J mouse	30-day treadmill- running training Quadricep muscle sample was extracted and analyzed	↓ DRP1 Ser616 phosphorylation levels ↑ DRP1 Ser637 phosphorylation levels	Unchanged	Unchanged
Konopka et al. (2014) [33]	Human	12-week cycling training Quadricep muscle sample extracted and analyzed	n/a	↑ MFN1 and MFN2 protein levels	n/a
Skelly et al. (2021) [34]	Human	MICT (cycling ~70% max heart rate) SIT (max effort sprints with 2-min intervals) Mixed muscle sample was extracted and analyzed	n/a	↑ MFN2 protein levels post MICT and SIT exercise training	↑ OPA1 protein levels post MICT and SIT exercise training
Marcangeli et al. (2022) [30]	Human (elderly and obese)	Participants with citrulline/placebo treatment for a 12- week HIIT elliptical exercise-training program Quadricep muscle sample extracted and analyzed	Uncharged	↑ MFN2 protein levels in placebo- and citrulline-treated participants	↑ OPA1 protein levels in citrulline-treated participants

Table 3

Pathological features of genetic mouse models with skeletal muscle-specific deletions of mitochondria-shaping genes. Unfolded protein response (UPR).

	MFN2 KO	MFN1::MFN2 DKO	OPA1 KO	DRP1 KO	OPA1::DRP1 DKO
Mitochondrial effect	Swollen mitochondria ↓ Mitochondrial respiration	Fragmented mitochondria ↑ mtDNA mutations ↑ Mitochondrial proliferation ↓ Mitochondrial respiration	Fragmented mitochondria ↓ Cristae number and aberrant cristae shape ↓ Mitochondrial respiration	Abnormal elongated mitochondria ↑ Mitochondrial Ca^{2+} uptake ↓ mtDNA levels ↓ Mitochondrial respiration	Abnormal elongated mitochondria with "onion-like" cristae morphology ↓ Complex-I and -IV activity ↑ Complex-V activity ↑ Mitochondrial depolarization
Muscle effect	↓ Myofiber CSA ↓ Muscle endurance and strength	↓ Myofiber CSA ↓ Fast-twitch type-IIB fibers	↓ Myofiber CSA ↓ Muscle strength ↑ FGF21 signaling	↓ Myofiber CSA ↓ Protein synthesis ↑ FGF21 signaling	↓ Myofiber CSA (mild) ↓ Muscle strength
Systemic effect	↑ ROS accumulation ↓ Glucose tolerance Impaired autophagy	↑ Post-exercise blood lactate levels ↓ Glucose tolerance	↑ FGF21 signaling ↑ Oxidative stress ↑ UPR/ER stress ↓ Glucose tolerance	↑ FGF21 signaling ↑ UPR/ER stress Hypoglycemia Growth- hormone resistance	↑ UPR/ER stress ↑ Oxidative stress Hypoglycemia Impaired autophagy
Lifespan	Normal	6–8 weeks postnatal	90–120 days post inducible deletion	30 days postnatal	Normal

diseases [68]. Based on this, designing novel therapeutics that target mitochondrial dynamics could be efficacious for patients with muscle problems, especially those unable to perform physical exercise. Of note, a recent study in humans demonstrated that excessive exercise can be maladaptive toward mitochondrial respiration [69]. Future work should therefore seek to delineate the optimal exercise intensity for maximizing mitochondria-related endurance adaptations. Elucidating this would have useful clinical applications, by improving the efficacy of exercise-referral schemes in patients with mitochondrial abnormalities. Importantly, unraveling further the relationship between the mitochondrial network and muscle mass may offer clues into unidentified molecular mechanisms governing the atrophy program. Muscle atrophy is a complex process and the signaling pathways initiated are stimuli-dependent [70–72]. For example, MuRF1-knockout mice were not protected from microgravity exposure, whereas in normal-gravity conditions, lack of MuRF1 expression in animals was protective against various atrophic stimuli [72]. Rapid muscle loss from microgravity remains a preeminent obstacle for active astronauts, highlighting the need to characterize the role of mitochondrial dynamics also in microgravity conditions.

Altogether, mitochondrial dynamics appears as an appealing toolkit to modulate mitochondrial and ultimately muscle function. Targeted therapeutics that impinge on the fusion/fission balance of these organelles in skeletal muscle might therefore be developed to counteract muscle atrophy and sarcopenia (Tables 1–3).

Authors contributions

AED and LS: conceptualization, writing the first draft, and revision; AED: figure preparation; LS: fund acquisition.

Declaration of Competing Interest

The authors declare no conflict of interest.

Acknowledgements

Research on this topic in LS lab is supported by Muscular Dystrophy Association (MDA), USA 603731 and Association Francaise contre les Myopathies (AFM), France 22326.

References and recommended reading

Papers of particular interest, published within the period of review, have been highlighted as:

- • of special interest
- •• of outstanding interest.

1. Pernas L, Scorrano L: **Mito-morphosis: mitochondrial fusion, fission, and cristae remodeling as key mediators of cellular function.** *Annu Rev Physiol* 2016, **78**:505-531.
2. Giacomello M, *et al.*: **The cell biology of mitochondrial membrane dynamics.** *Nat Rev Mol Cell Biol* 2020, **21**:204-224.
3. Tezze C, *et al.*: **Age-associated loss of OPA1 in muscle impacts muscle mass, metabolic homeostasis, systemic inflammation, and epithelial senescence.** *Cell Metab* 2017, **25**:1374-1389.e6.
4. Iqbal S, *et al.*: **Expression of mitochondrial fission and fusion regulatory proteins in skeletal muscle during chronic use and disuse.** *Muscle Nerve* 2013, **48**:963-970.
5. Cannavino J, *et al.*: **The role of alterations in mitochondrial dynamics and PGC-1alpha over-expression in fast muscle atrophy following hindlimb unloading.** *J Physiol* 2015, **593**:1981-1995.
6. Safdar A, *et al.*: **Endurance exercise rescues progeroid aging and induces systemic mitochondrial rejuvenation in mtDNA mutator mice.** *Proc Natl Acad Sci USA* 2011, **108**:4135-4140.
7. McKiernan SH, *et al.*: **Cellular adaptation contributes to calorie restriction-induced preservation of skeletal muscle in aged rhesus monkeys.** *Exp Gerontol* 2012, **47**:229-236.
8. Russell AP, *et al.*: **Skeletal muscle mitochondria: a major player in exercise, health and disease.** *Biochim Biophys Acta* 2014, **1840**:1276-1284.

9. Handschin C, Spiegelman BM: **The role of exercise and PGC1alpha in inflammation and chronic disease**. *Nature* 2008, **454**:463-469.

10. Glancy B, *et al.*: **Mitochondrial reticulum for cellular energy distribution in muscle**. *Nature* 2015, **523**:617-620.

11. Gaitanos GC, *et al.*: **Human muscle metabolism during intermittent maximal exercise**. *J Appl Physiol (1985)* 1993, **75**:712-719.

12. Zurlo F, *et al.*: **Skeletal muscle metabolism is a major determinant of resting energy expenditure**. *J Clin Invest* 1990, **86**:1423-1427.

13. Holloszy JO: **Biochemical adaptations in muscle. Effects of exercise on mitochondrial oxygen uptake and respiratory enzyme activity in skeletal muscle**. *J Biol Chem* 1967, **242**:2278-2282.

14. Penman KA: **Ultrastructural changes in human striated muscle using three methods of training**. *Res Q* 1969, **40**:764-772.

15. Gollnick PD, King DW: **Effect of exercise and training on mitochondria of rat skeletal muscle**. *Am J Physiol* 1969, **216**:1502-1509.

16. Lavorato M, *et al.*: **Elongated mitochondrial constrictions and fission in muscle fatigue**. *J Cell Sci* 2018, **131**:jcs221028.

17. Laker RC, *et al.*: **Ampk phosphorylation of Ulk1 is required for targeting of mitochondria to lysosomes in exercise-induced mitophagy**. *Nat Commun* 2017, **8**:548.

18. Jamart C, *et al.*: **Higher activation of autophagy in skeletal muscle of mice during endurance exercise in the fasted state**. *Am J Physiol Endocrinol Metab* 2013, **305**:E964-E974.

19. •• Moore TM, *et al.*: **The impact of exercise on mitochondrial dynamics and the role of Drp1 in exercise performance and training adaptations in skeletal muscle**. *Mol Metab* 2019, **21**:51-67.

This research revealed that mice subjected to chronic exercise training exhibited reduced levels of Drp1 phosphorylation at Ser616 (fission promoting) and higher Drp1 phosphorylation at Ser637 (fission inhibiting). This work offers an explanation to the adaptive mechanism in which exercise-induced fission is attenuated from repeated bouts of exercise.

20. Helle SCJ, *et al.*: **Mechanical force induces mitochondrial fission**. *Elife* 2017, **6**:e30292.

21. Fan X, Hussien R, Brooks GA: **H_2O_2-induced mitochondrial fragmentation in C_2C_{12} myocytes**. *Free Radic Biol Med* 2010, **49**:1646-1654.

22. Calvo E, *et al.*: **Functional role of respiratory supercomplexes in mice: SCAF1 relevance and segmentation of the Qpool**. *Sci Adv* 2020, **6**:eaba7509.

23. Kruse R, Pedersen AJ, Kristensen JM, Petersson SJ, Wojtaszewski JF, Højlund K: **Intact initiation of autophagy and mitochondrial fission by acute exercise in skeletal muscle of patients with Type 2 diabetes**. *Clin Sci (Lond).*, (1) 2017, **131**:37-47.

24. Picard M, *et al.*: **Acute exercise remodels mitochondrial membrane interactions in mouse skeletal muscle**. *J Appl Physiol (1985)* 2013, **115**:1562-1571.

25. Mishra P, *et al.*: **Mitochondrial dynamics is a distinguishing feature of skeletal muscle fiber types and regulates organellar compartmentalization**. *Cell Metab* 2015, **22**:1033-1044.

26. Romanello V, Sandri M: **Mitochondrial quality control and muscle mass maintenance**. *Front Physiol* 2015, **6**:422.

27. • Bell MB, *et al.*: **Adult skeletal muscle deletion of Mitofusin 1 and 2 impedes exercise performance and training capacity**. *J Appl Physiol (1985)* 2019, **126**:341-353.

This work demonstrated that single ablation of either MFN1 or MFN2 in mice is not sufficient enough to cause a detrimental effect towards exercise capacity. However, simultaneous deletion of MFN1 and MFN2 prevented any physiological adaptations from a long-term exercise training regime, indicating that mitochondrial fusion is essential for enhancing exercise capacity.

28. Cartoni F, *et al.*: **Altered skeletal muscle mitochondrial biogenesis but improved endurance capacity in trained OPA1-deficient mice**. *J Physiol* 2013, **591**:6017-6037.

29. Meinild Lundby AK, *et al.*: **Exercise training increases skeletal muscle mitochondrial volume density by enlargement of existing mitochondria and not de novo biogenesis**. *Acta Physiol* 2018, **222**:e12905.

30. Marcangeli V, Youssef L, Dulac M, Carvalho LP, Hajj-Boutros G, Reynaud O, Guegan B, Buckinx F, Gaudreau P, Morais JA, Maunège P, Noirez P, Aubertin-Leheudre M, Gouspillou G: **Impact of high-intensity interval training with or without l-citrulline on physical performance, skeletal muscle, and adipose tissue in obese older adults**. *J Cachexia Sarcopenia Muscle* (3) 2022, **13**:1526-1540.

31. Axelrod CL, *et al.*: **Exercise training remodels human skeletal muscle mitochondrial fission and fusion machinery towards a pro-elongation phenotype**. *Acta Physiol* 2019, **225**:e13216.

32. Huertas JR, Ruiz-Ojeda FJ, Plaza-Diaz J, Nordsborg NB, Martin-Albo J, Rueda-Robles A, Casuso RA: **Human muscular mitochondrial fusion in athletes during exercise**. *FASEB J.* (11) 2019, **33**:12087-12098.

33. Konopka AR, Suer MK, Wolff CA, Harber MP: **Markers of human skeletal muscle mitochondrial biogenesis and quality control: effects of age and aerobic exercise training**. *J Gerontol A Biol Sci Med Sci.* (4) 2014, **69**:371-378.

34. Skelly LE, Gillen JB, Frankish BP, MacInnis MJ, Godkin FE: **Tarnopolsky MA, Murphy RM, Gibala MJ. Human skeletal muscle fiber type-specific responses to sprint interval and moderate-intensity continuous exercise: acute and training-induced changes**. *J Appl Physiol* (4) 1985, **130**:1001-1014.

35. Houzelle A, *et al.*: **Human skeletal muscle mitochondrial dynamics in relation to oxidative capacity and insulin sensitivity**. *Diabetologia* 2021, **64**:424-436.

36. Cartoni R, *et al.*: **Mitofusins 1/2 and ERRalpha expression are increased in human skeletal muscle after physical exercise**. *J Physiol* 2005, **567**:349-358.

37. Shutt T, *et al.*: **The intracellular redox state is a core determinant of mitochondrial fusion**. *EMBO Rep* 2012, **13**:909-915.

38. Nielsen J, *et al.*: **Plasticity in mitochondrial cristae density allows metabolic capacity modulation in human skeletal muscle**. *J Physiol* 2017, **595**:2839-2847.

39. Cogliati S, *et al.*: **Mitochondrial cristae shape determines respiratory chain supercomplexes assembly and respiratory efficiency**. *Cell* 2013, **155**:160-171.

40. Acin-Perez R, Enriquez JA: **The function of the respiratory supercomplexes: the plasticity model**. *Biochim Biophys Acta* 2014, **1837**:444-450.

41. Greggio C, *et al.*: **Enhanced respiratory chain supercomplex formation in response to exercise in human skeletal muscle**. *Cell Metab* 2017, **25**:301-311.

42. • Gonzalez-Franquesa A, *et al.*: **Mass-spectrometry-based proteomics reveals mitochondrial supercomplexome plasticity**. *Cell Rep* 2021, **35**:109180.

Using mass spectrometry and native electrophoresis, complex II subunits were found to be elevated and incorporated into respiratory supercomplexes from exercise training in mouse skeletal muscle. These results show that respiratory supercomplexes assemble differently upon exercise training between mouse and human.

43. Zuchner S, *et al.*: **Mutations in the mitochondrial GTPase mitofusin 2 cause Charcot–Marie–Tooth neuropathy type 2A**. *Nat Genet* 2004, **36**:449-451.

44. Spiegel R, *et al.*: **Fatal infantile mitochondrial encephalomyopathy, hypertrophic cardiomyopathy and optic atrophy associated with a homozygous OPA1 mutation**. *J Med Genet* 2016, **53**:127-131.

45. Bartsakoulia M, *et al.*: **A novel mechanism causing imbalance of mitochondrial fusion and fission in human myopathies**. *Hum Mol Genet* 2018, **27**:1186-1195.

46. Koch J, *et al.*: **Disturbed mitochondrial and peroxisomal dynamics due to loss of MFF causes Leigh-like encephalopathy, optic atrophy and peripheral neuropathy.** *J Med Genet* 2016, **53**:270-278.

47. Shamseldin HE, *et al.*: **Genomic analysis of mitochondrial diseases in a consanguineous population reveals novel candidate disease genes.** *J Med Genet* 2012, **49**:234-241.

48. Chen H, *et al.*: **Mitochondrial fusion is required for mtDNA stability in skeletal muscle and tolerance of mtDNA mutations.** *Cell* 2010, **141**:280-289.

49. Sebastian D, *et al.*: **Mfn2 deficiency links age-related sarcopenia and impaired autophagy to activation of an adaptive mitophagy pathway.** *EMBO J* 2016, **35**:1677-1693.

50. Leboucher GP, *et al.*: **Stress-induced phosphorylation and proteasomal degradation of mitofusin 2 facilitates mitochondrial fragmentation and apoptosis.** *Mol Cell* 2012, **47**:547-557.

51. Xi QL, *et al.*: **Mitofusin-2 prevents skeletal muscle wasting in cancer cachexia.** *Oncol Lett* 2016, **12**:4013-4020.

52. Ainbinder A, *et al.*: **Role of Mitofusin-2 in mitochondrial localization and calcium uptake in skeletal muscle.** *Cell Calcium* 2015, **57**:14-24.

53. Boncompagni S, *et al.*: **Physical and functional cross talk between endo-sarcoplasmic reticulum and mitochondria in skeletal muscle.** *Antioxid Redox Signal* 2020, **32**:873-883.

54. Castro-Sepulveda M, *et al.*: **Low abundance of Mfn2 protein correlates with reduced mitochondria-SR juxtaposition and mitochondrial cristae density in human men skeletal muscle: examining organelle measurements from TEM images.** *FASEB J* 2021, **35**:e21553.

55. Pereira RO, *et al.*: **OPA1 deficiency promotes secretion of FGF21 from muscle that prevents obesity and insulin resistance.** *EMBO J* 2017, **36**:2126-2145.

56. Rodriguez-Nuevo A, *et al.*: **Mitochondrial DNA and TLR9 drive muscle inflammation upon Opa1 deficiency.** *EMBO J* 2018, **37**:e96553.

57. Varanita T, *et al.*: **The OPA1-dependent mitochondrial cristae remodeling pathway controls atrophic, apoptotic, and ischemic tissue damage.** *Cell Metab* 2015, **21**:834-844.

58. Civiletto G, *et al.*: **Opa1 overexpression ameliorates the phenotype of two mitochondrial disease mouse models.** *Cell Metab* 2015, **21**:845-854.

59. Romanello V, *et al.*: **Mitochondrial fission and remodelling contributes to muscle atrophy.** *EMBO J* 2010, **29**:1774-1785.

60. Touvier T, *et al.*: **Muscle-specific Drp1 overexpression impairs skeletal muscle growth via translational attenuation.** *Cell Death Dis* 2015, **6**:e1663.

61. • Favaro G, *et al.*: **DRP1-mediated mitochondrial shape controls calcium homeostasis and muscle mass.** *Nat Commun* 2019, **10**:2576.
In this study, mice lacking Drp1 specifically in skeletal muscle displayed distorted mitochondrial shape and developed a mitochondrial myopathy. This work provided evidence that Drp1-dependent fission is essential for regulating skeletal muscle homeostasis.

62. Durieux J, *et al.*: **Drp1 knockdown induces severe muscle atrophy and remodelling, mitochondrial dysfunction, autophagy impairment and denervation.** *J Physiol* 2020, **598**:3691-3710.

63. • Romanello V, *et al.*: **Inhibition of the fission machinery mitigates OPA1 impairment in adult skeletal muscles.** *Cells* 2019, **8**:597.
By simultaneously ablating Opa1 and Drp1 in mouse skeletal muscle, the authors showed that rebalancing mitochondrial dynamics has a rescue effect on skeletal muscle pathology characterized by unbalanced mitochondrial dynamics.

64. D'Amico D, *et al.*: **The RNA-binding protein PUM2 impairs mitochondrial dynamics and mitophagy during aging.** *Mol Cell* 2019, **73**:775-787.e10.

65. Rana A, *et al.*: **Promoting Drp1-mediated mitochondrial fission in midlife prolongs healthy lifespan of *Drosophila melanogaster*.** *Nat Commun* 2017, **8**:448.

66. Song M, *et al.*: **Abrogating mitochondrial dynamics in mouse hearts accelerates mitochondrial senescence.** *Cell Metab* 2017, **26**:872-883.e5.

67. Chen H, *et al.*: **Titration of mitochondrial fusion rescues Mff-deficient cardiomyopathy.** *J Cell Biol* 2015, **211**:795-805.

68. Luan X, *et al.*: **Exercise as a prescription for patients with various diseases.** *J Sport Health Sci* 2019, **8**:422-441.

69. •• Flockhart M, *et al.*: **Excessive exercise training causes mitochondrial functional impairment and decreases glucose tolerance in healthy volunteers.** *Cell Metab* 2021, **33**:957-970.e6.
In humans that exercised at various training loads, it was found that excessive exercise training led to impairments in mitochondrial function and glucose tolerance. This study uncovered that there is a bell-shaped relationship between exercise load and the physiological adaptations that ensue within the mitochondria.

70. Ciciliot S, *et al.*: **Muscle type and fiber type specificity in muscle wasting.** *Int J Biochem Cell Biol* 2013, **45**:2191-2199.

71. Talbot J, Maves L: **Skeletal muscle fiber type: using insights from muscle developmental biology to dissect targets for susceptibility and resistance to muscle disease.** *Wiley Interdiscip Rev Dev Biol* 2016, **5**:518-534.

72. Cadena SM, *et al.*: **Skeletal muscle in MuRF1 null mice is not spared in low-gravity conditions, indicating atrophy proceeds by unique mechanisms in space.** *Sci Rep* 2019, **9**:9387.